ISTANBUL TECHNICAL UNIVERSITY ★ GRADUATE SCHOOL

COGGING TORQUE AND PERFORMANCE OPTIMIZATION OF AN INTERIOR PERMANENT MAGNET SYNCHRONOUS MOTOR USED IN COMMERCIAL WASHING MACHINES

M.Sc. THESIS

Ege ÜNLÜTEPE KESKİN

Department of Electrical Engineering

Electrical Engineering Programme

JUNE 2021

ISTANBUL TECHNICAL UNIVERSITY ★ GRADUATE SCHOOL

COGGING TORQUE AND PERFORMANCE OPTIMIZATION OF AN INTERIOR PERMANENT MAGNET SYNCHRONOUS MOTOR USED IN COMMERCIAL WASHING MACHINES

M.Sc. THESIS

Ege ÜNLÜTEPE KESKİN
(504181017)

Department of Electrical Engineering

Electrical Engineering Programme

Thesis Advisor: Assoc. Prof. Dr. Derya Ahmet KOCABAŞ

JUNE 2021

ISTANBUL TEKNİK ÜNİVERSİTESİ ★ LİSANSÜSTÜ EĞİTİM ENSTİTÜSÜ

TİCARİ ÇAMAŞIR MAKİNELERİNDE KULLANILAN GÖMÜLÜ DAİMİ MIKNATISLI SENKRON MOTORLARIN TUTUNMA MOMENTİ VE PERFORMANS EN UYGUNLAŞTIRMASI

YÜKSEK LİSANS TEZİ

Ege ÜNLÜTEPE KESKİN
(504181017)

Elektrik Mühendisliği Anabilim Dalı

Elektrik Mühendisliği Programı

Tez Danışmanı: Doç. Dr. Derya Ahmet KOCABAŞ

HAZİRAN 2021

Ege ÜNLÜTEPE KESKİN, a M.Sc. student of İTU Graduate School 504181017, successfully defended the thesis entitled "COGGING TORQUE AND PERFORMANCE OPTIMIZATION OF AN INTERIOR PERMANENT MAGNET SYNCHRONOUS MOTOR USED IN COMMERCIAL WASHING MACHINES", which she prepared after fulfilling the requirements specified in the associated legislations, before the jury whose signatures are below.

Thesis Advisor :	**Assoc. Prof. Dr. Derya Ahmet KOCABAŞ** İstanbul Technical University	.....
Jury Members :	**Assoc. Prof. Dr. Derya Ahmet KOCABAŞ** Istanbul Technical University	.....
	Prof. Dr. İbrahim ŞENOL Yıldız Technical University	.....
	Assoc. Prof. Dr. Salih Barış ÖZTÜRK Istanbul Technical University	.....

Date of Submission : 11 June 2021
Date of Defense : 01 July 2021

To My Family,

FOREWORD

Firstly; I wish to express my sincere gratitude to my supervisor Assoc. Prof. Dr. Derya Ahmet Kocabaş for his valuable guidance and support throughout this thesis work. Besides, I would like to present my specific appreciation Arçelik Electronic Control R&D Manager Sezgin Parmaksız for his valuable support, sharing experience and guidance. Especially, I would like to express my sincere gratitude to my colleague Samet Gelme for his dedication to overcoming all difficulties of the project. My other specific appreciation goes Ferhat Coşkun for his eternal trust, encouragement and patience. In addition, I would like to express my appreciation to Halil Atilla, who has provided all kinds of support with his excellent coordination since the beginning of the project. I would like to state one of my special thanks to Eren Dalgakıran, for his guiding and supporting. Finally, I would like to thank my family for always supporting me.

June 2021

Ege ÜNLÜTEPE KESKİN
(Electrical Engineer)

TABLE OF CONTENTS

Page

FOREWORD ..... **ix**
TABLE OF CONTENTS ..... **xi**
ABBREVIATIONS ..... **xiii**
SYMBOLS ..... **xv**
LIST OF TABLES ..... **xvii**
LIST OF FIGURES ..... **xix**
SUMMARY ..... **xxiii**
ÖZET ..... **xxvii**
1. INTRODUCTION **1**
1.1 Purpose of Thesis 2
1.2 Motivation for Thesis 2
1.3 Literature Review 3
1.4 Organization of the Thesis 6
2. ELECTRICAL MOTORS IN WASHING MACHINE APPLICATIONS **8**
2.1 PMSM Structure 9
2.2 Washing Machine Application-Oriented PMSM Selection 14
2.2.1 Advantages of PMSM 15
2.2.2 Washing machine application requirements 16
2.3 PMSM Control Method for The Commercial Product 19
3. ANALYSIS OF REAL SAMPLE COMMERCIAL IPMSM **23**
3.1 Real Sample Motor 24
3.1.1 Real sample motor data 24
3.1.2 Real sample motor results 29
3.1.2.1 Disturbance effect results 30
3.1.2.2 Previous finite element modeling for transient analysis 31
3.1.2.3 Experimental results 32
3.2 Re-Analyzing and Confirmation of The Motor By FEA 35
3.2.1 Fundamentals of FEA 35
3.2.2 Motor design with ANSYS software program 38
3.2.3 Designed motor results 40
3.2.3.1 Disturbance effect results 41
3.2.3.2 Designed motor finite element modeling for transient analysis 44
3.2.3.3 Other results 46
3.3 Comparison of Real Sample and Designed Motor Results 50
3.4 Interpretation of Results 51
4. DESIGN OPTIMIZATION **53**
4.1 Parametric Modeling 54
4.2 Parametric Optimization Results 56
4.2.1 Cogging torque results 56
4.2.2 Torque ripple results 67
4.3 Multi-Objective Genetic Algorithm (MOGA) Optimization 73
4.4 Optimization Results 76

4.4.1 Simulation results 77
4.4.2 Comparison and interpretation 81
4.4.3 Prototyping 82
5. CONCLUSION 85
REFERENCES 91
CURRICULUM VITAE 95

ABBREVIATIONS

PMSM **:** Permanent Magnet Synchronous Motor

IPMSM **:** Interior Permanent Magnet Synchronous Motor

IPM **:** Interior Permanent Magnet

BEMF **:** Back Electromotive Force

MOGA **:** Multi-Objective Genetic Algorithm

rpm **:** Revolution Per Minute

FOC **:** Field Oriented Control

DTC **:** Direct Torque Control

FEM **:** Finite Element Method

FEA **:** Finite Element Analysis

SYMBOLS

k_e	: Back EMF coefficient
k_t	: Torque coefficient
θ	: The angle between the rotating and stationary references frames
V_α	: α reference frame component of stator voltages
V_β	: β reference frame component of stator voltages
w	: Electrical angular velocity of the rotor
R_a	: Armature resistance
Ψ_{PM}	: Magnet flux linkage
T_{avg}	: Nominal torque
$T_{peaktopeak}$	: Peak to peak torque
V_{line}	: Phase to phase voltage
V_{phase}	: Phase voltage
V_{rms}	: RMS voltage
B	: Magnetic flux density
E	: Electric field intensity
J	: Current density
H	: Magnetic field intensity

LIST OF TABLES

Page

Table 2.1 : Comparison for Interior PMs, Inset PMs and Surface PMs [23]. **10**
Table 3.1 : Real sample motor rated and maximum torque values for washing and spinning operations. **26**
Table 3.2 : Real sample motor stator current frequency for the wash and spin cycles in Hz. **27**
Table 3.3 : Motor design restrictions. **28**
Table 3.4 : Design criteria for the real sample IPMSM. **28**
Table 3.5 : Real sample motor model design specifications. **29**
Table 3.6 : Back EMF scenario. **47**
Table 3.7 : Back EMF and torque coefficients. **48**
Table 3.8 : Peak to peak cogging torque comparison. **50**

LIST OF FIGURES

Page

Figure 2.1 : Interior PM, Inset PM and Surface PM structures [24]. **9**
Figure 2.2 : A single-phase equivalent circuit model [24]. **10**
Figure 2.3 : A single-phase equivalent circuit model [24]. **12**
Figure 2.4 : The laundry positions on the drum for washing cycle [26]. **16**
Figure 2.5 : A sample washing machine torque-speed curve. **17**
Figure 2.6 : The field oriented control principle [28]. **20**
Figure 3.1 : A sample design of a front loading washing machine. **25**
Figure 3.2 : Core losses vs frequency. **26**
Figure 3.3 : The real sample motor cogging torque result [Nm]. **30**
Figure 3.4 : The real sample motor torque ripple result [Nm]. **31**
Figure 3.5 : The mesh structure of the real sample IPMSM. **31**
Figure 3.6 : The magnetic flux density of the real sample IPMSM. **32**
Figure 3.7 : The construction of the dynamic performance test system. **33**
Figure 3.8 : The real sample motor torque-current curve. **33**
Figure 3.9 : The real sample motor torque-efficiency curve. **34**
Figure 3.10 : The real sample motor line voltages [V]. **34**
Figure 3.11 : The real sample motor phase voltages [V]. **35**
Figure 3.12 : 2D design flow diagram. **39**
Figure 3.13 : The designed motor geometry. **40**
Figure 3.14 : The designed motor cogging torque result. **41**
Figure 3.15 : The designed motor torque ripple result. **42**
Figure 3.16 : The designed motor line back EMF harmonic spectrum. **43**
Figure 3.17 : The designed motor phase back EMF harmonic spectrum. **43**
Figure 3.18 : The mesh of the IPMSM model. **44**
Figure 3.19 : The magnetic flux density of the designed IPMSM model. **45**
Figure 3.20 : The equi-flux distribution of the designed IPMSM model. **45**
Figure 3.21 : The designed motor line voltages. **46**
Figure 3.22 : The designed motor phase voltages. **47**
Figure 3.23 : The designed motor phase currents. **48**
Figure 3.24 : The designed motor phase flux linkages. **48**
Figure 3.25 : The designed motor phase voltages. **49**
Figure 3.26 : The designed motor core losses on rotor and stator. **49**
Figure 4.1 : Cogging torque change for the different rotor pole face length. **57**
Figure 4.2 : The effect of the rotor pole face on the peak to peak cogging torque value and the cogging /nominal ratio change. **58**
Figure 4.3 : The effect of the rotor pole face on the peak to peak and average cogging torque. **58**
Figure 4.4 : The influence of cogging torque for the magnet opening. **59**
Figure 4.5 : The effect of the magnet opening on the peak to peak cogging torque value and the cogging /nominal ratio change. **60**
Figure 4.6 : The effect of the magnet opening on the peak to peak and average cogging torque. **60**

Figure 4.7 : The influence of cogging torque for the magnet thickness. **61**
Figure 4.8 : The effect of the magnet thickness on the peak to peak cogging torque value and the cogging /nominal ratio change. **62**
Figure 4.9 : The effect of the magnet thickness on the peak to peak and average cogging torque. **62**
Figure 4.10 : The influence of cogging torque for the air gap. **63**
Figure 4.11 : The effect of the magnet length on the peak to peak cogging torque value and the cogging /nominal ratio change. **64**
Figure 4.12 : The effect of the air gap on the peak to peak cogging torque value and the cogging /nominal ratio change. **64**
Figure 4.13 : The effect of the magnet length on the peak to peak and average cogging torque. **65**
Figure 4.14 : The effect of the air gap on the peak to peak and average cogging torque. **65**
Figure 4.15 : The cogging torque for the rotor slitless structure. **66**
Figure 4.16 : The influence of the rotor pole face change on motor torque ripple result. **67**
Figure 4.17 : The effect of the rotor pole face on back EMF coefficient (k_e) and torque coefficient (k_t). **68**
Figure 4.18 : The influence of the magnet opening change on motor torque ripple result. **69**
Figure 4.19 : The effect of the magnet opening on back EMF coefficient (k_e) and torque coefficient (k_t). **69**
Figure 4.20 : The influence of the magnet thickness change on motor torque ripple result. **70**
Figure 4.21 : The effect of the magnet thickness on back EMF coefficient (k_e) and torque coefficient (k_t). **71**
Figure 4.22 : The influence of the air gap change on motor torque ripple result. **72**
Figure 4.23 : The effect of the magnet length on back EMF coefficient (k_e) and torque coefficient (k_t). **72**
Figure 4.24 : The effect of the air gap on back EMF coefficient (k_e) and torque coefficient (k_t). **73**
Figure 4.25 : The cost-iteration graph. **76**
Figure 4.26 : Design 1 cogging torque analysis result. **78**
Figure 4.27 : Design 2 cogging torque analysis result. **78**
Figure 4.28 : Design 1 motor torque ripple result. **79**
Figure 4.29 : Design 2 motor torque ripple result. **79**
Figure 4.30 : Design 1 motor line voltages. **80**
Figure 4.31 : Design 1 motor phase voltages. **80**
Figure 4.32 : Design 2 motor line voltages. **81**
Figure 4.33 : Design 2 motor phase voltages. **81**
Figure 4.34 : Comparison of Design 1, Design 2 and existing motor simulation results. **82**
Figure 4.35 : The resultant design rotor part prototype. **822**
Figure 4.36 : The resultant design prototype. **83**

COGGING TORQUE AND PERFORMANCE OPTIMIZATION OF AN INTERIOR PERMANENT MAGNET SYNCHRONOUS MOTOR USED IN COMMERCIAL WASHING MACHINES

SUMMARY

Recent world-wide interest towards permanent magnet synchronous motors (PMSMs), especially impinge on various areas of applications such as home appliances, electric vehicles, robotics, industrial drives and vehicular propulsion. Utilizing accurate torque control capabilities and enabling variable speed motor drives yield a possibility to increase demand of PMSMs when compared to conventional universal motors. In addition; PMSMs outperform over other traditional motor types used in home appliances in terms of efficiency, power density (power to volume ratio), torque to mass ratio which enables compact structure, dynamic performance and low noise level.

One of the most dominated household appliances all around the world is the washing machine. Considering the washing machine performance improvement, standard features available in the washing machines are still being further developed so as to gathering maximum efficiency, low energy consumption, decreasing existing torque ripple and reduction of noise level for customer satisfaction.

Recently, researches related with the motor used for washing machine application are focused on to ensure the same output with smaller volume also decrease the cost of the used materials at the same time. In order to meet such requirements, instead of traditional universal motors PMSMs are preferable due to the reduced audible noise, long lifetime and more efficiency.

The fact that the washing machine has a high power density requirement as well as a cost constraint is made the spoke type IPMSM motors widely used. Because, these motors need airgap reduction and stack length reduction in order to meet the demanded power density requirement is caused the noise problem. The source of the unwanted noise in the spinning cycle, especially at high speeds, is the motor.

The most important components of the effects of harmonic torque distortions on the PMSMs are the back electromotive force (back EMF) harmonics, cogging torque and and torque ripple. It is proven with many researches that the disturbance effects on the machine are reduced by the geometric improvements on motor design and the development of the algorithms used in the motor control. Obtaining optimal pole pitch and pole ratio, different magnet design, reducing slot opening width, rotor or stator part skewing and slotless construction is the main contributers for motor geometrical parameters optimization to get low cogging torque effect.

The aim of this thesis is to develop and to improve the performance of an existing interior permanent magnet synchronous motor (IPMSM) which is being used in commercial washing machine applications while the disturbante effects are reduced. The actual motor used in commercial machine was modeled and analyzed numerically in order to obtain a trustable mathematical model. After obtaining a reliable analysis method and model, the motor was optimized by means of both parametric modeling

and multi-objective genetic algorithm. The disturbing effects based on cogging torque and torque ripple were decreased by changing major motor design parameter accoding to the optimization results. In the practical stage of the study the calculated numerical design was prototyped. Verification of the optimized design was proven with simulations and experiments. Studies on performance optimization with motor control technique were excluded from the scope of this thesis. The space occupied by the motor in the washing machine was kept constant.

Firstly; the design specifications and design data of a real sample IPMSM used for a typical horizontal belted-motor driven washing machine (H axis) were presented. The design criteria for the motor to be used for comparison were evaluated in accordance with the requirements and constraints for the washing machine application. Disturbance effect, simulation and experimental results were presented and discussed for existing IPMSM.

The real sample PMSM used in washing machine application with 12/8 slot-pole ratio was designed in ANSYS 2D software. 2D design steps of the real sample motor used in washing machine applications, which was aimed to improve cogging torque, were presented in ANSYS software program based on finite element method. After this step, disturbance effect, finite element modeling for transient analysis and other simulation results were obtained. Taking into consideration the requirements of the washing machine in order to fully evaluate the motor performance the designed motor results were evaluated under different scenarios including cogging torque, open circuit back EMF and on load. The results were given in this section should be very important in terms of evaluating and interpreting the performance of the designed motor.

It was aimed to verify 2D design by comparing the results obtained from the finite element analysis with the actual performance of the real sample motor. Considering all compatible results from the disturbance effect, finite element modeling for transient analysis and the other simulation results of the designed motor validation was proved. The simulation results were obtained with the designed model was found to be reliable when compared with the existing motor. Optimization process was continued via this model.

After confirming the reliability of the established model, the model was converted into a parametric analysis model. It was proven with many researches that the disturbance effects on the machine were reduced by the geometric improvements on motor design. For this purpose, the rotor of the designed motor was completely parametrically modeled.

The parametric analysis and design optimization were performed on the influence of several geometrical parameters which were the rotor pole face, magnet opening, magnet thickness, magnet length, air gap and rotor slit the investigated spoke type IPMSM. The parametric analysis was configured with definition reasonable ranges for each selected geometrical variable without ignoring the IPMSM motor requirements of the washing machine.

In next step, the effects of determined rotor geometrical parameters on cogging torque and torque ripple were investigated comprehensively. Taking into consideration the requirements of the washing machine in order to fully evaluate the infuence of the parameter on motor performance, results which were obtained from each paramater change were evaluated under different scenarios including cogging torque, open circuit back EMF and on load. Considering to the analyzes performed with the parametric

model, the parameters most affecting the cogging torque value were rotor pole face and magnet length.

In order to expand the data pool obtained cogging torque optimization of IPMSM was performed by using multi-objective genetic algorithm integrated with ANSYS software. It was obvious that the analysis results obtained by parametric modeling were the basic building blocks for the genetic algorithm. In line with the evaluation of the parametric analysis results, the most effective parameters were chosen on disturbance effect and determined ranges for each parameter were reconstructed considering the washing machine application motor requirements and restrictions. The computational complexity and calculation time for the genetic algorithm optimization was reduce with this approach.

Parametric values with the lowest cogging torque were selected from the data set to provide the cost function determined for the genetic algorithm optimization. From the analysis results on the parametric model, the approach of which parameter was effective on the cogging torque and the results that was given the lowest cogging torque value in the genetic algorithm were combined and the number of models obtained was reduced to the best two design.

Disturbance effect and simulation results were compared for the two best models obtained as a result of genetic algorithm and parametric optimization. According to these results, the design of the motor to be prototyped was decided.

These two model which were optimized in terms of rotor geometrical parameters cogging torque and torque ripple were investigated comprehensively. Taking into consideration the requirements of the washing machine in order to fully evaluate the infuence of the parameter on motor performance, results which were obtained from genetic algorithm and parametric modeling were evaluated under different scenarios including cogging torque, open circuit back EMF and on load. The optimized motors was given as “Design 1” and “Design 2” after this part.

If a comprehensive comparison was made between Design 1 and Design 2, it was observed that the Design 1 motor and Design 2 motor effect on reducing existing motor disturbance effect was highly. Since the prototyping of optimized motor was aimed when evaluating the appropriate results from the simulation results was taken into account the production capabilities. Considering the producibility capabilities of the prototype, the sample called Design 1 was chosen as resultant design.

In the final section, the prototyping of the resultant design was established. The resultant design that had been analyzed and simulated in the previous chapters were constructed in a real washing machine application. In this design, the rotor pole face parameter has been created and the magnet length has been reduced when compared to the existing motor design.

TİCARİ ÇAMAŞIR MAKİNELERİNDE KULLANILAN GÖMÜLÜ DAİMİ MIKNATISLI SENKRON MOTORLARIN TUTUNMA MOMENTİ VE PERFORMANS EN UYGUNLAŞTIRMASI

ÖZET

Sabit mıknatıslı senkron motorlara (PMSM'ler) yönelik son zamanlarda dünya çapında ilgi; özellikle ev aletleri, elektrikli araçlar, robotik, endüstriyel tahrikler ve taşıt tahriki gibi çeşitli uygulama alanlarına yöneliktir. Doğru tork kontrol yöntemlerinin ve değişken hızlı motor sürücülerinin aktif olarak kullanılması, geleneksel üniversal motorlarla karşılaştırıldığında PMSM'lere olan talebi artırma olanağı sağlar. Ek olarak; PMSM'ler, verimlilik, güç yoğunluğu (güç / hacim oranı), kompakt yapı, dinamik performans ve düşük gürültü seviyesi sağlayan tork / kütle oranı açısından ev aletlerinde kullanılan diğer geleneksel motor tiplerinden daha iyi performans gösterir.

Tüm dünyada en yaygın olarak kullanıla ev aletlerinden biri çamaşır makinesidir. Çamaşır makinesi performans iyileştirmesi göz önünde bulundurulduğunda, çamaşır makinelerinde bulunan standart özellikler; maksimum verim, mevcut tork dalgalanmasını azaltma ve müşteri memnuniyeti için gürültü seviyesini azaltma amacıyla daha da geliştirilmektedir.

Son zamanlarda, çamaşır makinesi uygulamasında kullanılan motorla ilgili araştırmalar, aynı çıktıyı daha küçük hacimde sağlamaya ve aynı zamanda kullanılan malzemelerin maliyetini düşürmeye odaklanmaktadır. Bu tür gereksinimleri karşılamak için; düşük gürültülü çalışma seviyesi, uzun ömür ve daha fazla verimlilik nedeniyle geleneksel universal motorlar yerine PMSM'ler tercih edilir.

Çamaşır makinesinin yüksek güç yoğunluğu gereksinimi ve maliyet kısıtlaması, spoke tip IPMSM motorların yaygın olarak kullanılmasını sağlamıştır. Çünkü bu motorlar, talep edilen güç yoğunluğu gereksinimini karşılamak için hava aralığının ve paket boyunun azaltılmasına ihtiyaç duyar, bu da gürültü sorununa neden olur. Sıkma devrinde, özellikle yüksek hızlarda, istenmeyen gürültünün kaynağı motordur.

Harmonik moment bozulmalarının PMSM'ler üzerindeki etkilerinin en önemli bileşenleri, endüklenen gerilim harmonikleri, tutunma momenti ve moment dalgalılığıdır. Motor tasarımında yapılan geometrik iyileştirmeler ve motor kontrolünde kullanılan algoritmaların geliştirilmesi ile makine üzerindeki bozucu etkilerin azaldığı birçok araştırma ile kanıtlanmıştır. Optimum kutup adımı ve kutup-oluk oranı elde edilmesi, farklı mıknatıs tasarımı, oluk ağzı açıklığının azaltılması, rotor veya statora kaykı verilmesi ve oluksuz yapı, düşük tutunma momenti etkisi elde etmek için motor geometrik parametrelerinin optimizasyonuna ana katkılardır.

Bu tezin amacı, ticari çamaşır makinesi uygulamalarında kullanılan mevcut bir dahili sabit mıknatıslı senkron motorun (IPMSM) bozucu etkilerinin azaltılarak motoru geliştirilmesi ve performansının iyileştirilmesidir. Güvenilir bir matematiksel model elde etmek için ticari makinede kullanılan gerçek motor sayısal olarak modellenmiş ve analiz edilmiştir. Güvenilir bir analiz yöntemi ve modeli elde edildikten sonra motor hem parametrik modelleme hem de çok amaçlı genetik algoritma ile optimize

edilmiştir. Optimizasyon sonuçlarına göre ana motor tasarım parametreleri değiştirilerek, tutunma momenti ve moment dalgalanmasına dayalı bozucu etkiler azaltılmıştır. Çalışmanın uygulama aşamasında, hesaplanan sayısal tasarım prototip haline getirilmiştir. Optimize edilmiş tasarımın doğrulanması simülasyonlar ile kanıtlanmıştır. Motor kontrol tekniği ile performans optimizasyonu üzerine yapılan çalışmalar bu tez kapsamından çıkarılmıştır. Motorun çamaşır makinesinde kapladığı alan sabit tutulmuştur.

İlk olarak; tipik bir yatay eksenli kayış kasnaklı çamaşır makinesi (H ekseni) için kullanılan gerçek bir örnek IPMSM'nin tasarım özellikleri ve tasarım verileri sunulmuştur. Karşılaştırma için kullanılacak motorun tasarım kriterleri, çamaşır makinesi uygulaması için gereksinimler ve kısıtlamalara göre değerlendirilmiştir. Bozucu etkiler, simülasyon ve deneysel sonuçlar sunulmuş ve mevcut IPMSM için tartışılmıştır.

12/8 oluk-kutup oranına sahip çamaşır makinesi uygulamasında kullanılan gerçek örnek PMSM, ANSYS 2D yazılımında tasarlanmıştır. Bozucu etkileri iyileştirilmesi amaçlanan çamaşır makinesi uygulamalarında kullanılan gerçek örnek motorun 2 boyutlu tasarım adımları, sonlu elemanlar yöntemine dayalı ANSYS yazılım programında sunulmuştur. Bu aşamadan sonra bozucu etkiler, geçici rejim analizi için sonlu eleman modellemesi ve diğer simülasyon sonuçları elde edilmiştir. Motor performansını tam olarak değerlendirmek için çamaşır makinesinin gereksinimleri göz önünde bulundurularak tasarlanan motor sonuçları, tutunma momenti, endüklenen gerilimve yükte olmak üzere farklı senaryolar altında değerlendirilmiştir. Bu bölümde verilen sonuçlar tasarlanan motorun performansının değerlendirilmesi ve yorumlanması açısından oldukça önemlidir.

Sonlu elemanlar analizinden elde edilen sonuçlar ile gerçek örnek motorun gerçek performansı karşılaştırılarak iki boyutlu tasarımın doğrulanması amaçlanmıştır. Bozucu etkilerden elde edilen tüm uyumlu sonuçlar göz önüne alındığında, geçici durum analizi için sonlu eleman modellemesi ve tasarlanan motor doğrulamasının diğer simülasyon sonuçları kanıtlanmıştır. Tasarlanan model ile elde edilen simülasyon sonuçları, mevcut motor ile karşılaştırıldığında güvenilir bulunmuştur. Bu model üzerinden optimizasyon işlemine devam edilmiştir.

Kurulan modelin güvenilirliği doğrulandıktan sonra model parametrik analiz modeline dönüştürülmüştür. Motor tasarımında yapılan geometrik iyileştirmeler ile makine üzerindeki bozucu etkilerin azaldığı birçok araştırma ile kanıtlanmıştır. Bu amaçla tasarlanan motorun rotoru tamamen parametrik olarak modellenmiştir.

Parametrik analiz ve tasarım optimizasyonu, rotor kutup yüzü, mıknatıs açıklığı, mıknatıs kalınlığı, mıknatıs uzunluğu, hava aralığı ve rotor yarığı gibi çeşitli geometrik parametrelerin etkisi üzerinde, araştırılan spoke tip IPMSM'de gerçekleştirilmiştir. Parametrik analiz, çamaşır makinesinin IPMSM motor gereksinimleri göz ardı edilmeden, seçilen her bir geometrik değişken için makul tanım aralıklarıyla yapılandırılmıştır.

Bir sonraki adımda, belirlenen rotor geometrik parametrelerinin tutunma momenti ve moment dalgalanması üzerindeki etkileri kapsamlı bir şekilde araştırılmıştır. Parametrenin motor performansı üzerindeki etkisini tam olarak değerlendirmek için çamaşır makinesinin gereksinimleri dikkate alınarak, her bir parametre değişikliğinden elde edilen sonuçlar, tutunma momenti, endüklenen gerilimve yükte olmak üzere farklı senaryolar altında değerlendirilmiştir. Parametrik model ile yapılan analizler dikkate

alındığında, tutunma momenti değerini en çok etkileyen parametreler rotor kutup yüzü ve mıknatıs uzunluğu olmuştur.

Elde edilen veri havuzunu genişletmek için ANSYS yazılımı ile entegre çok amaçlı genetik algoritma kullanılarak IPMSM'nin tutunma momenti optimizasyonu gerçekleştirilmiştir. Parametrik modelleme ile elde edilen analiz sonuçlarının genetik algoritmanın temel yapı taşları olduğu açıktır. Parametrik analiz sonuçlarının değerlendirilmesi doğrultusunda, bozucu etki üzerinde en etkili parametreler seçilmiş ve her bir parametre için belirlenen aralıklar, çamaşır makinesi uygulama motor gereksinimleri ve kısıtlamaları dikkate alınarak yeniden oluşturulmuştur. Bu yaklaşımla, genetik algoritma optimizasyonu için hesaplama karmaşıklığı ve hesaplama süresi kısaltılmıştır.

Genetik algoritma optimizasyonu için belirlenen maliyet fonksiyonunu sağlamak için veri setinden en düşük tutunma momentine sahip parametrik değerler seçilmiştir. Parametrik model üzerinde yapılan analiz sonuçlarından, tutunma momenti üzerinde hangi parametrenin etkili olduğu ile genetik algoritmada en düşük tutunma momenti değeri verilen sonuçlar birleştirilmiş ve elde edilen model sayısı en iyi iki tasarıma indirgenmiştir.

Genetik algoritma ve parametrik optimizasyon sonucunda elde edilen en iyi iki model için bozucu etkiler ve simülasyon sonuçları karşılaştırılmıştır. Bu sonuçlara göre prototipi yapılacak motorun tasarımına karar verilmiştir.

Rotor geometrik parametreleri, tutunma momenti ve moment dalgalanması açısından optimize edilen bu iki model kapsamlı bir şekilde incelenmiştir. Parametrenin motor performansı üzerindeki etkisini tam olarak değerlendirmek için çamaşır makinesinin gereksinimleri dikkate alınarak, genetik algoritma ve parametrik modellemeden elde edilen sonuçlar, tutunma momenti, endüklenen gerilimve yükte olmak üzere farklı senaryolar altında değerlendirilmiştir. Optimize edilmiş motorlar bu bölümden sonra “Tasarım 1” ve “Tasarım 2” olarak verilmiştir.

Tasarım 1 ve Tasarım 2 arasında kapsamlı bir karşılaştırma yapıldığında; Tasarım 1 motor ve Tasarım 2 motorlarının mevcut motorun bozulma etkisini azaltmadaki etkisinin yüksek olduğu gözlenmiştir. Optimize edilmiş motorun prototiplenmesi amaçlandığından, simülasyon sonuçlarından uygun sonuçlar değerlendirilirken üretim yetenekleri göz önünde bulundurulmuştur. Prototipin üretilebilirlik yetenekleri göz önünde bulundurularak ortaya çıkan tasarım olarak Tasarım 1 adı verilen örnek seçilmiştir.

Son bölümde, ortaya çıkan tasarımın prototipine yer verilmiştir. Önceki bölümlerde analiz edilen ve simüle edilen nihayi tasarım, gerçek bir çamaşır makinesi uygulaması için gerçeklenmiştir. Bu tasarımda rotor kutup yüzü parametresi oluşturulmuş ve mevcut motor tasarımına göre mıknatıs boyu kısaltılmıştır.

1. INTRODUCTION

One of the most dominated household appliances all around the world is the washing machine. Standard features available in the washing machines are still being further developed so as to gathering maximum efficiency, reaching maximum power, decreasing existing torque ripple and reduction of noise level for customer satisfaction. In order to meet washing machine requirements, instead of traditional universal motors PMSMs are preferable due to the reduced audible noise, long lifetime and more efficiency [1].

The fact that the washing machine has a high power density requirement as well as a cost constraint is made the spoke type IPMSM motors widely used. Because, these motors need airgap reduction and stack length reduction in order to meet the demanded power density requirement is caused the noise problem [2]. The source of the unwanted noise in the spinning cycle, especially at high speeds, is the motor.

The most important components of the effects of harmonic torque distortions on the PMSMs are the back electromotive force (back EMF) harmonics, cogging torque and and torque ripple. Obtaining optimal pole pitch and pole ratio, different magnet design, reducing slot opening width, rotor or stator part skewing and slotless construction is the main contributers for motor geometrical parameters optimization to get low cogging torque effect [3].

Cogging torque is mostly related with motor structure because the cogging torque effect is occured when flux passes under each stator teeth due to the permanent magnets inside the rotor. Due to the magnetic fluxes are intended to direction of rotation the spoke-type PMSM has harmonics and air-gap magnetic flux density deformation which are caused to cogging torque [4].

Torque ripple occurs at loaded condition and is undesirable because it causes vibration in the load response. Electromagnetic torque, reluctance torque results from saliency and cogging torque is the major components which lead to torque ripple. The non-sinusoidal flux distribution, saturation, incompatible slots structure in PMSMs will

decrease the motor starting and steady-state performances due to cause the torque ripple. Reducing torque ripple is essential which is corresponding to a dynamic oscillation during steady-state operation to use PMSMs more effectively. Thus, unwanted mechanical impacts are reduced such as vibration, noise and rotor stress [4].

1.1 Purpose of Thesis

The purpose of the thesis is to develop and to improve the performance of an existing interior permanent magnet synchronous motor (IPMSM) which is being used in commercial washing machine applications while the disturbante effects are reduced. The actual motor used in commercial machine was modeled and analyzed numerically in order to obtain a trustable mathematical model. After obtaining a reliable analysis method and model, the motor was optimized by means of both parametric modeling and multi-objective genetic algorithm. The disturbing effects based on cogging torque and torque ripple were decreased by changing major motor design parameter accoding to the optimization results. In the practical stage of the study the calculated numerical design was prototyped. Verification of the optimized design was proven with simulations. Studies on performance optimization with motor control technique were excluded from the scope of this thesis. The space occupied by the motor in the washing machine was kept constant.

1.2 Motivation for Thesis

The fact that the washing machine has a high power density requirement as well as a cost constraint is made the spoke type IPMSM motors widely used. Because, these motors need airgap reduction and stack length reduction in order to meet the demanded power density requirement is caused the noise problem. The source of the unwanted noise in the spinning cycle, especially at high speeds, is the motor [2]. This overall noise should be evaluated not only as an increase in noise level, but also as general harmonic noise.

The most important components of the effects of harmonic torque distortions on the PMSMs are the back electromotive force (back EMF) harmonics, cogging torque and and torque ripple. There are many studies in the literature to eliminate disturbance effects by reducing cogging torque and torque ripple. It is proven with many researches

that the disturbance effects on the machine are reduced by the geometric improvements on motor design and the development of the algorithms used in the motor control. Obtaining optimal pole pitch and pole ratio, different magnet design, reducing slot opening width, rotor or stator part skewing and slotless construction is the main contributers for motor geometrical parameters optimization to get low cogging torque effect [3].

Torque ripple occurs at loaded condition and is undesirable because it causes vibration in the load response. Electromagnetic torque, reluctance torque results from saliency and cogging torque is the major components which lead to torque ripple. Thus, the most crucial parameter should be evaluated for IPMSMs used in washing machine disturbance effect will be the cogging torque [4].

The non-sinusoidal flux distribution, saturation, incompatible slots structure in PMSMs will decrease the motor starting and steady-state performances due to cause the torque ripple. Reducing torque ripple is essential which is corresponding to a dynamic oscillation during steady-state operation to use PMSMs more effectively. Thus, unwanted mechanical impacts are reduced such as vibration, noise and rotor stress [4].

The definitions mentioned as disturbance effect on the IPMSM throughout this study are included back EMF harmonics, cogging torque and torque ripple, similar to the researches in the related literature.

1.3 Literature Review

One of the most dominated household appliances all around the world is the washing machine. According to the resent researches based on washing machine performance improvement, standard features available in the washing machines are still being further developed so as to gathering maximum efficiency, low energy consumption, decreasing existing disturbance effects and reduction of noise level for customer satisfaction. In order to meet such requirements, instead of traditional universal motors PMSMs are preferable due to the reduced audible noise, long lifetime and more efficiency [1].

Various techniques have been adopted to get low cogging torque effect such as obtaining optimal pole pitch and pole-slot ratio, different magnet design, reducing slot

opening width, rotor or stator part skewing and slotless construction which are the main contributers for motor geometrical parameter optimization [2].

One of the most important component of the effect of harmonic torque distortions on the PMSMs is the cogging torque. Cogging torque is mostly related with motor structure because the cogging torque effect is occured when flux passes under each stator teeth due to the permanent magnets inside the rotor. Due to the magnetic fluxes are intended to direction of rotation the spoke-type PMSM has harmonics and air-gap magnetic flux density deformation which are caused to cogging torque [4].

Torque ripple occurs at loaded condition and is undesirable because it causes vibration in the load response. Electromagnetic torque, reluctance torque results from saliency and cogging torque is the major components which lead to torque ripple [4].

Recent world-wide interest towards permanent magnet synchronous motors (PMSMs), especially impinge on various areas of applications such as home appliances, electric vehicles, robotics, industrial drives and vehicular propulsion. Utilizing accurate torque control capabilities and enabling variable speed motor drives yield a possibility to increase demand of PMSMs when compared to conventional universal motors [5].

In addition; PMSMs outperform over other traditional motor types used in home appliances in terms of efficiency, power density (power to volume ratio), torque to mass ratio which enables compact structure, dynamic performance and noise level [6].

Recently, a various number of methods have been proposed by researchers to eliminate disturbance effects. It is proven with many researches that the disturbance effects on the machine are reduced by the geometric improvements on motor design and the development of the algorithms used in the motor control [7].

Considering the most important effects of harmonic torque distortions on PMSMs which are back EMF harmonics, cogging torque and torque ripple, and the producibility conditions of the motor to be optimized, researches in the field of these areas are formed the basis of this study.

In [8], combinations with various different pole number and slot design have been created to be able to reduce the cogging torque value for better motor control at low speeds in white goods application. It has been emphasised stator topology improvement for cogging torque reduction in [9]. Cogging torque effect was decreased in line with inserted wedges from soft magnetic composite to the stator tooth-slot area.

Besides, slot opening and skewing to the stator laminations for a sample PMSM have been evaluated in terms of cogging torque, torque ripples and back EMF harmonics in [10]. An appropriate skew angle use had eliminated cogging torque as possible, reduced torque ripples and improved the back EMF harmonic spectrum.

Besides, it has been determined that magnet selection and magnet geometry had an influence on cogging torque. Especially, it has been shown the magnet embrace was an effective parameter directly on the cogging torque [11]. In [12], it has been stated that optimizing the iron and the magnet materials on stator and rotor poles was decreased the mechanical vibration and the acoustic noise arises from cogging torque.

In [13], an optimization has been proposed in order to reduce the torque ripple for the interior permanent magnet (IPM) motor via permanent magnet (PM) and ferromagnetic material (FM) part of the rotor design. These different materials, referred to as PM, FM and air, were formulated to minimize torque ripple under volume constraints. It has been emphasised that changing rotor permanent magnet structure was directly associated with reluctance torque which was lead to increase torque ripple [14]. An optimization has been implemented regarding to the rotor shape to improve performance of IPM motor.

It has been proposed the various barrier shape designs for IPMSM used in a direct drive washing machine to reduce high magnetic torque which was inversely proportional with torque ripple at low speeds corresponding to the wash cycle [15].

In [16], the rotor of V type IPMSM has been parametrically modeled to ensure the average torque, torque ripple, cogging torque, efficiency optimization. As a result of the analyzes carried out for the selected parameters, it was determined which parameter had more effect on the target size for improvement. By limiting the results obtained within the limits and constraints, the most suitable design parameters have been reached.

On the other hand, electromagnetic nosie in the washing machines has been anayzed by load torque and radial force at stator tooth harmonics components. Stator tooth shoe was redesigned as can be minimized the change in magnetic flux to eliminate the harmonics of noise [17].

In [18], a genetic algorithm optimization of PMSM in order to ensure the high power density and high speed requirement has been presented. By using high optimization

techniques such as genetic algorithm small volume with high power requirement was satisfied. In [19], in order to minimize the cogging torque provided that the same output power, torque or current, rotor structure has been changed in terms of thickness and shape of the magnets and pole span by using a genetic algorithm optimization tool. In addition; genetic algorithm has been used for minimum cogging torque requirement by changing magnet shape [20]. For this purpose, permanent magnet pole slice arrangement was performed with optimization tool in order to be able to define exact values.

A novel method by using genetic algorithm has been conducted to be able to minimize the magnitude and phase of the harmonic currents for an IPMSM [21]. Providing this goal, genetic algorithm were applied to achieve decreasing the peak to peak torque ripple, reducing the harmonic currents, and increasing the average torque component. As a result of optimization the objectives have been achieved regarding to chosen parameters.

1.4 Organization of the Thesis

In Chapter 2, electrical motor requirements in washing machine applications are given. PMSM structure, washing machine application-oriented PMSM selection and washine machine application requirements are the main topics that are covered in this part.

Analysis of real sample commercial IPMSM is proposed in Chapter 3. In this chapter, real sample motor data is shared and re-analyzing and confirmation of the motor by FEM is presented. After design step, comparison between real sample motor and designed motor results are given. Verification of the designed model has been proven.

Optimization process has been implemented in Chapter 4. The designed model is transferred to the parametric model and re-analyzed. In order to confirm the parametric model, multi-objective genetic algorithm optimization has been performed. In line with the genetic algorithm and parametric modeling results, the best two models are selected and the analysis results are compared. Prototyping of the best design is carried out and experimental results are presented.

Finally, conclusion is given in Chapter 5. The results obtained throughout the study are summarized.

2. ELECTRICAL MOTORS IN WASHING MACHINE APPLICATIONS

One of the most dominated household appliances all around the world is the washing machine. According to the literature review based on washing machine performance improvement, standard features available in the washing machines are still being further developed so as to gathering maximum efficiency, low energy consumption, decreasing existing torque ripple and reduction of noise level for customer satisfaction [1].

Recent world-wide research towards to motor used for washing machine application is to ensure the same output with smaller volume also decrease the cost of the used materials at the same time. In order to meet such requirements, instead of traditional universal motors PMSMs are preferable due to the reduced audible noise, long lifetime and more efficiency [1]. Considering this approach, IPMSMs are well suited for such applications enabling miniaturisation and cost competitiveness with better performance. Additionally, PMSMs make possible incorporating precise torque control features with sensorless control techniques to the system to utilize the maximum motor torque required for motor acceleration while the motor/drum start-up.

The washing machine application is complicated with regard to motor control due to a wide speed range and load variation. Considering the dynamic drum load characteristics of the washing machine, the motor start-up torque is changed according to the load conditions, low speeds in washing mode and high speeds in spin mode. PMSMs are designed to accomplish not only in the constant torque mode (washing cycle) when their speed is below-rated speed but also in the constant power mode (spinning cycle) when above-rated speed. PMSMs are used in washing machines have a wide operating range because voltage control is performed below-rated speed and field weakening control is applied above-rated speed [2].

In this chapter, the specifications of the IPMSM used for a typical horizontal belted-motor driven washing machine (H axis) is presented. This features can be listed as IPMSM structure, equivalent circuit and mathematical modelling. Also, it is

mentioned about the advantages of the PMSM over other conventional universal motors used in today's washing machines. According to the washing machine application requirements; the selection of the PMSM motor is discussed for a belted-motor type washing machine which is composed of two pulleys with the belt transmitting the speed, torque and power from the motor to the drum. Finally, the PMSM control method, based on washing machine application, is mentioned.

The topics mentioned in this chapter are considered as the basic building blocks, beacuse they form the basis of determining the requirements of the selected application and improving the motor design accordingly.

2.1 PMSM Structure

Literature and patent researches includes different permanent magnet synchronous motor topologies in various slot-pole ratio combination. PMSMs are divided into three main categories according to the position of the magnet on rotor: interior permanent magnet motor (Interior PM), inset permanent magnet motor (Inset PM), and surface permanent magnet motor (Surface PM). The configurations of these structures are presented in Figure 2.1.

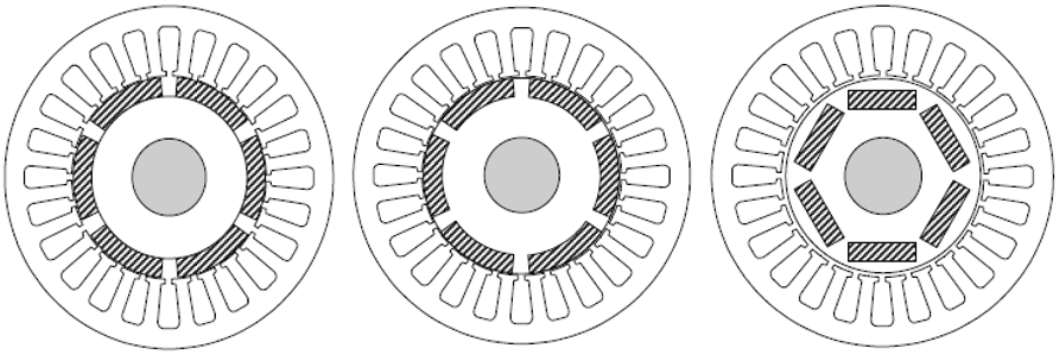

Figure 2.1 : Interior PM, Inset PM and Surface PM structures, respectively [22].

The flux distribution, rotor structure complexibility, high speed response capability and the characteristics of the control structure are compared for Interior PMs, Inset PMs and Surface PMs in Table 2.1.

Table 2.1 : Comparison for Interior PMs, Inset PMs and Surface PMs [23].

Concepts	Surface PMs	Inset PMs	Interior PMs
Flux Distribution	Trapezoidal	Trapezoidal or Sinusoidal	Sinusoidal
Rotor Structure Complexibility	Simple	Medium	Complex
High Speed Response Capability	Cannot be used without protection.	Possible	Possible
Characteristics of The Control Structure	Simple	Medium	Complex

According to the requirements of the application to be used; PMSM stator structure can be designed in various forms such as concentrated or distributed winding with integer or fractional slot. PMSMs are constructed with fractional slot concentrated winding with less end turns instead of distributed one for applications requiring higher power density. In similar approach, spoke type interior permanent magnet (spoke IPM) structure should be preferred to achieve maximum power density as well as satisfying load demands. In literature, different radial flux interior or surface magnet synchronous motor topologies with different slot-pole ratio are observed.

Permanent magnets in the rotor create the magnetic field in IPMSMs. According to the Ampere's Law, the fundemental interaction between rotating magnetic field of the stator which is created by the currents and constant magnetic field of the rotor produces the electromagnetic torque that creates rotating torque. Due to the rotor rotation, time varying magnetic field induces voltage in the stator windings. In this cycle, induced voltage is called back electromotive force (EMF) based on Faraday's law. A single-phase equivalent circuit model is demonstrated as below in Figure 2.2.

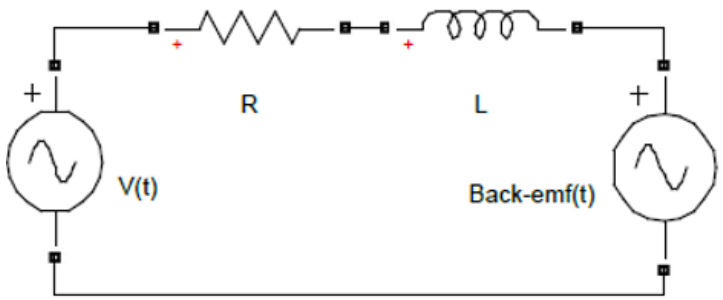

Figure 2.2 : A single-phase equivalent circuit model [24].

Three phase equations are obtained as follow according to Faraday's law via equivalent circuit depicted in Equation (2.1), where EMF(t) is the induced back electromotive force [24].

$$\begin{aligned} v_u(t) &= Ri_u(t) + L_u \frac{di_u(t)}{dt} + EMF_u(t) \\ v_v(t) &= Ri_v(t) + L_v \frac{di_v(t)}{dt} + EMF_v(t) \\ v_w(t) &= Ri_w(t) + L_w \frac{di_w(t)}{dt} + EMF_w(t) \end{aligned} \tag{2.1}$$

Back EMF expressions are expressed as the time derivative of stator flux linkages to recover equations from time dependency. The stator flux linkages for each phase are defined in Equation (2.2) [24].

$$\begin{aligned} \psi_u^S &= L_u i_u + \psi_u^{PM} \\ \psi_v^S &= L_v i_v + \psi_v^{PM} \\ \psi_w^S &= L_w i_w + \psi_w^{PM} \end{aligned} \tag{2.2}$$

In order to obtain general representation Equation (2.1) and Equation (2.2) are combined and the expressions are given in Equation (2.3) [24].

$$\begin{aligned} v_u &= Ri_u + \frac{d\psi_u^S}{dt} \\ v_v &= Ri_v + \frac{d\psi_v^S}{dt} \\ v_w &= Ri_w + \frac{d\psi_w^S}{dt} \end{aligned} \tag{2.3}$$

Three phase system is transferred into to an equivalent two phase system by shifting uvw reference frame to αβ frame with Clarke transformation, because IPMSMs are satisfied below in Equation (2.4) [25].

$$\begin{aligned} v_u + v_v + v_w &= 0 \\ i_u + i_v + i_w &= 0 \end{aligned} \tag{2.4}$$

The Clarke transformation is shown with Figure 2.3 and transformation matrix is represented as below Equation (2.5);

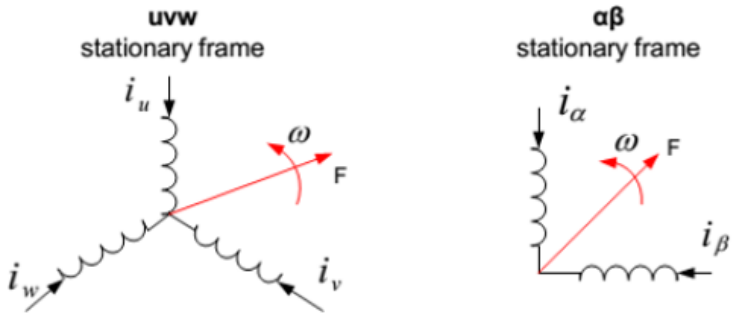

Figure 2.3 : A single-phase equivalent circuit model [24].

$$\begin{bmatrix} f_\alpha \\ f_\beta \end{bmatrix} = \begin{bmatrix} 1 & -\frac{1}{2} & -\frac{1}{2} \\ 0 & \frac{\sqrt{3}}{2} & -\frac{\sqrt{3}}{2} \end{bmatrix} \begin{bmatrix} f_a \\ f_b \\ f_c \end{bmatrix} \tag{2.5}$$

The two phase system can be depicted both in the fixed reference frame of the stator and in the rotating reference frame of the rotor which is called *d-q.* The rotor position which is denoted by θ, is represented the angle between the rotating and stationary references frames. Park transformation is expressed as transformation from stationary to rotating reference frame [25].

If Clarke transformation is applied to the Equation (2.1) and Equation (2.2), three phase model is reduced two phase in matrix form as follows in Equation (2.6);

$$\begin{bmatrix} V_\alpha \\ V_\beta \end{bmatrix} = \begin{bmatrix} R_a + \frac{di_\alpha}{dt}(L_0 + L_1 \cos 2\theta) & \frac{di_\alpha}{dt} L_1 \sin 2\theta \\ \frac{di_\alpha}{dt} L_1 \sin 2\theta & R_a + \frac{di_\alpha}{dt}(L_0 - L_1 \cos 2\theta) \end{bmatrix} \begin{bmatrix} i_\alpha \\ i_\beta \end{bmatrix} + w\psi_{PM} \begin{bmatrix} -\sin\theta \\ \cos\theta \end{bmatrix} \tag{2.6}$$

where; i_α and i_β are armature currents, V_α and V_β are stator voltages, w is electrical angular velocity of the rotor, θ is electrical angular position of the rotor, R_a armature and ψ_{PM} is magnet flux linkage.

In addition L_0 and L_1, which are d and q axes inductances respectively is formulated follow in Equation (2.7);

$$L_0 = \frac{L_d + L_q}{2}$$
$$L_1 = \frac{L_d - L_q}{2} \tag{2.7}$$

Due to the d and q axes inductances are not equal in IPMSMs, obtained expressions and equations are more complex. Besides, terms connected with torque and flux is not seen obviously which are the critical parameters for motor control in αβ reference frame equations. If model is fictionalised in rotational reference frame substituted for stationary reference frame, the model is simplified. In this way, it is possible to use DC components instead of AC components that change with time [25].

By using Park transformation, stationary reference frame is transferred into rotating reference frame with Equation (2.8).

$$\begin{bmatrix} f_d \\ f_q \end{bmatrix} = \begin{bmatrix} \cos\theta & \sin\theta \\ -\sin\theta & \cos\theta \end{bmatrix} \begin{bmatrix} f_\alpha \\ f_\beta \end{bmatrix} \tag{2.8}$$

Mathematical expression complexity is reduced by using rotating reference frame representation and IPMSM model is demonstrated as below matrix with Equation (2.9), where i_d and i_q are armature currents, V_d and V_q are stator voltages. Differential operator is symbolized as *p* [25].

$$\begin{bmatrix} V_d \\ V_q \end{bmatrix} = \begin{bmatrix} R_a + p(L_d) & -wL_q \\ wL_d & R_a + p(L_d) \end{bmatrix} \begin{bmatrix} i_d \\ i_q \end{bmatrix} + \begin{bmatrix} 0 \\ w\psi_{PM} \end{bmatrix} \tag{2.9}$$

As mentioned previously, torque and flux related terms are obtained with *d-q* reference frame representation. In addition; unlike stationary frame transformations, position-dependent terms are also avoided. IPMSM torque equation is obtained as below in Equation (2.10), where *P* is the pole pairs number [25].

$$T_e = \frac{3}{2} P\left[\psi_{PM} + (L_d - L_q) i_d\right] i_q \tag{2.10}$$

Torque equation is demonstrated that q axis current component (i_q) is contributed to torque production and d axis current component (i_d) is related with flux linkage.

2.2 Washing Machine Application-Oriented PMSM Selection

One of the most dominated household appliances all around the world is the washing machine. According to the literature review based on washing machine performance improvement, standard features available in the washing machines are still being further developed so as to gathering maximum efficiency, low energy consumption, decreasing existing torque ripple and reduction of noise level for customer satisfaction [1].

The washing machine application is complicated with regard to motor control due to a wide speed range and load variation. Considering the dynamic drum load characteristics of the washing machine, the motor start-up torque is changed according to the load conditions, low speeds in washing mode and high speeds in spin mode. Permanent magnet synchronous motors (PMSMs) make possible incorporating precise torque control features with sensorless control techniques to the system to utilize the maximum motor torque required for motor acceleration while the motor/drum start-up. PMSMs are designed to accomplish not only in the constant torque mode (washing cycle) when their speed is below-rated speed but also in the constant power mode (spinning cycle) when above-rated speed. PMSMs are used in washing machines have a wide operating range because voltage control is performed below-rated speed and field weakening control is applied above-rated speed [2].

Recent world-wide interest towards PMSMs, especially impinge on various areas of applications such as home appliances, electric vehicles, robotics, industrial drives and vehicular propulsion. Utilizing accurate torque control capabilities and enabling variable speed motor drives yield a possibility to increase demand of PMSMs when compared to conventional universal motors [5]. In addition; PMSMs outperform over other traditional motor types used in home appliances in terms of efficiency, power density (power to volume ratio), torque to mass ratio which enables compact structure, dynamic performance and low noise level.

A recent focus for the motor used in washing machine application is to ensure the same output with smaller volume also decrease the cost of the used materials at the same time. In order to meet such requirements, instead of traditional universal motors PMSMs are preferable due to the reduced audible noise, long lifetime and more

efficiency. Considering this approach, IPMSMs are well suited for such applications enabling miniaturisation and cost competitiveness with better performance.

In this section, the advantages of the PMSMs are presented over other conventional universal motors used in today's washing machines. The most commonly used washing machine specifications which is a typical horizontal belted-motor driven washing machine (H axis) are introduced. According to the washing machine application requirements; the selection of the PMSM motor is discussed for a belted-motor type washing machine which is composed of two pulleys with the belt transmitting the speed, torque and power from the motor to the drum.

2.2.1 Advantages of PMSM

Recent world-wide interest towards permanent magnet synchronous motors (PMSMs), especially impinge on various areas of applications such as home appliances, electric vehicles, robotics, industrial drives and vehicular propulsion. Utilizing accurate torque control capabilities and enabling variable speed motor drives yield a possibility to increase demand of PMSMs when compared to conventional universal motors. In addition; PMSMs outperform over other traditional motor types used in home appliances in terms of efficiency, power density (power to volume ratio), torque to mass ratio which enables compact structure, dynamic performance and low noise level [5].

Considering the requirements of commercial products, long lifetime and low noise level are the most important factors to emphasise. It is observed that the universal motor noise level is extremely high due to the brush and collector structure when the universal motor performance on the washing machine is tested. In the spinnig operation, where the washing machine operates at high speeds, unwanted audible noise is occured due to the brush and collector structure of the universal motor. In addition, the deteriation on brushes is reduced the motor lifetime. In order to meet such requirements, instead of traditional universal motors PMSMs are preferable due to the reduced audible noise, long lifetime and more efficiency. As a result, IPMSMs are well suited for such applications enabling miniaturisation and cost competitiveness with better performance [26].

2.2.2 Washing machine application requirements

One of the most dominated household appliances all around the world is the washing machine. In order to better understanding to the working of the washing machine, washing and spinning operations are also examined. The washing cycle is the main operation for cleaning and is also the longest operating period. Washing mode can basically be interpreted as circulating dirty laundry with detergent and water. This wash cycle, in which the laundry is constantly tumbled, can take up to 60 minutes. In the patents related to the washing machine, it is stated that the drum should be rotated at a speed of 40 to 80 rpm in order to provide an effective laundry cleaning. The water pumped into the drum at the starting of cycle is created a heavy load for the motor and is required a high startup torque. Washing machine load torque is not only affected by weight of laundry, also it is showed periodic variation depending on the load drum speed. The falling movement of the laundry causes a sudden change in speed [2,26]. The balance points of laundry on the drum for washing cycle is shown in Figure 2.4.

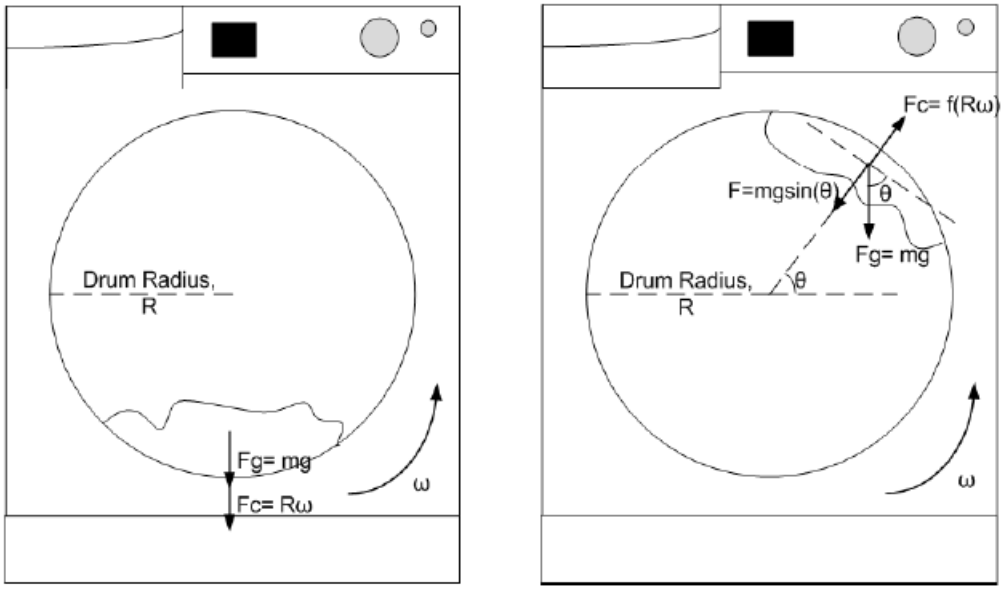

Figure 2.4 : The laundry positions on the drum for washing cycle [26].

Washing machine rinse mode is the operation cycle in which the dirty water with detergent is discharged and washed again with cold water only. The rinsing operation, where the drum speed is lower than the washing cycle speed, is created a heavy load and low speed condition for motor operation [2,26].

Lastly, in spinning mode washing machine operates in high speed and low torque. In the spinning cycle, the main purpose is to drain the rinsed water. The main problem in

spinning is the imbalance created by the loads that cannot be dissipated in distribution cycle by sticking to the drum surface. To solve this problem, known as unbalanced load, algorithms are used to determine the load is occurred at the which point of the drum [2,26].

The washing machine application is complicated with regard to motor control due to a wide speed range and load variation. Considering the dynamic drum load characteristics of the washing machine, the motor start-up torque is changed according to the load conditions, low speeds in washing mode and high speeds in spin mode. PMSMs make possible incorporating precise torque control features with sensorless control techniques to the system to utilize the maximum motor torque required for motor acceleration while the motor/drum start-up. PMSMs are designed to accomplish not only in the constant torque mode (washing cycle) when their speed is below-rated speed but also in the constant power mode (spinning cycle) when above-rated speed. PMSMs are used in washing machines have a wide operating range because voltage control is performed below-rated speed and field weakening control is applied above-rated speed [2]. A generic torque-speed curve of the washing machine which includes both washing and spinning operations is given in Figure 2.5.

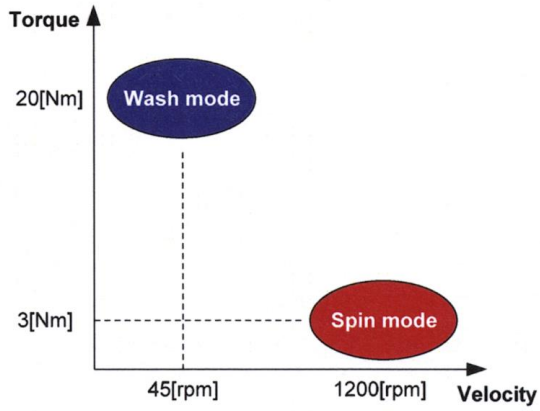

Figure 2.5 : A sample washing machine torque-speed curve.

According to the literature review based on washing machine performance improvement, standard features available in the washing machines are still being further developed so as to gathering maximum efficiency, low energy consumption, decreasing existing torque ripple and reduction of noise level for customer satisfaction.

A recent focus for the motor used in washing machine application is to ensure the same output with smaller volume also decrease the cost of the used materials at the same

time. In order to meet such requirements, instead of traditional universal motors PMSMs are preferable due to the reduced audible noise, long lifetime and more efficiency. Considering this approach, IPMSMs are well suited for such applications enabling miniaturisation and cost competitiveness with better performance.

Considering to the washing machine requirements and the expected outputs from the motor performance, there should be certain restrictions in the motor selection. According to the washing machine application requirements; the selection of the PMSM motor is important for a belted-motor type washing machines which are composed of two pulleys with the belt transmitting the speed, torque and power from the motor to the drum. The belt is used for connection between motor and drum. The washing machine pulley is attached to the pulley of the motor through a belt. The motor speed and the drum speed is not equal for this kind of washing machines, due to the belt use, the speed is transferred in proportion with a transmission ratio. In line with this information, the transmission ratio between the motion of the motor shaft and drum is obtained. Considering this transmission ratio, drum torque-speed and motor torque-speed data is interpreted [26].

In order to provide a higher power density, IPMSMs are commonly designed with fractional slot concentrated winding with less end turns instead of distributed one. In similar approach, interior permanent magnet (mostly spoke type) structure is preferred to achieve maximum power density as well as satisfying load requirements. Apart from this structure, surface magnet rotor topologies for washing machine application are introduced in the literature. The advantages and disadvantages of the IPMSMs to have an interior permanent magnet structure instead of surface or inset permanent magnet are presented below based on the requirements of the application [27].

Advantages:

1. Achieving high speeds in the spinning mode using field weakening
2. High torque/weight ratio
3. Mechanical robustness
4. Lower cogging torque

Disadvantages:

1. Complex and higher cost for rotor production
2. Current I_d component

Due to the cost-optimization constraint of the washing machine, permanent magnet (PM) material is chosen usually sintered ferrite instead of bonded rare earth PMs which are inclined to increase since 2020 for IPMSMs.

Some of the important performance criteria are related to motor thermal performance regarding to operation conditions. As an example, motor heating performance on washing machine at different load and operation conditions is very essential to satisfy IEC standarts. The fundamental standards that should be satisfied for washing machine application as a commercial product are given as follows;

- EN 60335-1 / Safety general requirements
- EN 60335-2-7 / Safety particular requirements for washing machines
- IEC/EN 60704-2-4 / Particular requirements for washing machines and spin extractors
- TS EN 55014-1 & 55014-2 / Electromagnetic compatibility (EMC)
- EN 61000-3-2 & EN 61000-3-3 / Electromagnetic compatibility (EMC) Limits

2.3 PMSM Control Method for The Commercial Product

Determination of the rotor position information is critical to obtain an efficient control for IPMSMs. Rotor position can be obtained by using sensors or estimating with sensorless control methods. Using a rotor position sensor such as encoders, resolvers and hall effect sensors on the motor shaft is not preferable for cost competitive applications such as washing machine. Since the use of extra sensors in the motor increase the cost of the product, it creates a disadvantage for product groups where competition is critical. Therefore, in such kind of applications position estimation techniques are preferred instead of mechanical sensor which measures the rotor position directly. To summarize, the use of sensors might be lead to complex cable structure, operation speed range limitation, misalignment on assembling and needing calibration [24].

The direction of the rotor magnetization flux direction relative to the stator windings should be constantly known in order to effectively manage the control algorithms in IPMSMs and to create a rotating stator magnetic field in syncronized with the rotor magnetic field created by the permanent magnets. Field oriented control (FOC) and direct torque control (DTC) are aimed to control angle between stator magnetic field ile rotor magnetic field to reduce the torque ripple which is mentioned as one of the major disturbing effects. The core structure of field oriented control principle is summarized in Figure 2.6.

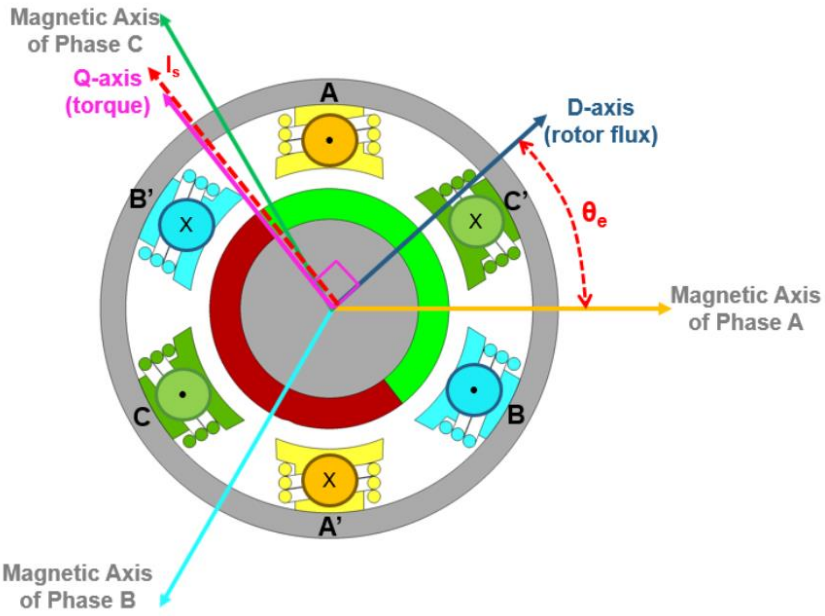

Figure 2.6 : The field oriented control principle [28].

On the other hand, in sensorless control estimators are used instead of rotor position sensors. Estimators use the stator voltages and the stator currents which are the results of applied voltages as an input to the driver software implementation. Advanced motor control algorithms are demanded more exactly motor electrical parameters such as L_d (d axis synchronous inductance), L_q (q axis synchronous inductance) and k_e (back EMF constant). Electrical parameters are required to achieve the desired closed loop performance and for back EMF observer constants by setting the PI controller gains. By means of this electrical parameter implementation to the system, position and speed of the motor is estimated properly.

At low speeds which is corresponding to the washing cycle, open loop start-up technique is preferred in order to spin the motor in the case of high back EMF for back EMF observer. If spinning cycle is considered, due to the high speed operation, d-q

reference frame is used for back EMF observer. The field weakening algorithm is needed for above the machine base speed operations. By using this algorithm speed limitation obstacle is coped with. In these regions where high speed is required, the negative d-axis current is applied with field weakening algorihtm and the back EMF voltage is reduced by rotor field weakening in response to the need to provide an output voltage higher than the output voltage limited by DC link voltage. As a result, a higher stator current is allowed related with voltage limited by DC link voltage [25,28].

3. ANALYSIS OF REAL SAMPLE COMMERCIAL IPMSM

The initial step of the studies related to IPMSM motor design is to determine the requirements of the application in which the motor will be used and to evaluate the different motor topologies used for this application in the literature. In this thesis; since it is aimed to improve the performance of a real sample motor for washing machine application, the performance of the designed motor should match with the requirements of the application. Recent world-wide research towards to motor used for washing machine application is to ensure the same output with smaller volume also decrease the cost of the used materials at the same time. Considering this approach, IPMSMs are well suited for such applications enabling miniaturisation and cost competitiveness with better performance. These principles are taken into account when evaluating the real sample motor and designed data presented in this section.

First of all, the design specifications and design data of a real sample motor used in a washing machine are given. Disturbance effect, simulation and experimental results are presented and discussed. After the details of the existing IPMSM and the motor results are given, 2D design is created with ANSYS software program based on current motor specifications. In order to make the analysis, simulation and experimentation feasible and sustainable, the model is created to be accurate enough to represent existing production.

Taking into consideration the requirements of the washing machine in order to fully evaluate the motor performance both real sample motor and designed motor results are assessed under different scenarios including cogging torque, open circuit back EMF and on load. For these different scenarios, the matching of the data of both motor is checked and compared.

In this chapter is focused on proving the accuracy of the model created in Maxwell 2D by making a comparison between designed motor and existing motor. The topics mentioned in this section include the design and validation of the real sample model in terms of electrical performance that will be the base for the parametric analysis and multi-objective genetic algorithm which are the main targets for the following chapters.

3.1 Real Sample Motor

In this section, the design specifications and design data of a real sample IPMSM used for a typical horizontal belted-motor driven washing machine (H axis) is presented. The design criteria for the motor to be used for comparison is evaluated in accordance with the requirements and constraints for the washing machine application. Disturbance effect, simulation and experimental results are presented and discussed for existing IPMSM.

3.1.1 Real sample motor data

One of the most dominated household appliances all around the world is the washing machine. According to the literature review based on washing machine performance improvement, standard features available in the washing machines are still being further developed so as to gathering maximum efficiency, low energy consumption, decreasing existing torque ripple and reduction of noise level for customer satisfaction [1].

Recent world-wide research towards to motor used for washing machine application is to ensure the same output with smaller volume also decrease the cost of the used materials at the same time. In order to meet such requirements, instead of traditional universal motors PMSMs are preferable due to the reduced audible noise, long lifetime and more efficiency. Considering this approach, IPMSMs are well suited for such applications enabling miniaturisation and cost competitiveness with better performance. Additionally, PMSMs make possible incorporating precise torque control features with sensorless control techniques to the system to utilize the maximum motor torque required for motor acceleration while the motor/drum start-up [2].

In this scope, the design specifications and design data of a real sample IPMSM used for a typical horizontal belted-motor driven washing machine (H axis) is presented. A sample design of a front loading belted-motor type washing machine is given in Figure 3.1.

Figure 3.1 : A sample design of a front loading belted motor type washing machine.

A belted-motor type washing machine composed of two pulleys with the belt transmitting the speed, torque and power from the motor to the drum as given in Figure 3.1. A large pulley is combined on the drum shaft with a diameter of 300 mm whereas a smal pulley is mounted on the motor shaft whose diameter is 20 mm. As a consequence, for the real sample IPMSM, the transmission ratio between the motion of the motor shaft to drum is obtained approximately 1:15. This means if the motor to drum transmission ratio is 1:15, the drum speed for 1200 rpm at spinning cycle with 1.08 Nm rated torque, motor torque-speed values can be computed straightforwardly which are corresponding to the spinning cycle: speed as 18000 rpm and rated torque as 0.07 Nm. The selected IPMSM for washing machine application has two load characteristics as a washing mode at 780 rpm and a spinning mode at 18000 rpm. The rated torque and maximum torque values of this motor both washing and spinning operations (operational torques) are given in Table 3.1.

Table 3.1: Real sample motor rated and maximum torque values for washing and spinning operations.

Drum Torque-Speed				Turn Ratio	Motor Torque-Speed		
Operation Mode	Speed	T_{nom}	T_{peak}		Speed	T_{nom}	T_{peak}
Washing	52 rpm	14.0 Nm	28.5 Nm	15	780 rpm	0.93 Nm	1.90 Nm
Spininng	1200 rpm	1.08 Nm	2.95 Nm	15	18000 rpm	0.07 Nm	0.20 Nm

The washing machine application is complicated with regard to motor control due to a wide speed range and load variation. Considering the dynamic drum load characteristics of the washing machine, the motor start-up torque is changed according to the load conditions, low speeds in washing mode and high speeds in spin mode. PMSMs are designed to accomplish not only in the constant torque mode (washing cycle) when their speed is below-rated speed but also in the constant power mode (spinning cycle) when above-rated speed. PMSMs are used in washing machines have a wide operating range because voltage control is performed below-rated speed and field weakening control is applied above-rated speed. Torque-speed characteristics of the real sample IPMSM in the washing mode representing high torque, low speed and in the spinning mode representing high speed, low torque are discussed by considering motor control approach [2].

One of the critical disadvantage is the increased core losses depending on the frequency for the operating conditions where the shaft power is kept constant and the motor rotates at higher speed and requires low torque and is presented in Figure 3.2.

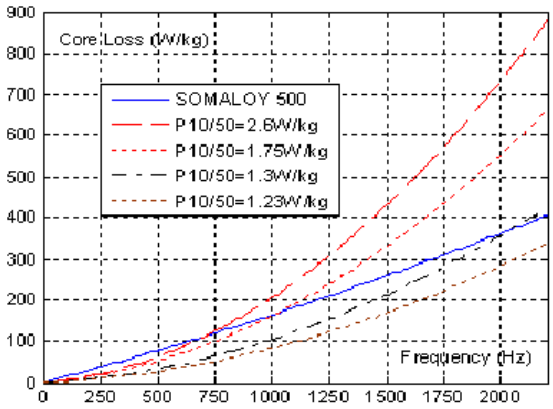

Figure 3.2 : Core losses vs frequency.

For the real sample IPMSM model with 8 pole, the stator current frequency in [Hz] is calculated for wash and spin cycles as given in Table 3.2, where f_s is the frequency of the stator supply, N is the synchronous speed and p is the number of poles by using Equation (3.1).

$$N = \frac{120.\,\mathrm{fs}}{\mathrm{p}} \tag{3.1}$$

Table 3.2: Real sample motor stator current frequency for the wash and spin cycles in Hz.

Number of Pole: 8			
Operation Mode	Speed	Turn Ratio	Stator Current Frequency [Hz]
Washing	52 rpm	15	52.0
Spininng	1200 rpm	15	1200

The sample model is reached maximum torque up to 780 rpm through the voltage control with in proportion to the incereased speed. In the case of the voltage limit is reached at the rated speed, the voltage can be no increased in proportional to the speed. That is why the voltage control can not be applied. After this phase, as the speed increases, the constant power region becomes active and the magnetic flux is reduced step by step with field weakening operation. The sample model is achieved a constant torque region of 0.93 Nm nominal at 780 rpm rated speed through voltage control in the washing mode. Similary, for spinning cycle which is executed a high-speed operation, 0.07 Nm nominal torque is required for 18000 rpm through field weakening control.

The real sample IPMSM model is used for comparison has a 12/8 slot-pole ratio with concentrated windings on the stator. According to the washing machine application requirements; in order to provide a higher power density, sample motor is designed with fractional slot concentrated winding with less end turns instead of distributed one [14]. In similar approach, spoke type interior permanent magnet (spoke IPM) structure is preferred to achieve maximum power density as well as satisfying load requirements [29]. Literature and patent researches includes different radial flux interior or surface magnet synchronous motor topologies in similar slot-pole ratio combination. The advantages and disadvantages of the

sample motor to have an interior permanent magnet structure instead of surface or inset permanent magnet are presented below based on the requirements of the application [27].

Advantages:

1. Achieving high speeds in the spinning mode using field weakening
2. High torque/weight ratio
3. Mechanical robustness
4. Lower cogging torque

Disadvantages:

1. Complex and higher cost for rotor production
2. Current I_d component

According to the washing machine requirements and the expected outputs from the motor performance, there should be certain restrictions in the motor design and given in Table 3.3.

Table 3.3: Motor design restrictions.

Motor Design Restrictions
Line EMF THD < %3
Bst. Peak < 1.7 T
J_{rms} < 8.0 A/mm^2
Magnet Demagnetization < %5

Design criteria for the real sample IPMSM is presented in Table 3.4.

Table 3.4: Design criteria for the real sample IPMSM.

Motor Design Criteria
Ferrite Magnet B_r: 0.40 T
Slot Fill Factor < 0.80
Torque for Wash / Spin: 0.65 / 0.15 Nm
n (speed) for Wash / Spin: 780 / 18000 rpm
T_{peak}: 2.0 Nm
n_{base}: 5000-6500 rpm
Max. Shaft Power: 400W

Considering the cost-optimized criterion of the washing machine, the permanent magnet (PM) material is sintered ferrite for the real sample motor, despite bonded rare earth PMs are inclined to increase since 2020 [30]. In addition, as a result of the studies aimed at enabling the use of rare-earth magnets, it is revealed that the cogging torque and back EMF THD components obtained extremely high when taking into account the washing machine motor design restrictions. As a different approach, when the PM material is chosen NdFeB the existing magnet cross-sectional area could not be kept constant, requiring an alternative mounting process which is required additional cost for production.

The existing motor model design specifications and design criteria are explained up to this point based on the washing machine requirements are summarized below in Table 3.5.

Table 3.5: Real sample motor model design specifications.

Contents	Washing	Spininng
Speed [rpm]	780	18000
Load Torque [Nm]	0,65	0,15
Power [W]	55W	400W
DC Bus Voltage [V]	310 V	
Rated Voltage [V]	220 V AC	
Rated Current [A_{rms}]	1,2 A	

In the following part, current IPMSM motor results is examined in terms of the disturbance effect, simulation and experimental results.

3.1.2 Real sample motor results

In this part of the thesis; the results of the real sample motor which is structurally introduced and design criteria are given, is demonstrated. Disturbance effect, simulation and experimental results are presented and discussed. Taking into consideration the requirements of the washing machine in order to fully evaluate the motor performance real sample motor results are evaluated under different scenarios including cogging torque, open circuit back EMF and on load. The results given in this section are very important in terms of evaluating and interpreting the performance of the existing motor. As a result, determining the existing condition of disturbance effects, which are resulted from motor through analysis and experimental test results, and the goal of improving motor performance is realized on the basis of these data.

3.1.2.1 Disturbance effect results

The most important components of the effects of harmonic torque distortions on the permanent magnet synchronous motor are the back electromotive force (back EMF) harmonics, cogging torque and and torque ripple. There are many studies in the literature to eliminate disturbance effects by reducing cogging torque and torque ripple. It is proven with many researches that the disturbance effects on the machine are reduced by the geometric improvements on motor design and the development of the algorithms used in the motor control. Obtaining optimal pole pitch and pole ratio, different magnet design, reducing slot opening width, rotor or stator part skewing and slotless construction is the main contributers for motor geometrical parameters optimization to get low cogging torque effect [2].

Torque ripple occurs at on-load condition and is undesirable because it causes vibration in the load response. Electromagnetic torque, reluctance torque results from saliency and cogging torque is the major components which lead to torque ripple. For this part; the most crucial parameter to be evaluated while giving the results of the existing motor's disturbance effect will be the cogging torque. The real sample motor cogging torque result which is obtained from numerical analysis is presented in Figure 3.3.

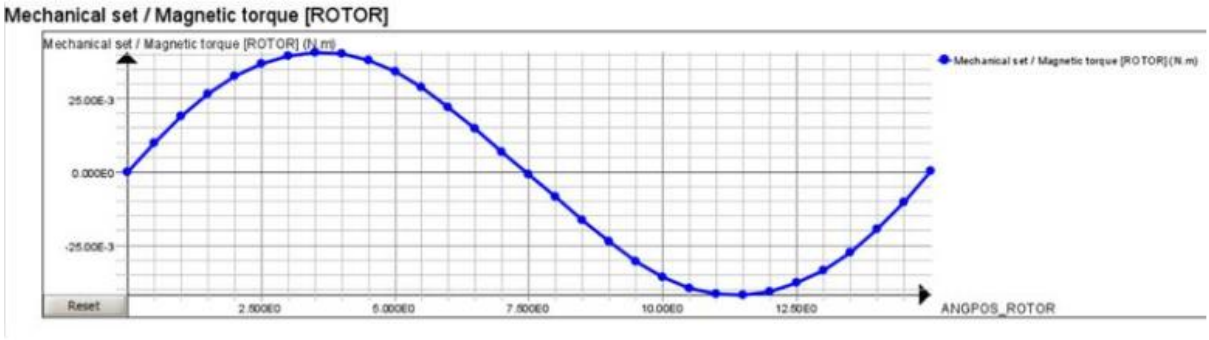

Figure 3.3 : The real sample motor cogging torque result [Nm].

The real sample motor torque changing depending on rotor position is presented in Figure 3.4.

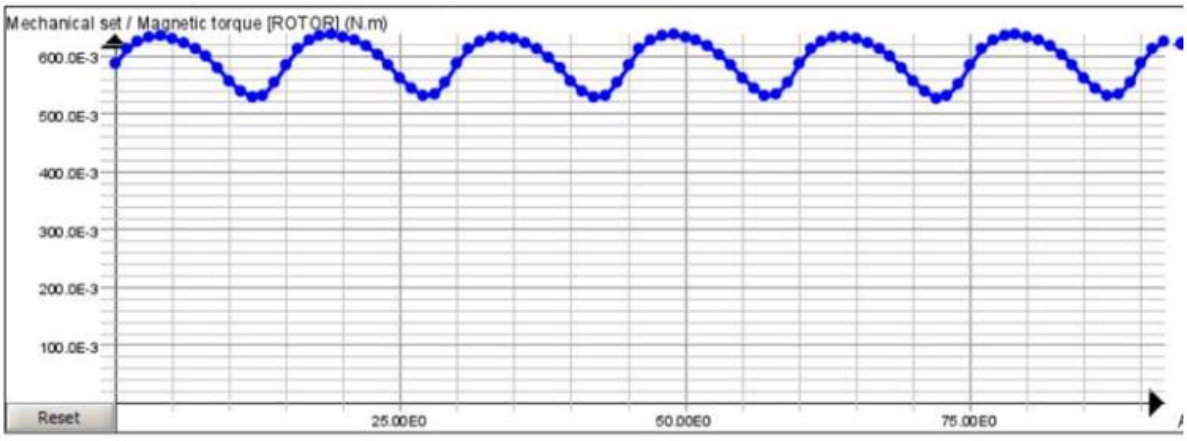

Figure 3.4 : The real sample motor torque ripple result [Nm].

Based on the results given in this section, the undesirable effects of the existing motor are revealed. Concordantly, the real sample IPMSM peak to peak cogging torque value is found as 81.12 [mNm]. It is noticed that the cogging torque and torque ripple are opened to improve to obtain better performance.

3.1.2.2 Previous finite element modeling for transient analysis

In this section, the results of 2D transient magnetic analysis of the real sample motor are presented. The mesh structure of the existing IPMSM via whole model and cross sectional area are shown in Figure 3.5.

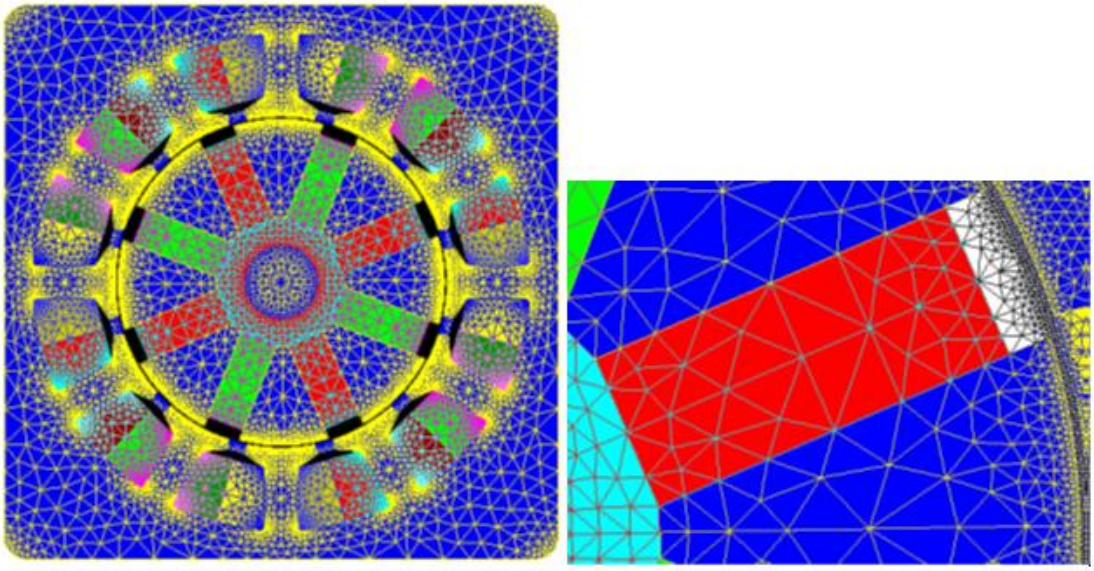

Figure 3.5 : The mesh structure of the real sample IPMSM.

The magnetic flux density distribution of the real sample IPMSM is shown in Figure 3.6.

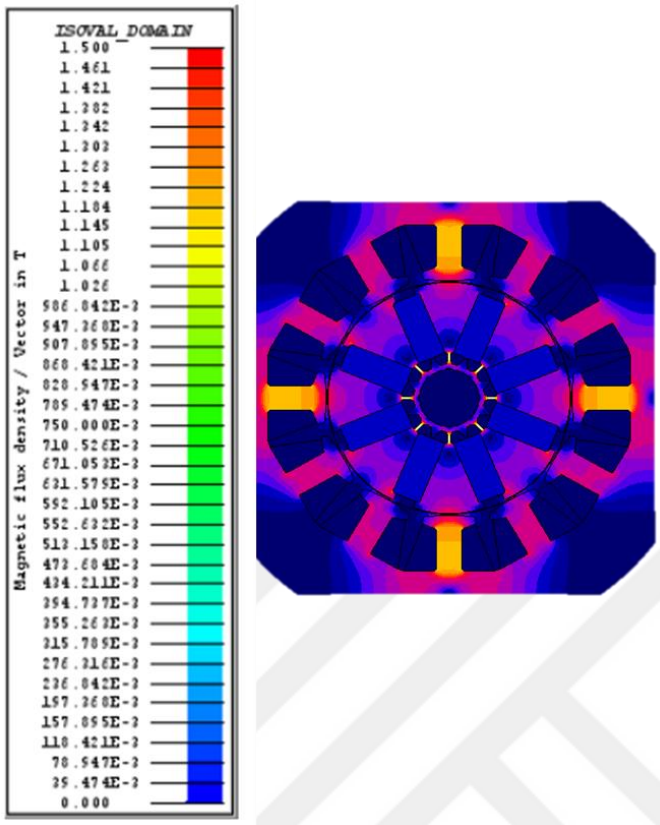

Figure 3.6 : The magnetic flux density distribution of the real sample IPMSM.

Magnetic analysis are given at no-load condition to provide the created total magnetic field by permanent magnets without stator effect. In line with this approach, the connection between permanent magnets and the stator-rotor magnetic circuit is controlled. The results of the magnetic analysis performed under no load condition are demonstrated that the flux distributions are smooth and magnetic flux density distribution is not exceeded the Bst. Peak < 1.7 T limit value as discussed in Section 3.1.1. This result proved that the real sample motor was designed in accordance with washing machine application magnetic field restrictions. As expected, it is concluded that the flux density at no load condition is become higher in rotor shape around magnets arising from permanent magnets.

3.1.2.3 Experimental results

At this stage, the solo performance curves of the real sample motor are indicated on the dynamometer. The construction of the dynamic performance test system is presented in Figure 3.7.

Figure 3.7 : The construction of the dynamic performance test system.

The existing motor characteristics curves in other words torque-current and torque-efficiency are presented in below Figure 3.8 and Figure 3.9, respectively.

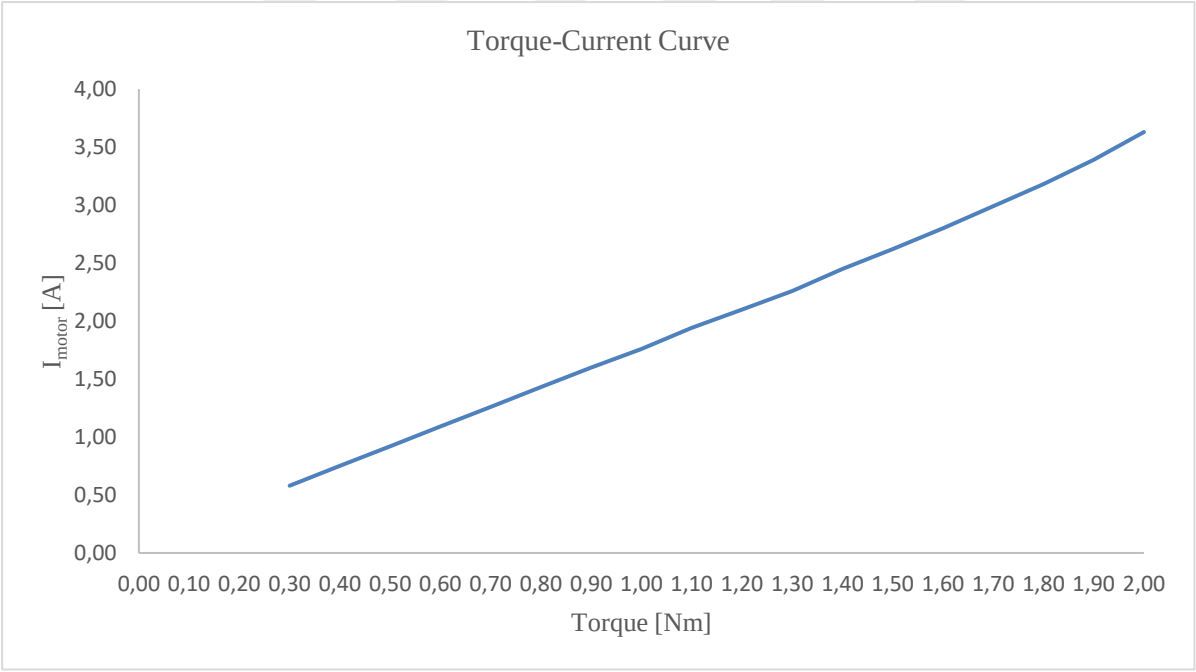

Figure 3.8 : The real sample motor torque-current curve.

In the torque current graph, the point where the graph starts to go linear is represented the saturation point.

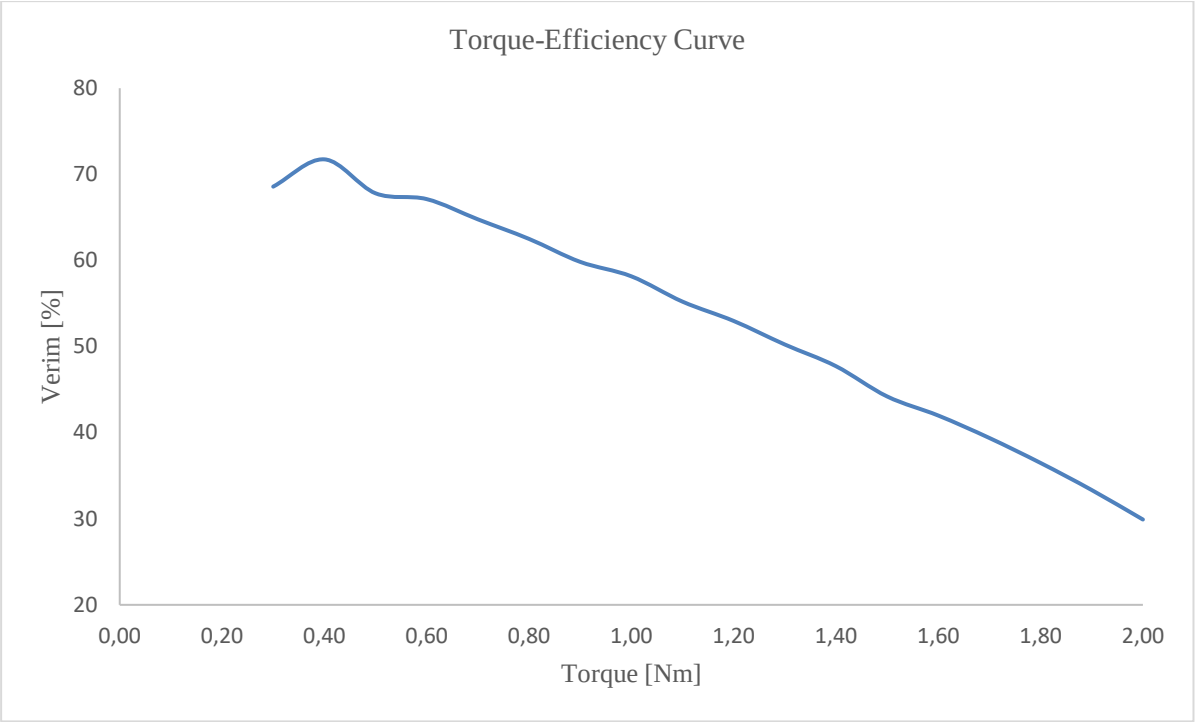

Figure 3.9 : The real sample motor torque-efficiency curve.

Besides, line (phase to phase) voltages and phase voltages were obtained as below in Figure 3.10 and Figure 3.11, respectively.

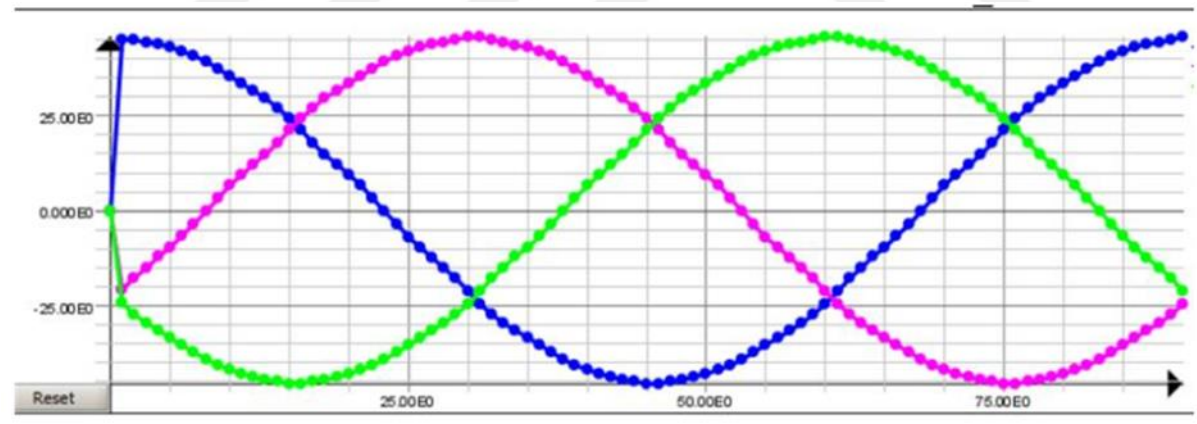

Figure 3.10 : The real sample motor line voltages [V].

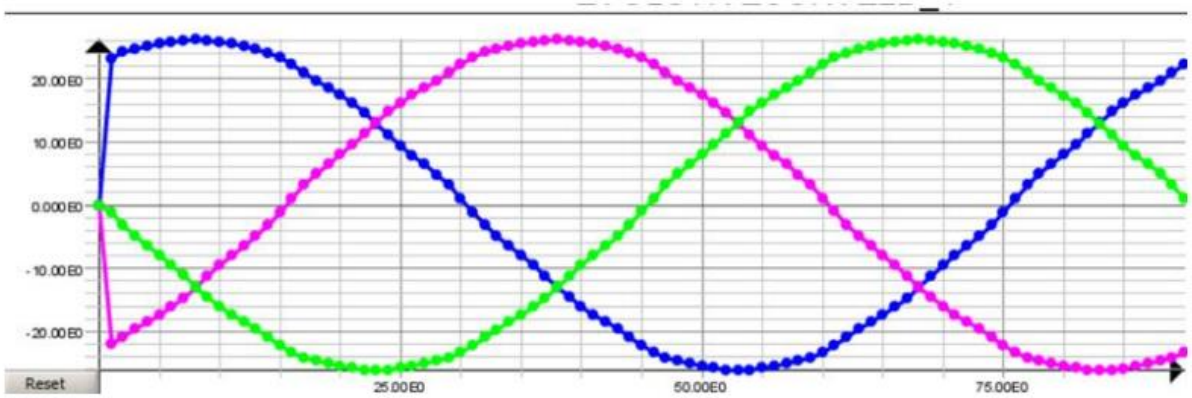

Figure 3.11 : The real sample motor phase voltages [V].

In this section, the experimental results of the current motor are shared. The data obtained experimental results will be compared with the motor to be designed, and model validation will be checked based on the reliability of the simulation results.

3.2 Re-Analyzing and Confirmation of The Motor By FEA

In this section, the basic structure of the finite element analysis (FEA), which is widely used in solving engineering problems, is explained. 2D design steps of the real sample motor used in washing machine applications, which is aimed to improve cogging torque, presented in ANSYS software program based on finite element method. After this step, disturbance effect, finite element modeling for transient analysis and other simulation results are presented. Taking into consideration the requirements of the washing machine in order to fully evaluate the motor performance the designed motor results are evaluated under different scenarios including cogging torque, open circuit back EMF and on load. The results given in this section are very important in terms of evaluating and interpreting the performance of the designed motor.

3.2.1 Fundamentals of FEA

Solving engineering problems consists of two main steps as formulating the problem mathematically, and numerical analysis of created mathematical model. The most commonly used method for this analysis is finite element method. Finite element analysis is a numerical modeling technique developed for the analysis of engineering problems involving nonlinear materials and complex geometrical structure [31].

A system expressed mathematically by performing finite element analysis can be considered as a modeling consisting of sub-parts. In line with this approach; geometry is divided into a large number of smaller parts that can numerically solve the problem with a specific approximation. Nodal points are formed on the volume or surface geometry separated by these structures called meshes. The properties of the defined material are assigned to each node. The equations are solved so that the potential function for each node is the smallest. The solution of each element is expressed as the combination of solutions obtained from the nodes that consist of this element. Since finite element analysis is usually perform in two or three dimensions for many applications, by using the symmetry and periodicity properties, the dimensions of the problems are adapted [31,32].

The solution of the finite element equations is based on the analysis of static, frequency domain and time varying electromagnetic and electric fields using basic Maxwell's equations. PMSMs are consisted of a stationary magnetic flux source which is permanent magnets located on the rotor part and the rotating magnetic field of the stator. Depending on the rotation, magnetic fields that change with time induce electric fields which is given in Equation (3.2) with Faraday's law, where B is magnetic flux density and E is electric field intensity [31,32].

$$rot\,\vec{E} = \vec{\nabla} \times \vec{E} = -\frac{\partial \vec{B}}{\partial t} \tag{3.2}$$

In case of electric field causes current according to Ohm's law is given in Equation (3.3), where J is current density.

$$\vec{J} = \sigma \times \vec{E} \tag{3.3}$$

According to the Ampere's Law; interaction between the magnetic field of the rotor and synchronous alternating current of the stator windings creates force (F) for rotor to rotate. As soon as the rotor begins to rotate at synchronous speed with the stator field, the rotor poles are interlaced with the rotating magnetic field of the stator. The equations proving that the current density (J) is the source of the magnetic field intensity (H) are given as follows in Equation (3.4), where D is the electric flux density [31,32].

$$\vec{F} = \vec{J} \times \vec{B}$$
$$rot\,\vec{H} = \vec{\nabla} \times \vec{H} = \vec{J} + \frac{\partial D}{\partial t} \tag{3.4}$$

Gauss law is related with two main approach: the distribution of electric charge (ρ) is the source of electric flux density and in an enclosed loop total magnetic field is zero, as expressed in Equation (3.5).

$$\vec{\nabla} . \vec{D} = \rho$$
$$\vec{\nabla} . \vec{B} = 0 \tag{3.5}$$

In the simplest expression, FEA method is the division of geometry into small parts to eliminate the difficulty of complex boundary conditions for engineering problems where it is not possible to define the potential function to cover the entire solution. Then, equations are obtained for the each element created and analytical analysis is performed by applying boundary conditions to these equations.

PMSM electromagnetic field analytical calculation is based on Laplacian and Poisson equations of a magnetic vector potential and magnetic scalar potential within the respective regions. In this manner; conducting region of the permanent magnets and non-conducting regions of air gap and rotor can be modelled by using magnetic vector potential (A) and magnetic scalar potential (ϑ), where H_T is total magnetic field intensity. Concordantly, relevant correlations and Laplacian type equations are given for non-conducting regions as expressed in Equation (3.6), where μ is the permeance [31].

$$H_T = -\nabla . \vartheta$$
$$\nabla . \mu . \nabla . \vartheta = 0 \tag{3.6}$$

Similar way; conducting regions can be formed as below Equation (3.7) by using magnetic flux density (B) and electric field intensity (E) concepts, where V is scalar electric potential, ω is the speed [31].

$$B = \nabla \times A$$
$$E = -\frac{\partial A}{\partial t} - \nabla.V + \omega \times \nabla \times A \tag{3.7}$$

In order to obtain the scalar potential function (V) equation; scalar electric potential is denominated in terms of magnetic vector potential (A) and speed (ϖ) values and is given in Equation (3.8) [31].

$$V = A.\omega \tag{3.8}$$

Ampere's Law and divergence theorem are combined as below in Equation (3.9) [31].

$$\nabla \times \frac{1}{\mu} \times \nabla \times A = \sigma\left(-\frac{\partial A}{\partial t} - \omega \times \nabla \times A + \nabla.V \right)$$
$$\nabla.\sigma\left(-\frac{\partial A}{\partial t} - \omega \times \nabla \times A + \nabla.V \right) = 0 \tag{3.9}$$
$$\nabla \times \frac{1}{\mu} \times \nabla \times A = \sigma\left(-\frac{\partial A}{\partial t} - (\omega.\nabla)A - (A.\nabla)\omega - A \times (\nabla \times \omega) \right)$$

As a result; the electromagnetic field change of rotating electrical machines is mathematically expressed with FEA basic Maxwell equations by applying the boundary conditions.

3.2.2 Motor design with ANSYS software program

A real sample PMSM used in washing machine application with 12/8 slot-pole ratio is designed in ANSYS 2D software. It is aimed to verify 2D design by comparing the results obtained from the finite element analysis with the actual performance values of the real sample motor. The flow diagram built for ANSYS 2D design is given in Figure 3.12.

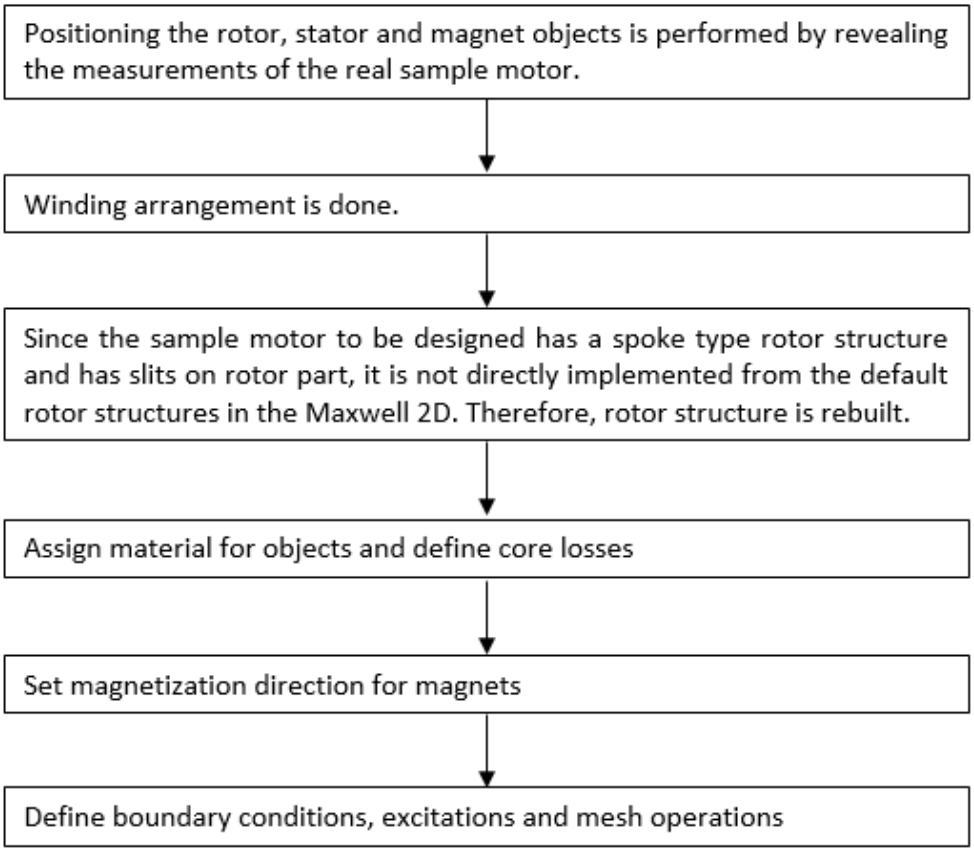

Figure 3.12 : 2D design flow diagram.

The geometry of the designed motor that exactly matches with the mass production is shown in Figure 3.13.

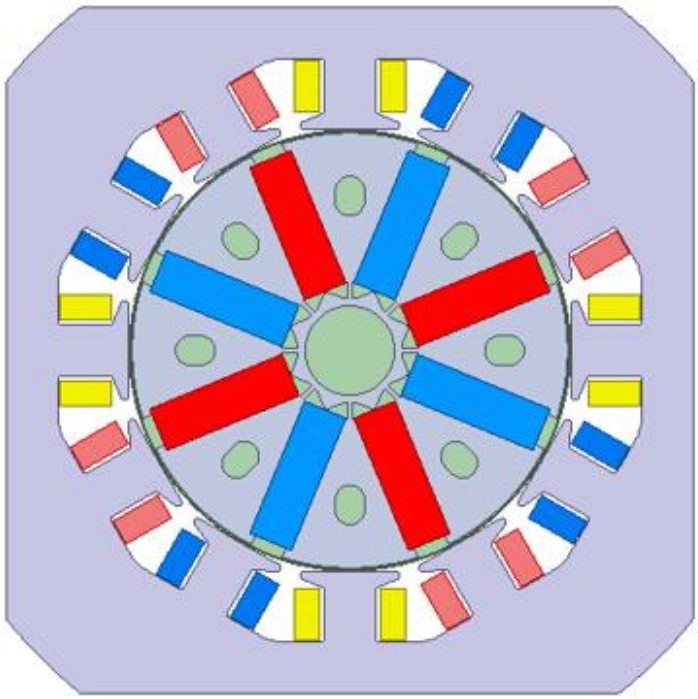

Figure 3.13 : The designed motor geometry.

3.2.3 Designed motor results

In this study, ANSYS Maxwell 2D transient analysis is used for finite element analysis of the designed sample motor. Transient analysis takes much longer than magnetostatic analysis. Although it will extend the analysis process time, in order to obtain more accurate results and to take into account the geometrical problems transient analysis is preferred. The reason is that the problem is solved again for each time in transient analysis until reach the steady state. This allows transients in the system to be taken into account. In addition, the more complex transient equations extend the analysis time.

2D transient analyzes are performed using ANSYS software program based on finite element method. The geometry of the problem is automatically split into small triangles in Maxwell 2D to obtain the set of algebraic equations to solve. Maxwell 2D adaptive meshing capability provides the assembly of all triangles automatically which is called the finite element mesh of the model. The materials, boundaries and source conditions are assigned for the created 2D model and the electromagnetic field problems are solved by applying Maxwell's equations over a finite space region with Maxwell 2D.

In this step, disturbance effect, finite element modeling for transient analysis and other simulation results are presented. Taking into consideration the requirements of the washing machine in order to fully evaluate the motor performance the designed motor results are evaluated under different scenarios including cogging torque, open circuit back EMF and on load. The results given in this section are very important in terms of evaluating and interpreting the performance of the designed motor.

3.2.3.1 Disturbance effect results

For this part; the most crucial parameter to be evaluated while giving the results of the designed motor's disturbance effect is the cogging torque. Cogging torque analysis is performed at no-load condition in Maxwell 2D. Therefore, the cogging torque effect is occured when flux passes under each stator teeth due to the permanent magnets inside the rotor. Due the fact that the real sample IPMSM used in washing machine application with 12/8 slot-pole ratio, as proportional to the number of poles, there should be 24 cogging steps in one rotor mechanical turn. In this case, the cogging torque period is calculated to be 15 degree. Since the speed is held constant at 1.0 deg/sec, 15 degree is corresponded to be 15 second. The designed motor cogging torque analysis result is presented as below in Figure 3.14.

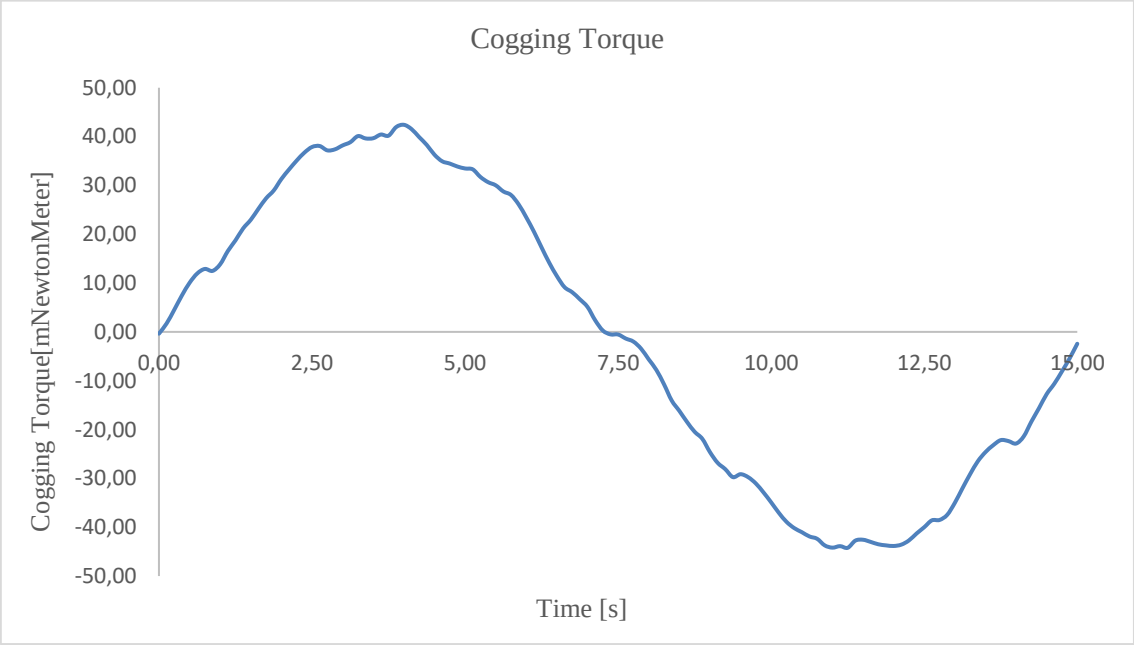

Figure 3.14 : The designed motor cogging torque result.

The designed motor torque changing depending on rotor position is presented in Figure 3.15.

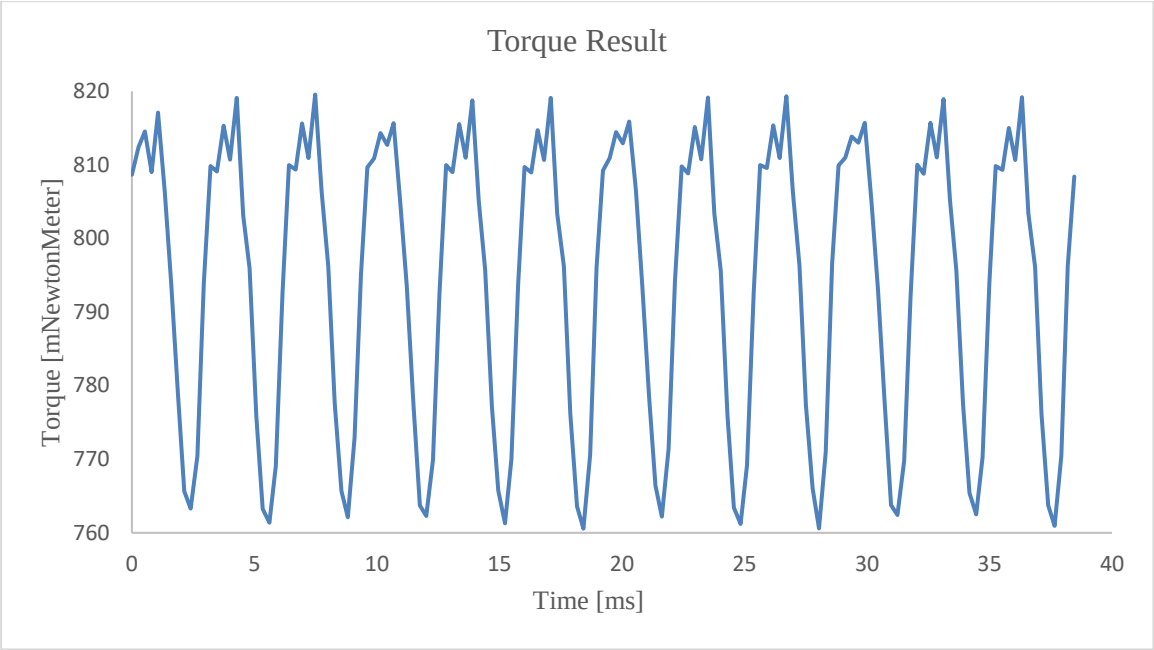

Figure 3.15 : The designed motor torque ripple result.

Accorrding to the above results, torque ripple, which is the other unwanted effect is computed at loaded condition in 780 rpm with below Equation (3.10) and depends on peak to peak torque ($T_{peaktopeak}$) and mean torque (T_{avg}), where is sembolized as T_{ripple}.

$$T_{ripple} = \frac{T_{peaktopeak}}{T_{avg}} \tag{3.10}$$

Torque ripple percentage is computed as below for the designed motor in Equation (3.11).

$$T_{ripple}(\%) = \frac{T_{peaktopeak}}{T_{avg}} = \frac{58{,}99[\text{mNm}]}{794{,}35[\text{mNm}]} \times 100 = 7{,}43\,\% \tag{3.11}$$

Based on the results are given until this part, the undesirable effects of the designed motor are revealed. Concordantly, the designed sample IPMSM peak to peak cogging torque value is found as 86,62 [mNm] and torque ripple percentage is defined as 7,43%. In the parametric optimization to be capabled, it is aimed to reduce the cogging torque value.

Besides, back EMF THD results are presented for single phase and phase to phase voltages in Figure 3.16 and Figure 3.17, respectively.

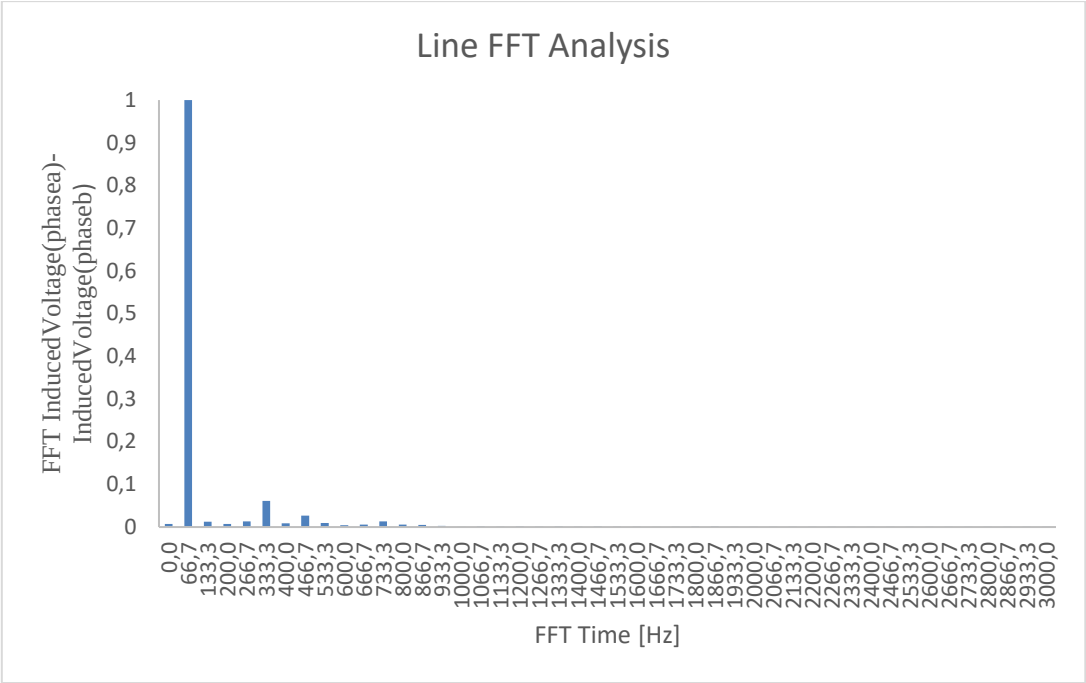

Figure 3.16 : The designed motor line back EMF harmonic spectrum.

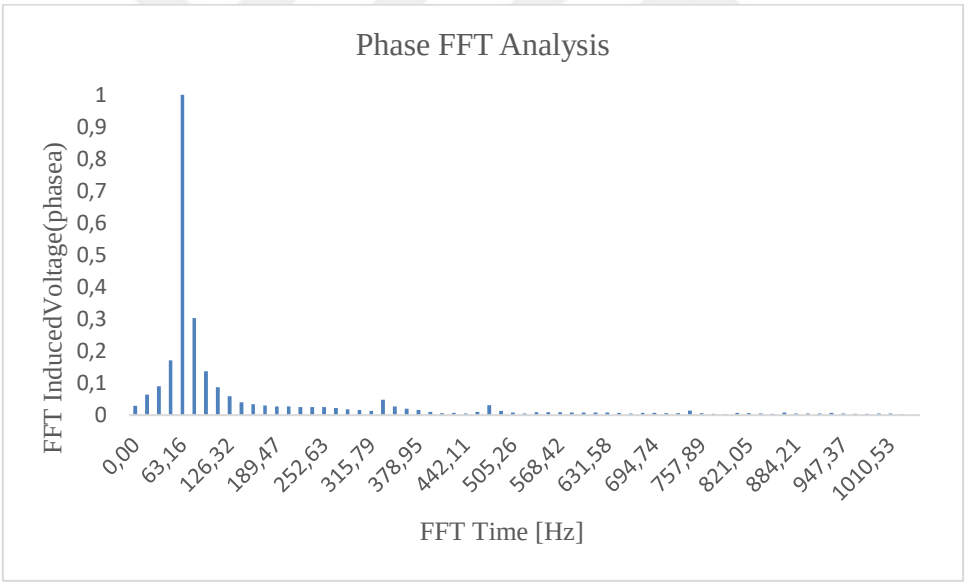

Figure 3.17 : The designed motor phase back EMF harmonic spectrum.

FFT analysis for single phase back EMF is performed up to 1000 Hz in order to focus on the frequency spectrum better. Thus, fundamental components of the harmonics are selected obviously.

The results given in this section are very important in terms of evaluating and interpreting the validation of the designed motor.

3.2.3.2 Designed motor finite element modeling for transient analysis

In this section, the results of Maxwell 2D transient magnetic analysis of the designed motor are presented. The mesh of the model automatically generated by ANSYS for simulation is given in Figure 3.18.

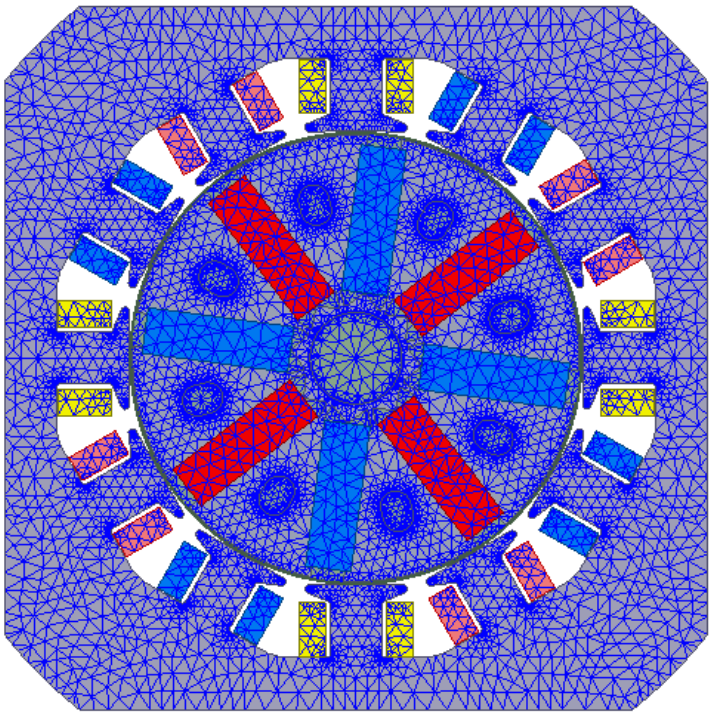

Figure 3.18 : The mesh of the IPMSM model.

The magnetic flux density and equi-flux distribution of the created IPMSM are shown in Figure 3.19 and Figure 3.20, respectively.

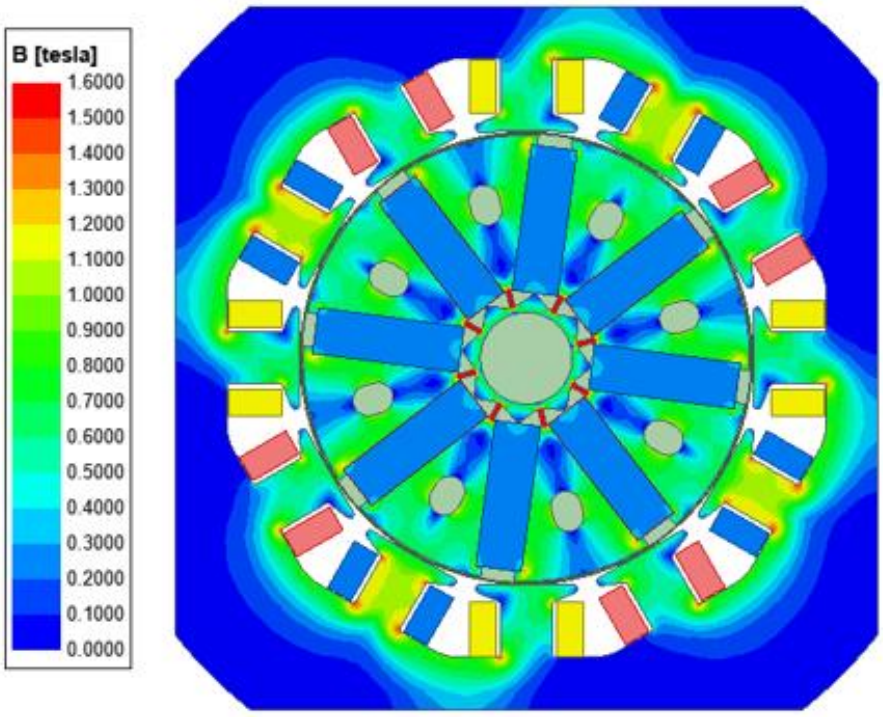

Figure 3.19 : The magnetic flux density distribution of the designed IPMSM model.

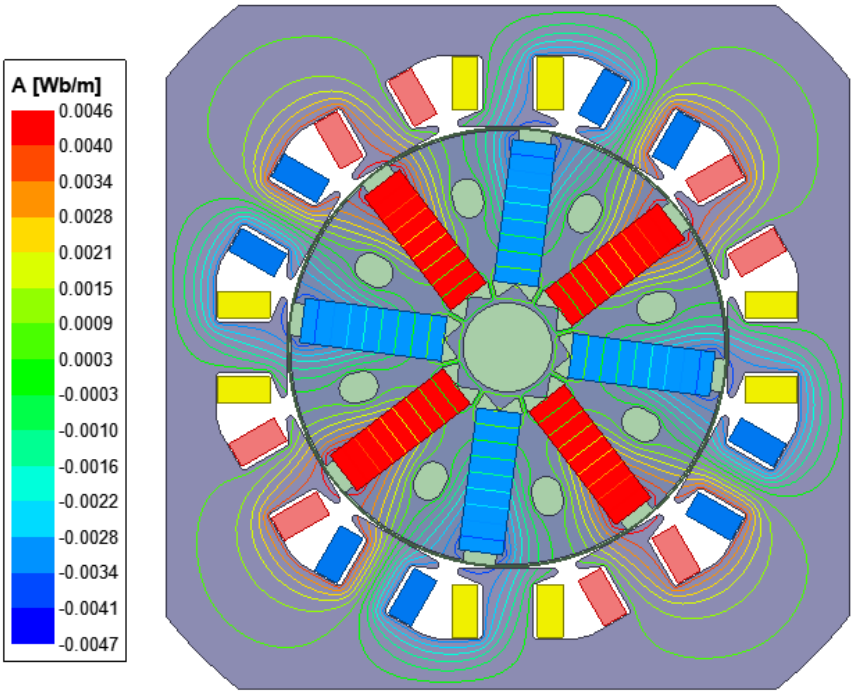

Figure 3.20 : The equi-flux distribution of the designed IPMSM model.

Magnetic analysis are performed at no-load condition to provide the created total magnetic field by permanent magnets without stator effect. In this way, the interaction between permanent magnets and the stator-rotor magnetic circuit is examined. The results of the magnetic analysis performed under no load condition are demonstrated that the flux distributions are smooth and magnetic flux density distribution is not exceeded the Bst. Peak < 1.7 T limit value. Accordingly, it is concluded that the flux density is high where the area is rotor shape around magnets resulting from permanent magnets.

3.2.3.3 Other results

In this stage, open circuit back EMF analysis is performed to obtain line peak to peak, line rms, phase peak to peak and phase rms values in Maxwell 2D. Open circuit analysis are carried out under 1000 rpm to obtain easy transition to degree/per second. Line and phase voltages are presented in Figure 3.21 and Figure 3.22, respectively.

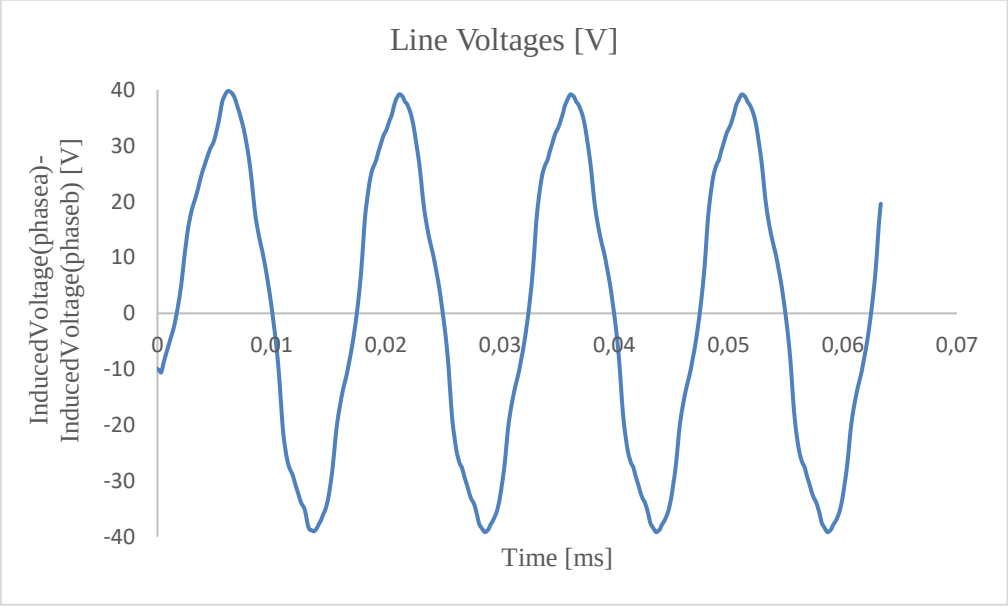

Figure 3.21 : The designed motor line voltages.

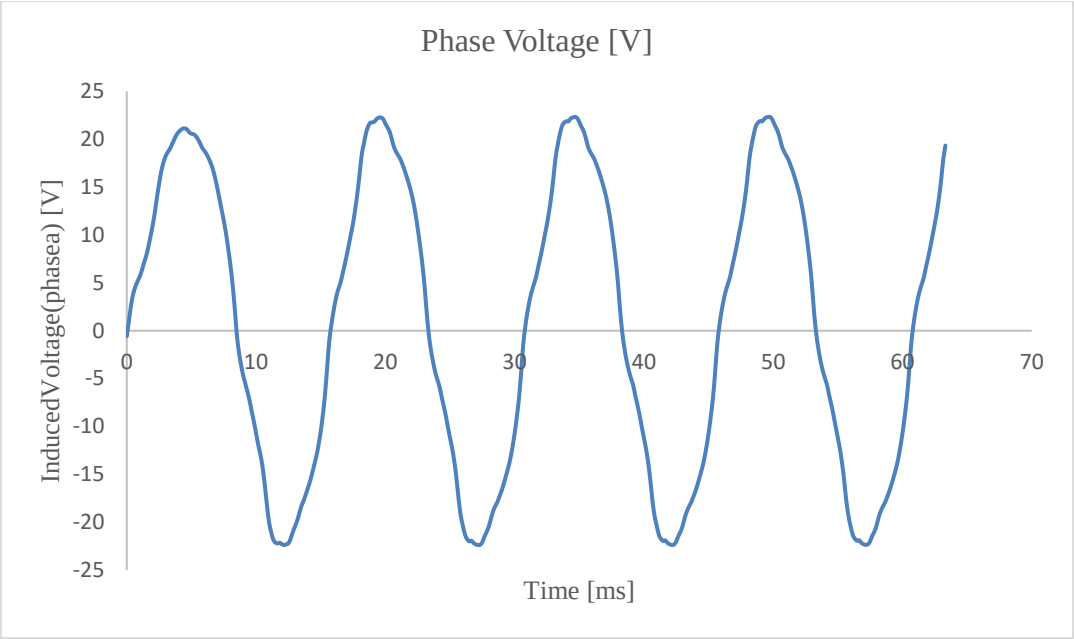

Figure 3.22 : The designed motor phase voltages.

In line with these curves obtained, line peak to peak, line rms, phase peak to peak and phase rms values that form the basis of the back EMF scenario are obtained and shown in the Table 3.6.

Table 3.6: Back EMF scenario.

Back EMF Scenario
Line peak to peak voltage: 78.9931 [V]
Line rms voltage: 27.1225 [V]
Phase peak to peak voltage: 44.7196 [V]
Phase rms voltage: 15.6474 [V]

After meausrement of the line-to-line and phase voltages, equivalent parameter determination, which primarily show the characteristics of the motor, is performed. Because, today's advanced motor control algorithms are demanded more exactly motor electrical parameters such as L_d (d axis synchronous inductance), L_q (q axis synchronous inductance) and k_e (back EMF constant). Electrical parameters are required to achieve the desired closed loop performance and for BEMF observer constants by setting the PI controller gains. Necessary equation for back EMF coefficient (k_e) [V.s/rad] and torque coefficient (k_t) which are the quantities to be controlled for the motor to be optimized, are given in Table 3.7.

Table 3.7: Back EMF and torque coefficients.

Back EMF and Torque Coefficients
Back EMF Coefficient (k_e) : 0,377
Torque Coefficient (k_t) : 0,562

The designed motor phase currents, phase flux linkages, phase voltages and core losses on rotor and stator are presented in below at 780 rpm in Figure 3.23, Figure 3.24, Figure 3.25, and Figure 3.26, respectively.

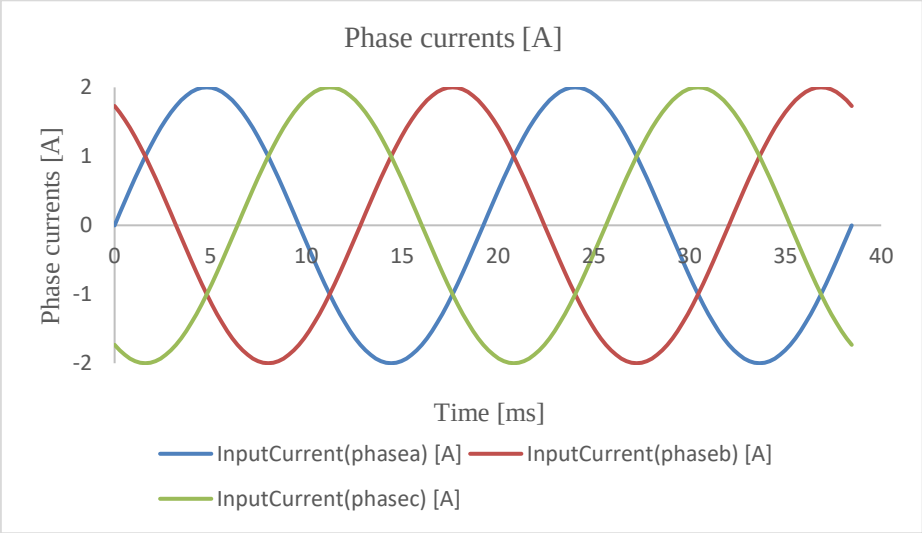

Figure 3.23 : The designed motor phase currents.

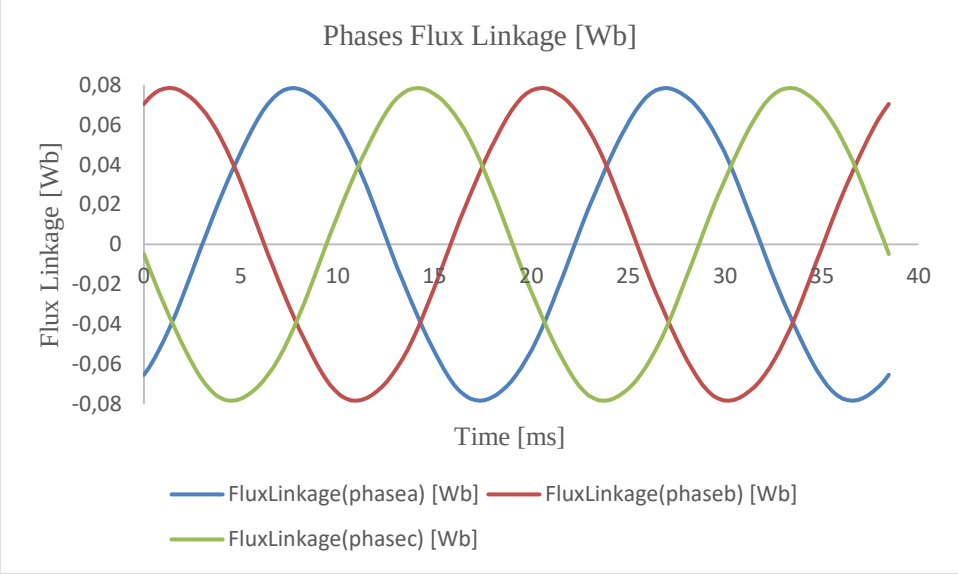

Figure 3.24 : The designed motor phase flux linkages.

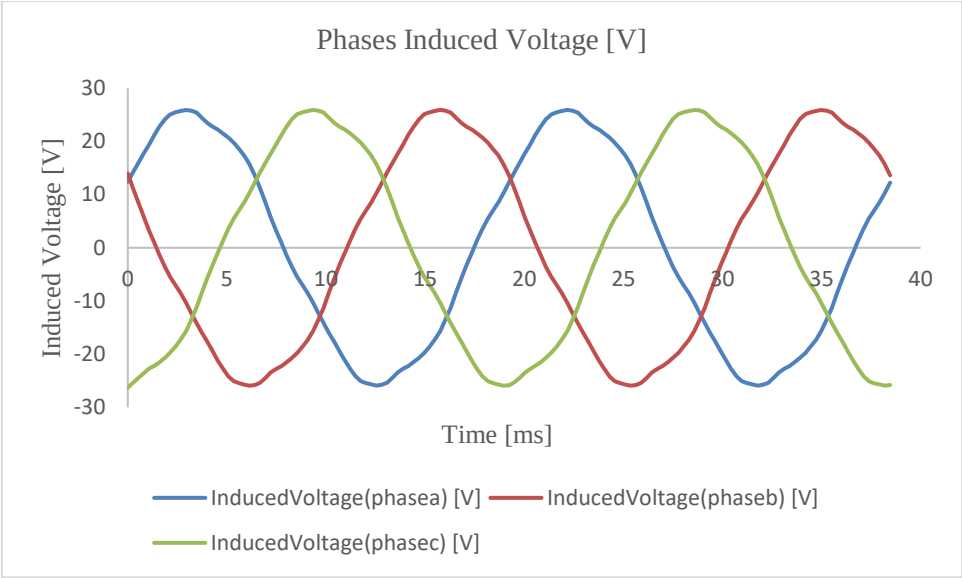

Figure 3.25 : The designed motor phase voltages.

Figure 3.26 : The designed motor core losses on rotor and stator.

Throughthout this study, since analysis and examinations are performed under constant frequency, the losses are given only for the existing motor, the evaluation of the losses for optimization is not given priority.

In this section, the simulation results of the designed motor are shared. The data obtained simulation results will be compared with the real sample motor results, and model validation will be checked based on the reliability of the simulation results.

3.3 Comparison of Real Sample and Designed Motor Results

In this section, the disturbance effect, finite element modeling for transient analysis, simulation and experimental results of the real sample motor and designed motor are compared. Actually, the data obtained simulation results is compared with the real sample motor simulation results, and model validation is checked based on the reliability of the simulation results. Taking into consideration the requirements of the washing machine in order to fully evaluate the designed motor performance both real sample and designed motor results are compared under different scenarios including cogging torque, open circuit back EMF and on load. According to the results given in previous section are used for evaluating and interpreting the design verification.

The results of the finite element modeling for transient analysis, disturbance effect, and other simulation results are compared for the existing model and the designed model, respectively.

Firstly; the existing and the designed motor finite element modeling transient analysis results are confirmed each other in terms of magnetic flux density.

The most crucial parameter to be evaluated while giving the results of the motor's disturbance effect is cogging torque. The peak to peak cogging torque values are compared both the existing model and the designed model in Table 3.8.

Table 3.8: Peak to peak cogging torque comparison.

Contents	Peak to Peak Cogging Torque Result [mNm]
The Existing Model	81,12
The Designed Model	86,62

It is observed that the cogging torque peak to peak values are close to each other.

Another important parameter to be evaluated while giving the results of the motor's disturbance effect is torque ripple. The obtained torque ripple simulation results are confirmed each other.

On the other hand, when the back EMF scenarios are compared both the existing model and the designed model according to the simulation results, line peak to peak and phase peak to peak voltages are so close and are confirmed each other.

3.4 Interpretation of Results

Consequently, determining the disturbance effects which are obtained from analysis results and the goal of improving motor performance is realized on the basis of these compared data.

Considering all compatible results from the disturbance effect, finite element modeling for transient analysis and the other simulation results of the designed motor validation is proved. The simulation results are performed with the designed model is found to be reliable when is compared with the existing motor. Optimization process is continued via this model.

4. DESIGN OPTIMIZATION

The first stage of parametric modeling is to determine the motor geometric parameters that will most affect the quantities which are the optimization targets and to evaluate the different geometric optimization methods used for this application in the related literature. In order to be able to evaluate and interpret the effects of geometric parameters on motor performance more comprehensively, many studies have been presented in the literature related with the optimization of geometric parameters. It is proven with many researches that the disturbance effects on the machine are reduced by the geometric improvements on motor design. For this purpose, the rotor of the designed motor is completely parametrically modeled.

First of all, the parametric analysis and design optimization are proposed on the influence of several geometrical parameters which are the rotor pole face, magnet opening, magnet thickness, magnet length, air gap and rotor slit the investigated spoke type IPMSM. The parametric analysis is configured with definition reasonable ranges for each selected geometrical variable without ignoring the IPMSM motor requirements of the washing machine.

After creating parametric model, the effects of determined rotor geometrical parameters on cogging torque and torque ripple are investigated comprehensively. Taking into consideration the requirements of the washing machine in order to fully evaluate the infuence of the parameter on motor performance, results which are obtained from each paramater change are evaluated under different scenarios including cogging torque, open circuit back EMF and on load. Considering to the analyzes performed with the parametric model, the parameters most affecting the cogging torque value are rotor pole face and magnet length.

It is obvious that the analysis results are obtained from parametric modeling are the basic building blocks for the genetic algorithm. In line with the evaluation of the parametric analysis results, the most effective parameters are chosen on disturbance effect and determined ranges for each parameter are reconstructed considering the

washing machine application motor requirements and restrictions. The computational complexity and calculation time for the genetic algorithm optimization is reduce with this approach.

In second part, genetic algorithm optimization is performed with several geometrical parameters which are the rotor pole face, magnet opening, magnet thickness, magnet length and air gap parameters the investigated spoke type IPMSM with appropriate intervals and results are obtained as minimizing the cogging torque. In order to achieve the most proper design, the parametric analysis results and genetic algorithm results are evaluated both the individual and the combined. From the analysis results on the parametric model, the approach of which parameter is effective on the cogging torque and the results that give the lowest cogging torque value in the genetic algorithm are combined and the number of models obtained is reduced to the best two design.

Since the prototyping of optimized motor is aimed when evaluating the appropriate results from the genetic algorithm are taken into account the production capabilities. Disturbance effect, finite element modeling for transient analysis and the other simulation results are compared for the two best models obtained as a result of genetic algorithm and parametric optimization. According to these results, the design of the motor to be prototyped is decided. After this step, a prototype is constructed base on the best design.

4.1 Parametric Modeling

In this chapter is focused on constructing a parametric model using the motor design validated in the previous section. The first stage of parametric modeling is to determine the motor geometric parameters that will most affect the quantities which are the optimization targets, similar to the design section, and to evaluate the different geometric optimization methods used for this application in the related literature. In order to be able to evaluate and interpret the effects of geometric parameters on motor performance more comprehensively, many studies have been presented in the literature related with the optimization of geometric parameters.

Recently, a various number of methods have been proposed by researchers to eliminate disturbance effects. It is proven with many researches that the disturbance effects on the machine are reduced by the geometric improvements on motor design [7].

Besides, it has been determined that magnet selection and magnet geometry had an influence on cogging torque. Especially, it has been shown the magnet embrace was an effective parameter directly on the cogging torque [11]. In [13], an optimization has been proposed in order to reduce the torque ripple for the interior permanent magnet (IPM) motor via permanent magnet (PM) and ferromagnetic material (FM) part of the rotor design. These different materials, referred to as PM, FM and air, were formulated to minimize torque ripple under volume constraints. It has been emphasised that changing rotor permanent magnet structure was directly associated with reluctance torque which was lead to increase torque ripple [14]. An optimization has been implemented regarding to the rotor shape to improve performance of IPM motor.

On the other hand, it has been proposed the various barrier shape designs for IPMSM used in a direct drive washing machine to reduce high magnetic torque which was inversely proportional with torque ripple at low speeds corresponding to the wash cycle [15]. In [16], the rotor of V type IPMSM has been parametrically modeled to ensure the average torque, torque ripple, cogging torque, efficiency optimization. As a result of the analyzes carried out for the selected parameters, it was determined which parameter had more effect on the target size for improvement. By limiting the results obtained within the limits and constraints, the most suitable design parameters have been reached.

Moreover, in [19], in order to minimize the cogging torque provided that the same output power, torque or current, rotor structure has been changed in terms of thickness and shape of the magnets and pole span by using a genetic algorithm optimization tool. In addition; genetic algorithm has been used for minimum cogging torque requirement by changing magnet shape [20]. For this purpose, permanent magnet pole slice arrangement was performed with optimization tool in order to be able to define exact values.

According to the aforementioned literature researches, it is determined that the rotor geometric structure optimization is the most effective in order to achieve cogging torque, torque ripple and back EMF harmonics improvement. For this purpose, the rotor of the designed motor is completely parametrically modeled.

In this study, the parametric analysis and design optimization are proposed on the influence of several geometrical parameters which are the rotor pole face, magnet

opening, magnet thickness, magnet length, air gap and rotor slit the investigated spoke type IPMSM. One of the reason why the selected parameters include especially magnets, magnetomotive force is created by permanent magnets. Also, permanent magnet geomery is directly affected the cogging torque [16]. The parametric analysis is configured with definition reasonable ranges for each selected geometrical variable without ignoring the IPMSM motor requirements of the washing machine.

4.2 Parametric Optimization Results

In this part, the effects of determined rotor geometrical parameters on cogging torque and torque ripple are investigated comprehensively. Disturbance effect and simulation results are presented and discussed as similar with Section 3.1.2 and Section 3.2.3.

Taking into consideration the requirements of the washing machine in order to fully evaluate the infuence of the parameter on motor performance, results which are obtained from each paramater change are evaluated under different scenarios including cogging torque, open circuit back EMF and on load.

In order to achieve the most proper design, the parametric analysis results are evaluated both the individual and the combined by considering on the interaction effects of depicted parameters.

It is obvious that the analysis results to be obtained by parametric modeling are the basic building blocks for the genetic algorithm. In next part, in line with the evaluation of the parametric analysis results, the most effective parameters will be chosen on disturbance effect and determined ranges for each parameter will be reconstructed considering the washing machine application motor requirements and restrictions. It is aimed to reduce the computational complexity and calculation time for the genetic algorithm optimization.

4.2.1 Cogging torque results

For this part, the most crucial criteria to be evaluated while giving the results of the the determined rotor geometrical parameters on disturbance effect is the cogging torque.

Cogging torque analysis is performed at no-load condition in Maxwell 2D as similary mentioned in previous sections. In this case, the cogging torque period is calculated to

be 15 degree. Since the speed is held constant at 1.0 deg/sec, 15 degree is corresponded to be 15 second.

In this part, the parametric analysis results are presented for the influence of cogging torque for each parameter which are the rotor pole face, magnet opening, magnet thickness, magnet length, air gap and rotor slit, respectively. Since it is a trade secret, geometrical dimensions are not shared in the analysis results given in this section. In order to better interpret the analysis results, the minimum and maximum points of the defined intervals on the result graphs are specified for each geometric quantity and the increase and decrease of these values within the defined interval are explained.

The parametric analysis results are presented for the influence of cogging torque for the rotor pole face parameter as below in Figure 4.1. In this analysis, all parameters except the rotor pole face were kept the same as the existing motor.

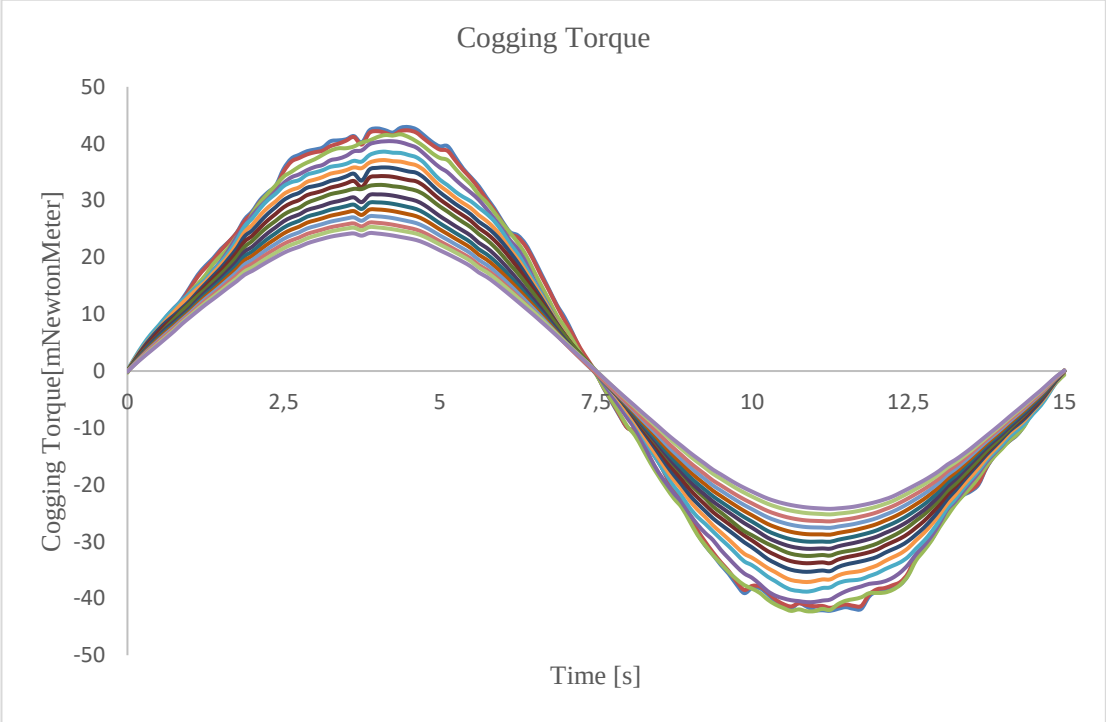

Figure 4.1 : Cogging torque change for the different rotor pole face length.

The top curve is represented the existing motor without a pole face. The bottom curve is represented the highest pole face value. The pole face value was solved by increasing in the given range.

The effect of the rotor pole face on the peak to peak cogging torque value and the cogging /nominal ratio change are given in the Figure 4.2, where nominal term is corresponded to the cogging torque value of the real sample current motor.

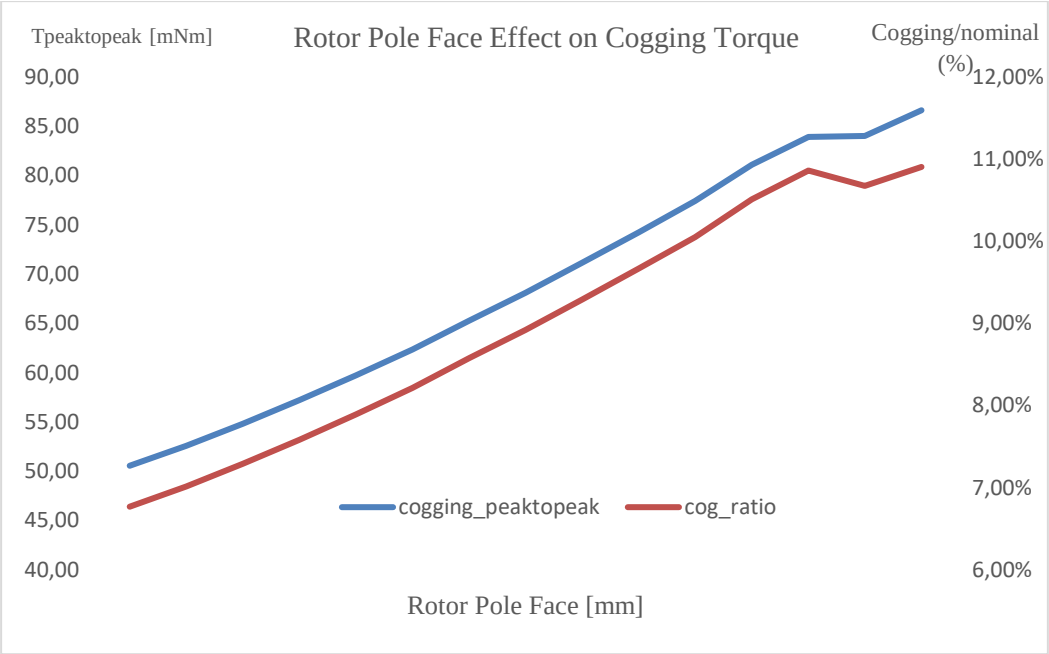

Figure 4.2 : The effect of the rotor pole face on the peak to peak cogging torque value and the cogging /nominal ratio change.

The rotor pole face value is given by decreasing from left to right. The leftmost dot represents the highest pole face value, and the rightmost dot represents the lowest pole face value.

The effect of the rotor pole face on the peak to peak and average cogging torque are given in the Figure 4.3.

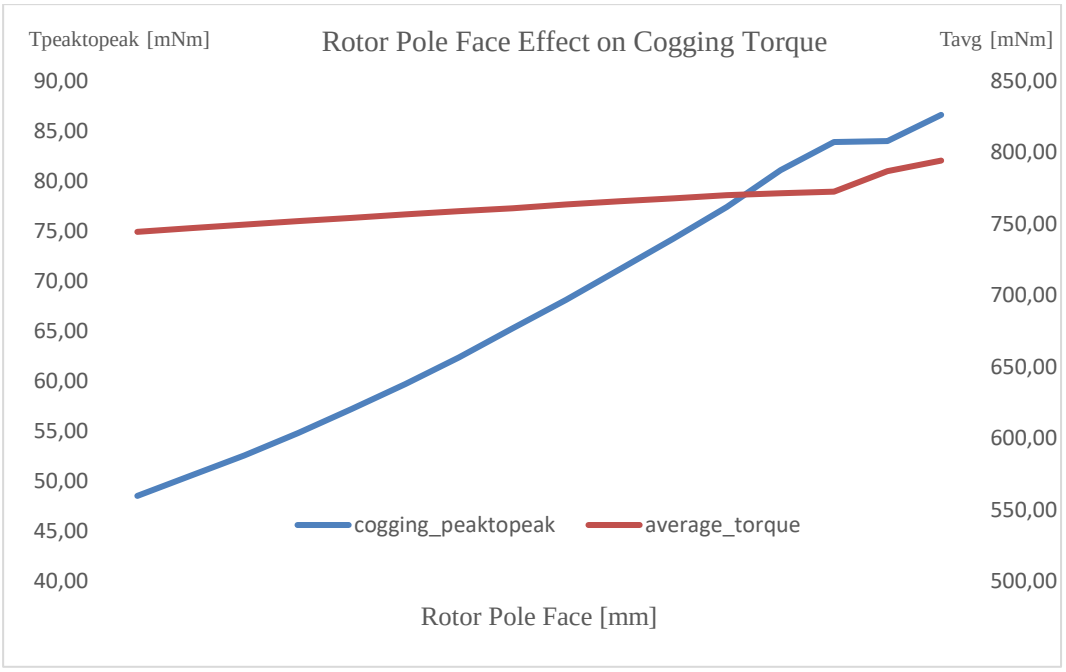

Figure 4.3 : The effect of the rotor pole face on the peak to peak and average cogging torque.

The rotor pole face value is given by decreasing from left to right. The leftmost dot represents the highest pole face value, and the rightmost dot represents the lowest pole face value.

As a result of the analysis, when the change of the rotor pole face parameter in specified range on the cogging torque is examined, it is observed that this parameter is quite effective on the cogging torque. Increase in rotor pole face parameter is lead to cogging torque decrease. Minimum cogging torque value is obtained at maximum pole face length which is corresponding to the lowest cogging torque graph.

The parametric analysis results are presented for the influence of cogging torque for the magnet opening parameter as below in Figure 4.4. In this analysis, all parameters except the magnet opening and rotor pole face were kept the same as the existing motor. The rotor pole face value was analyzed as maximum value.

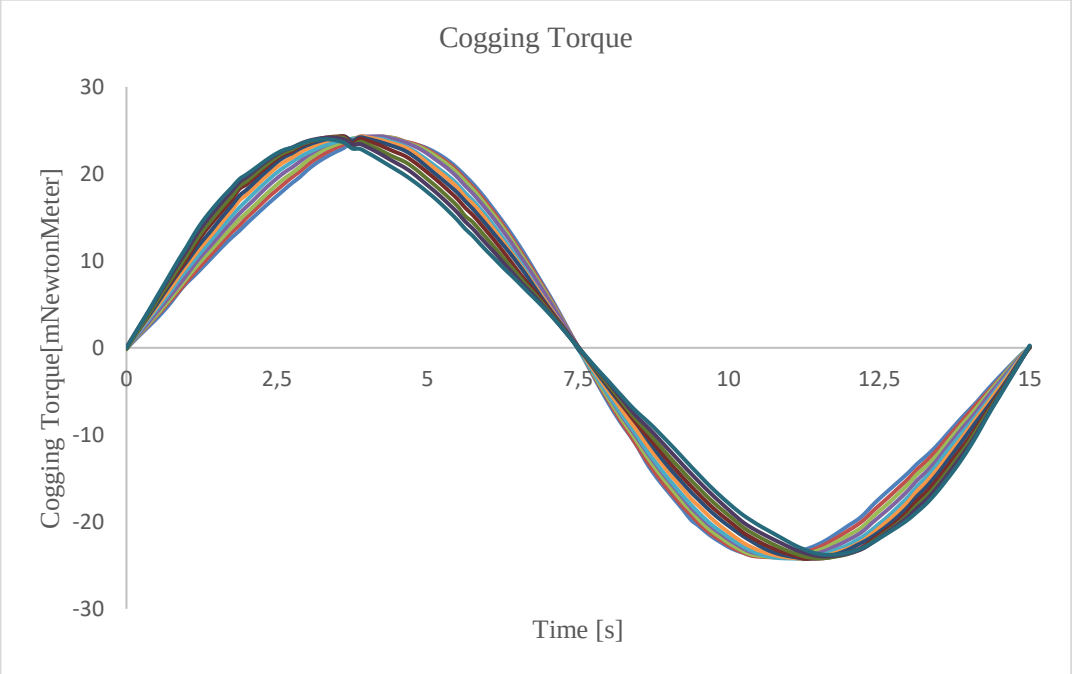

Figure 4.4 : The influence of cogging torque for the magnet opening.

The top curve is represented the highest magnet opening length. The bottom curve is represented the lowest magnet opening length. The magnet opening length was solved by increasing in the given range.

The effect of the magnet opening on the peak to peak cogging torque value and the cogging /nominal ratio change are given in the Figure 4.5, where nominal term is corresponded to the cogging torque value of the real sample current motor.

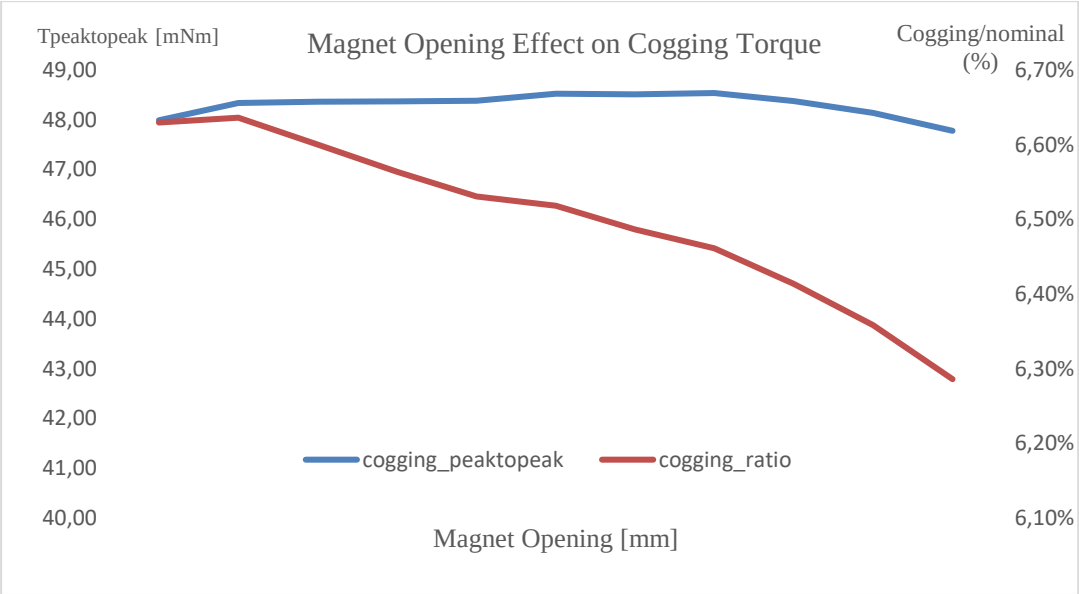

Figure 4.5 : The effect of the magnet opening on the peak to peak cogging torque value and the cogging /nominal ratio change.

The magnet opening length is given by increasing from left to right. The leftmost dot represents the lowest magnet opening length, and the rightmost dot represents the highest magnet opening length.

The effect of the magnet opening on the peak to peak and average cogging torque are given in the Figure 4.6.

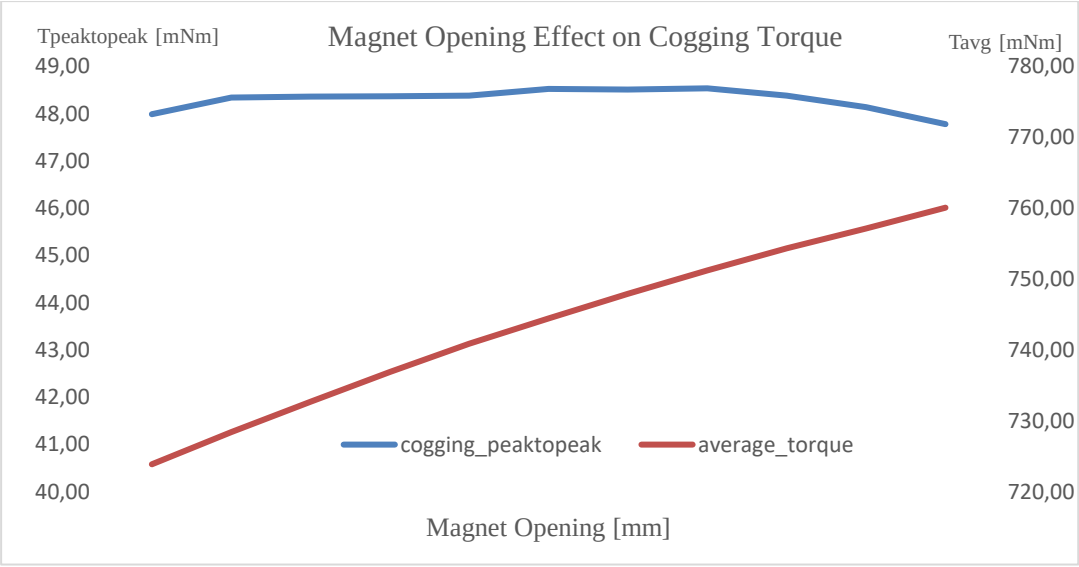

Figure 4.6 : The effect of the magnet opening on the peak to peak and average cogging torque.

The magnet opening length is given by increasing from left to right. The leftmost dot represents the lowest magnet opening length, and the rightmost dot represents the highest magnet opening length.

As a result of the analysis, when the change of the magnet opening parameter in specified range on the cogging torque is examined, it is observed that this parameter is effective on the cogging torque. Increase in magnet opening parameter is lead to cogging/nominal ratio decrease.

The parametric analysis results are presented for the influence of cogging torque for the magnet thickness parameter as below in Figure 4.7. In this analysis, all parameters except the magnet thickness and rotor pole face were kept the same as the existing motor. The rotor pole face value was analyzed as maximum value.

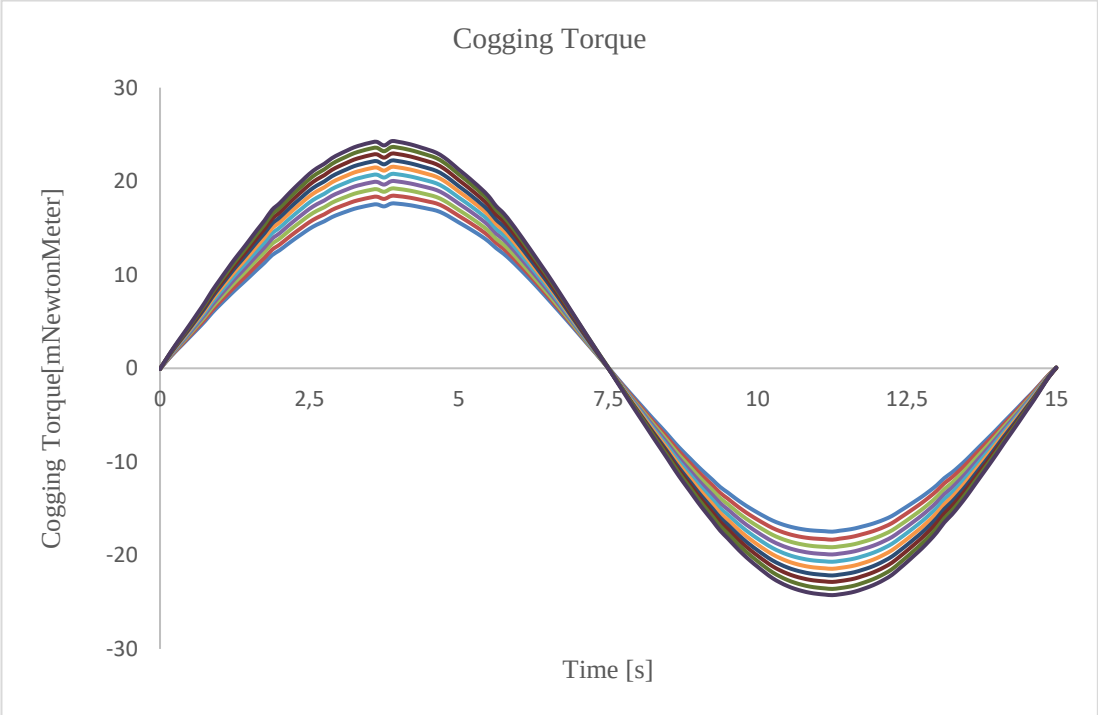

Figure 4.7 : The influence of cogging torque for the magnet thickness.

The top curve is represented the highest magnet thickness length. The bottom curve is represented the lowest magnet thickness length. The magnet thickness length was solved by increasing in the given range.

The effect of the magnet thickness on the peak to peak cogging torque value and the cogging /nominal ratio change are given in the Figure 4.8, where nominal term is corresponded to the cogging torque value of the real sample current motor.

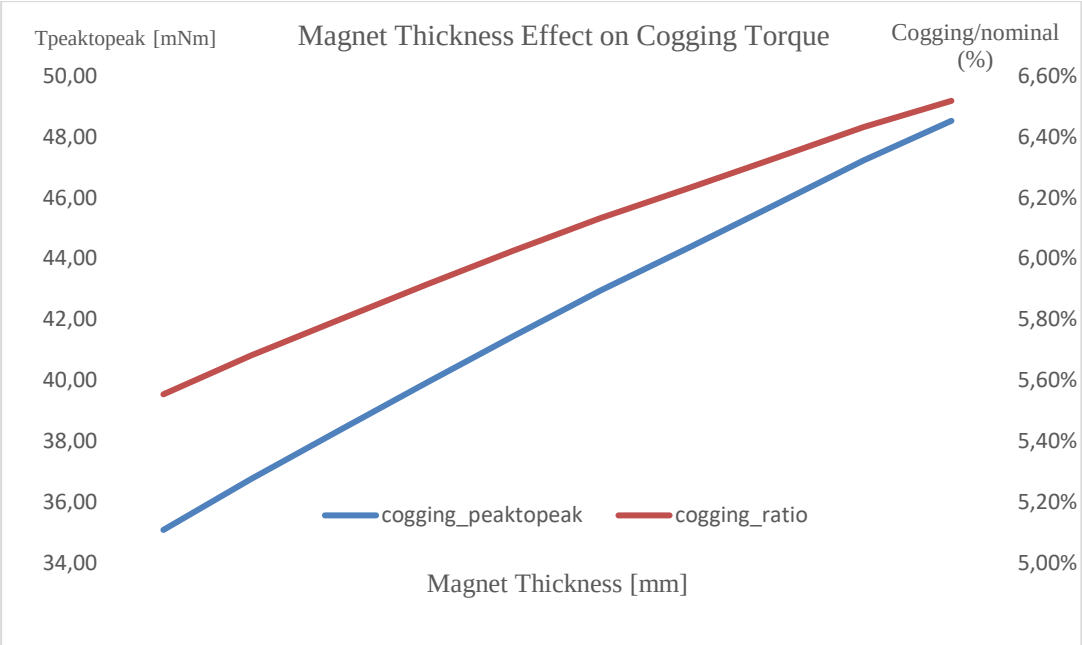

Figure 4.8 : The effect of the magnet thickness on the peak to peak cogging torque value and the cogging /nominal ratio change.

The magnet thickness length is given by increasing from left to right. The leftmost dot represents the lowest magnet thickness length, and the rightmost dot represents the highest magnet thickness length.

The effect of the magnet thickness on the peak to peak and average cogging torque are given in the Figure 4.9.

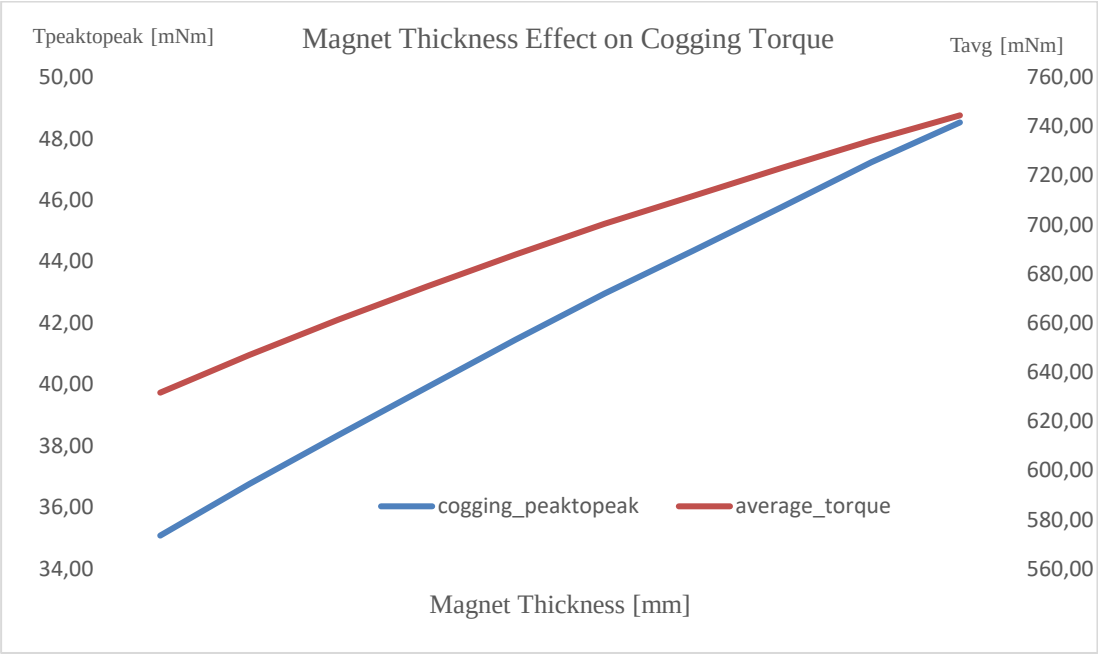

Figure 4.9 : The effect of the magnet thickness on the peak to peak and average cogging torque.

The magnet thickness length is given by increasing from left to right. The leftmost dot represents the lowest magnet thickness length, and the rightmost dot represents the highest magnet thickness length.

As a result of the analysis, when the change of the magnet thickness parameter in specified range on the cogging torque is examined, it is observed that this parameter is quite effective on the cogging torque. Increase in rotor magnet thickness parameter is lead to cogging torque increase also.

The parametric analysis results are presented for the influence of cogging torque for the magnet length and air gap parameters as below in Figure 4.10. Since changes in magnet length directly correspond to air gap change, the evaluation of these parameters is given together considering their interactions with each other. In this analysis, all parameters except the magnet length, air gap and rotor pole face were kept the same as the existing motor. The rotor pole face value was analyzed as maximum value.

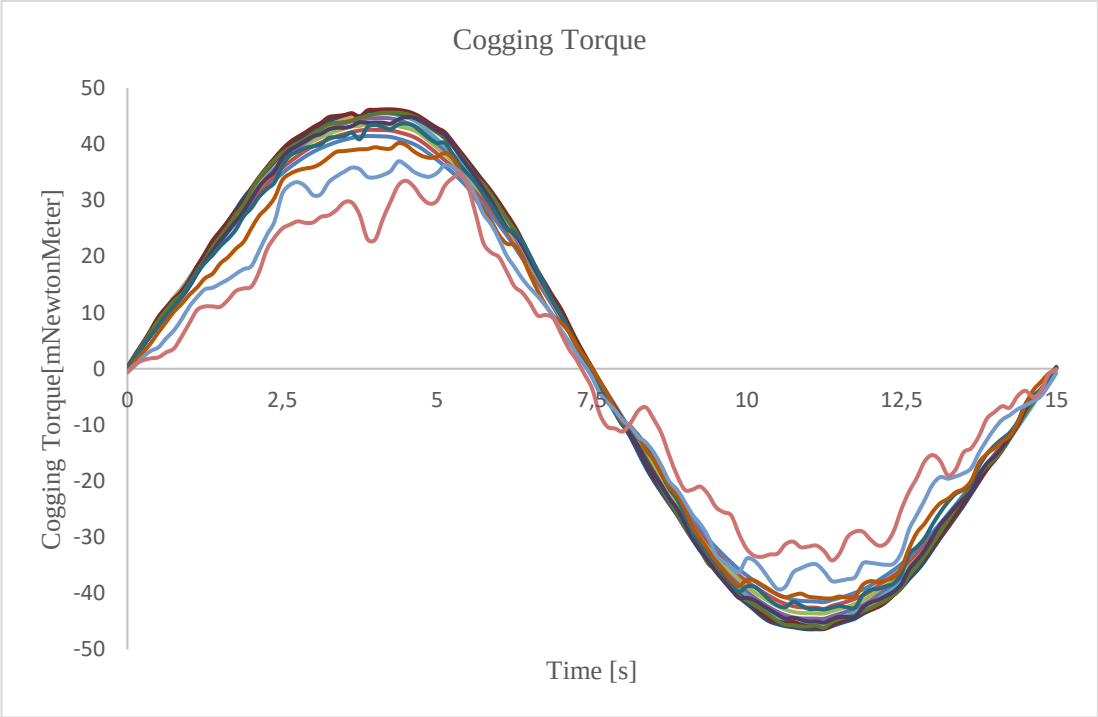

Figure 4.10 : The influence of cogging torque for the air gap.

The top curve is represented the higher air gap and lower magnet length when compared to the existing motor. The bottom curve is represented the higher magnet length and lower air gap. The magnet length was solved by decreasing and the air gap was solved by increasing in the given range.

The effect of the magnet length and air gap on the peak to peak cogging torque value and the cogging /nominal ratio change are given in the Figure 4.11 and Figure 4.12, respectively where nominal term is corresponded to the cogging torque value of the real sample current motor.

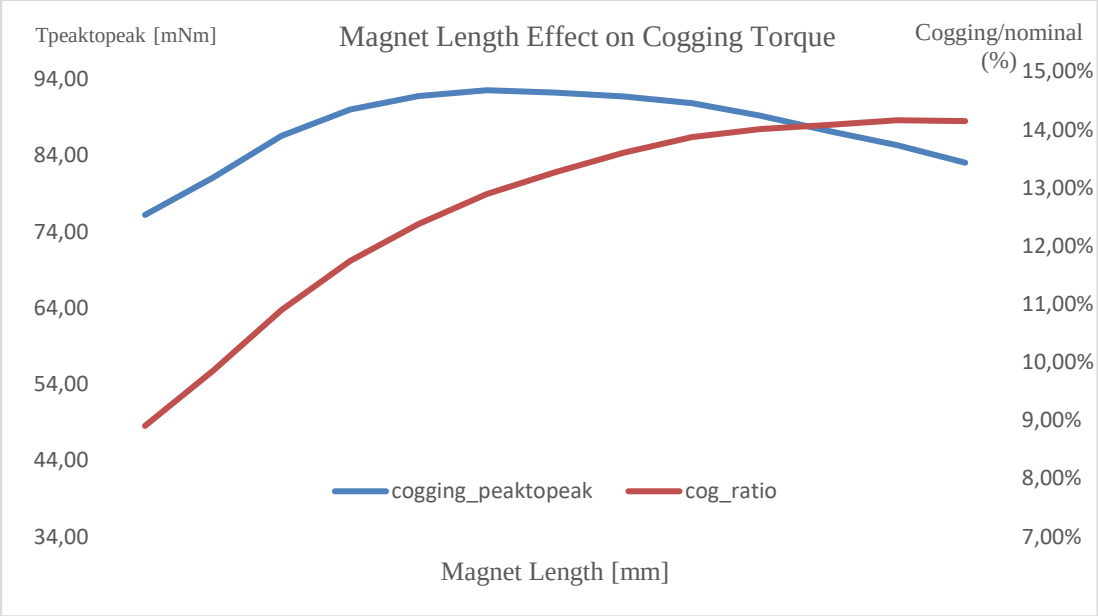

Figure 4.11 : The effect of the magnet length on the peak to peak cogging torque value and the cogging /nominal ratio change.

The magnet length is given by decreasing from left to right. The leftmost dot represents the highest magnet length, and the rightmost dot represents the lowest magnet length.

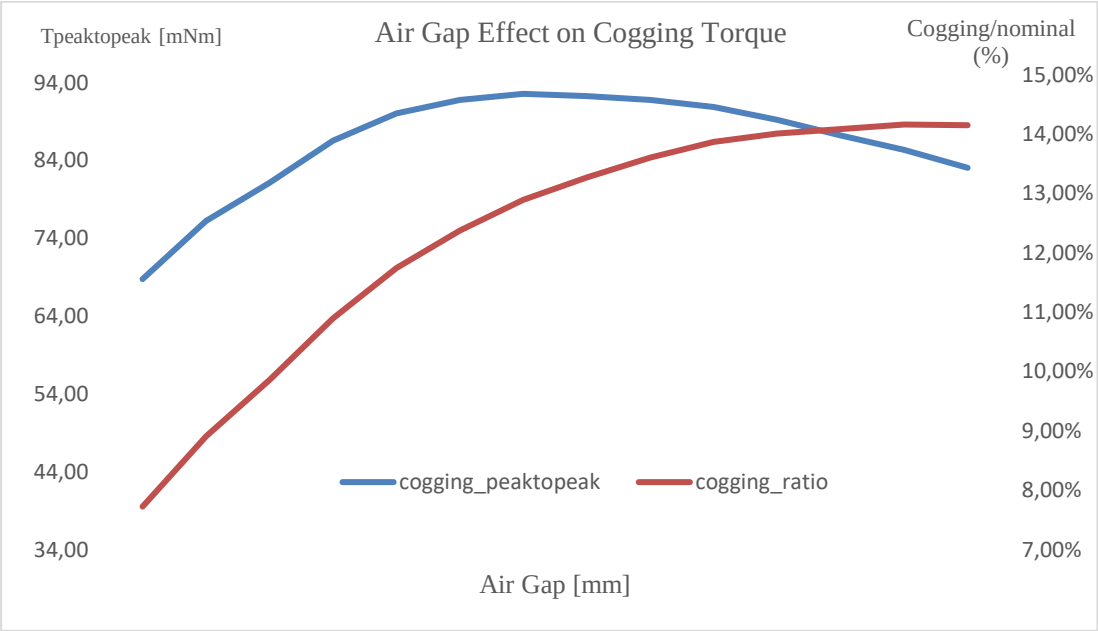

Figure 4.12 : The effect of the air gap on the peak to peak cogging torque value and the cogging /nominal ratio change.

The air gap is given by increasing from left to right. The leftmost dot represents the lowest air gap, and the rightmost dot represents the highest air gap.

The effect of the magnet length and air gap on the peak to peak and average cogging torque are given in the Figure 4.13 and Figure 4.14, respectively.

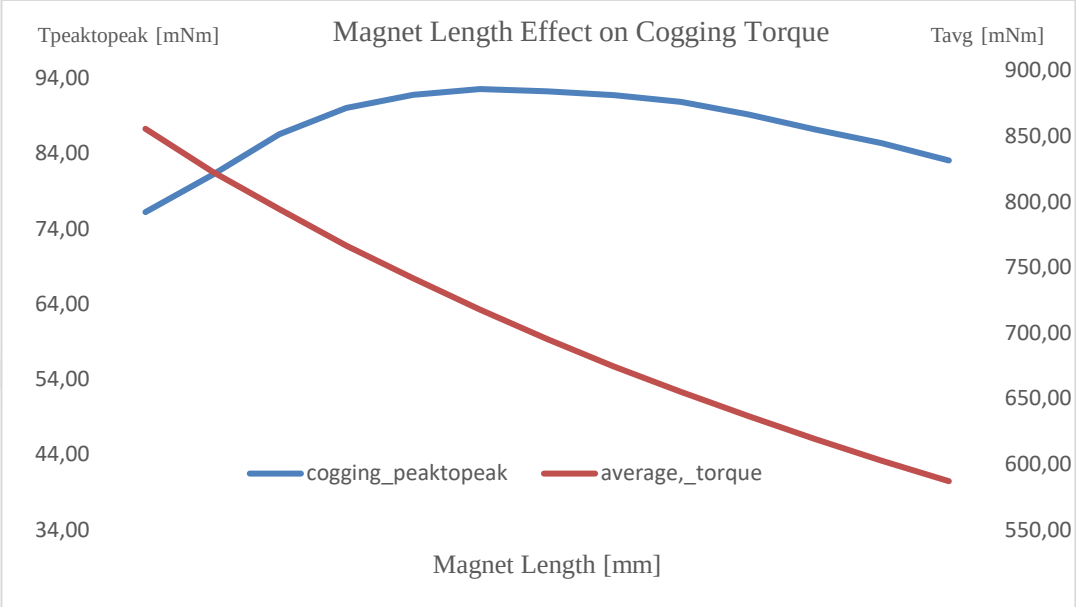

Figure 4.13 : The effect of the magnet length on the peak to peak and average cogging torque.

The magnet length is given by decreasing from left to right. The leftmost dot represents the highest magnet length, and the rightmost dot represents the lowest magnet length.

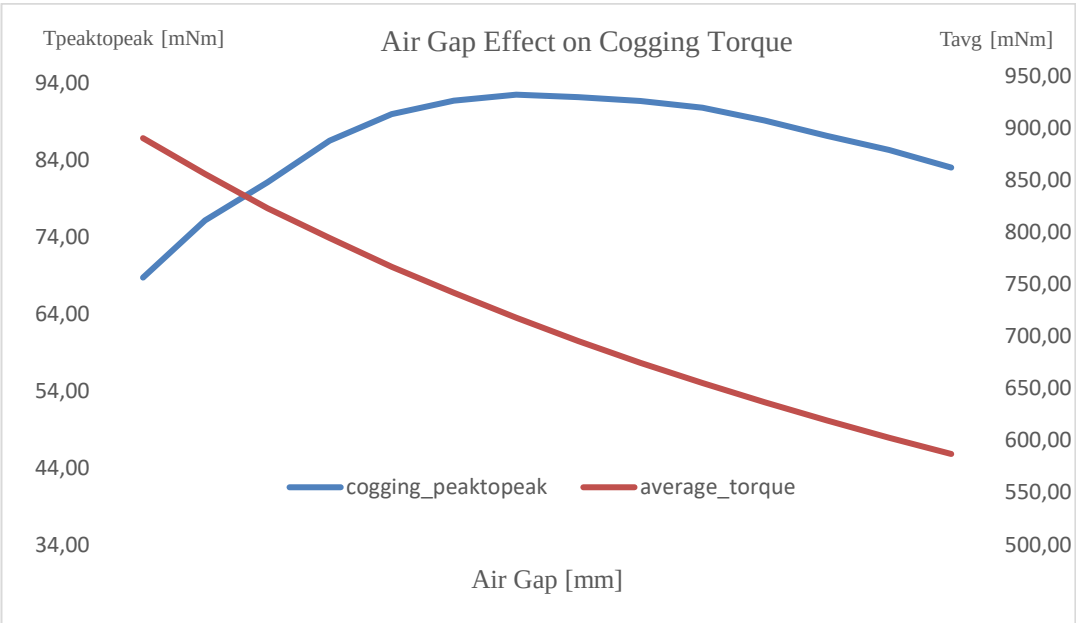

Figure 4.14 : The effect of the air gap on the peak to peak and average cogging torque.

The air gap is given by increasing from left to right. The leftmost dot represents the lowest air gap, and the rightmost dot represents the highest air gap.

As a result of the analysis, when the change of the air gap in specified range on the cogging torque is examined, it is observed that this parameter is quite effective on the cogging torque. The decrease of the air gap below a certain value caused a decrease in the cogging torque value, but also increased the ripple ratio. In addition, since reducing the air gap below a specific value affects the producibility, this case is taken into account in the changes applied for this parameter.

The parametric analysis results are presented for the influence of cogging torque for the rotor slit parameter as below in Figure 4.15. The effect of this parameter is evaluated as structure with and without rotor slit. Since the real sample motor has rotor slit, the effect of cogging on torque is given for the slitless construction. In this analysis, all parameters except the rotor slit and rotor pole face were kept the same as the existing motor. The rotor pole face value was analyzed as maximum value.

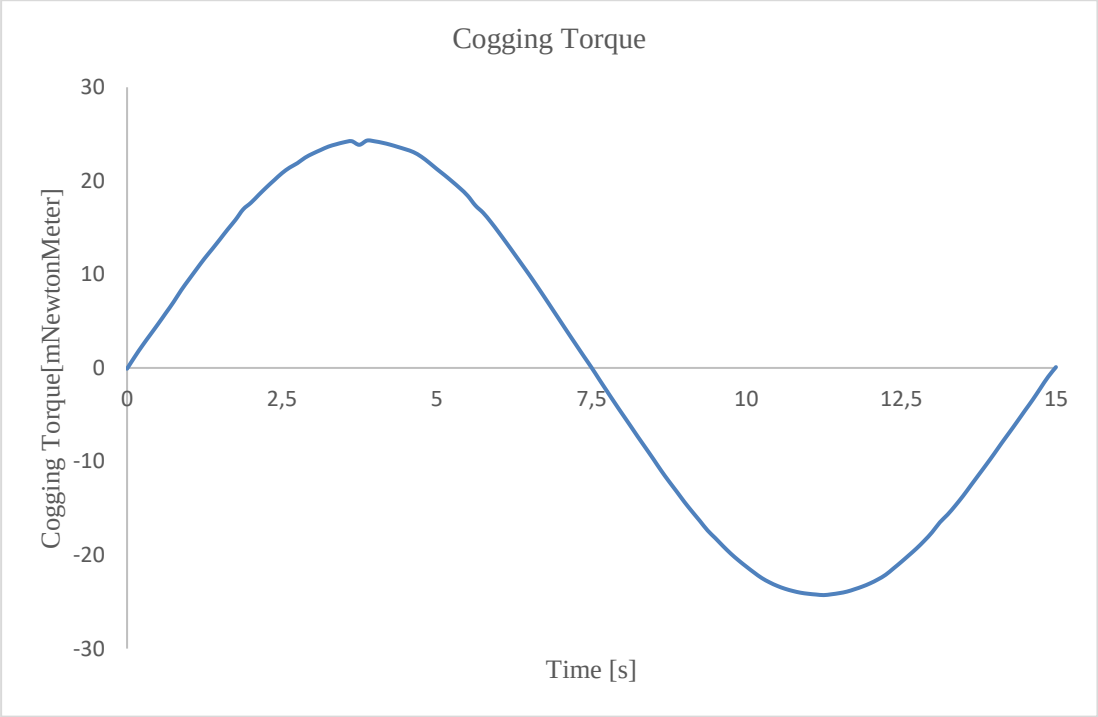

Figure 4.15 : The cogging torque for the rotor slitless structure.

As a result of the analysis, when the change of the rotor slit parameter in specified range on the cogging torque is examined, it is observed that the slitless structure has a lower cogging torque value. However, since the slit structure is preferred for applications with high speed requirements, only the effect of this parameter on the

cogging torque is shown. This parameter is not included in the genetic algorithm optimization process.

4.2.2 Torque ripple results

For this part, the most crucial criteria to be evaluated while giving the results of the the determined rotor geometrical parameters on disturbance effect is the torque ripple. The parametric analysis results are presented for the influence of torque ripple for each parameter which are the rotor pole face, magnet opening, magnet thickness, magnet length, and air gap, respectively. Since it is a trade secret, geometrical dimensions are not shared in the analysis results given in this section. In order to better interpret the analysis results, the minimum and maximum points of the defined intervals on the result graphs are specified for each geometric quantity and the increase and decrease of these values within the defined interval are explained.

The parametric analysis results are presented for the change of the rotor pole face parameter according to the motor torque changing depending on rotor position as below in Figure 4.16. In this analysis, all parameters except the rotor pole face were kept the same as the existing motor.

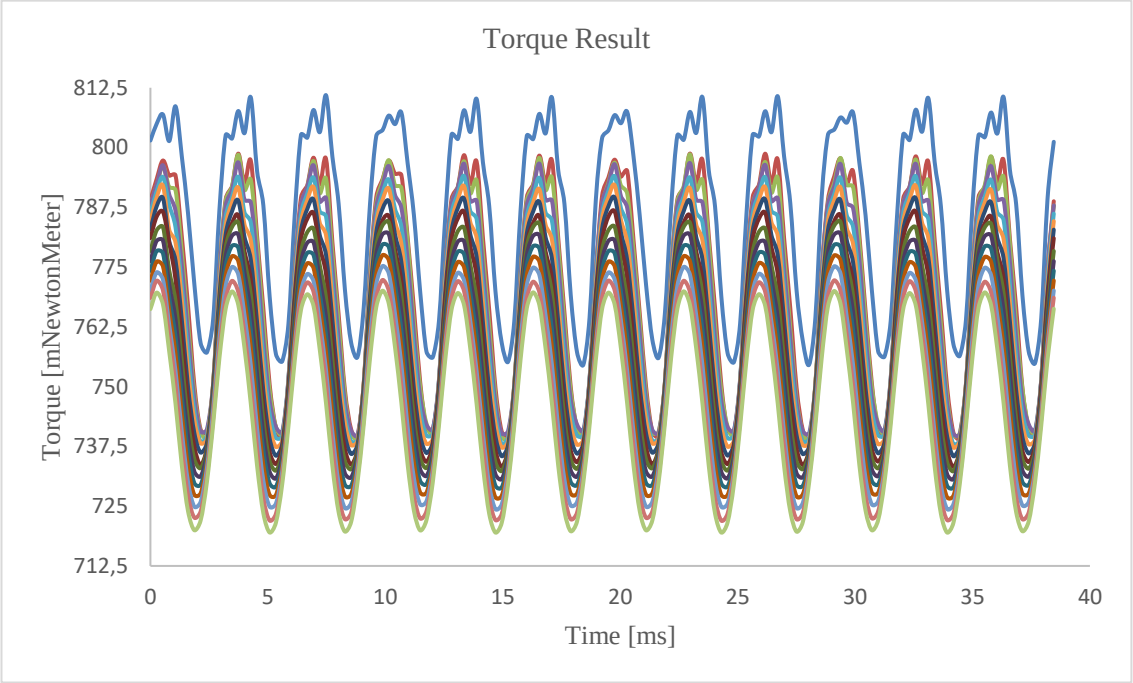

Figure 4.16 : The influence of the rotor pole face change on motor torque ripple result.

The top curve is represented the existing motor without a pole face. The bottom curve is represented the highest pole face value. The pole face value was solved by increasing in the given range.

The parametric analysis results are presented for the change of the rotor pole face parameter on back EMF coefficient (k_e) and torque coefficient (k_t) results as below in Figure 4.17.

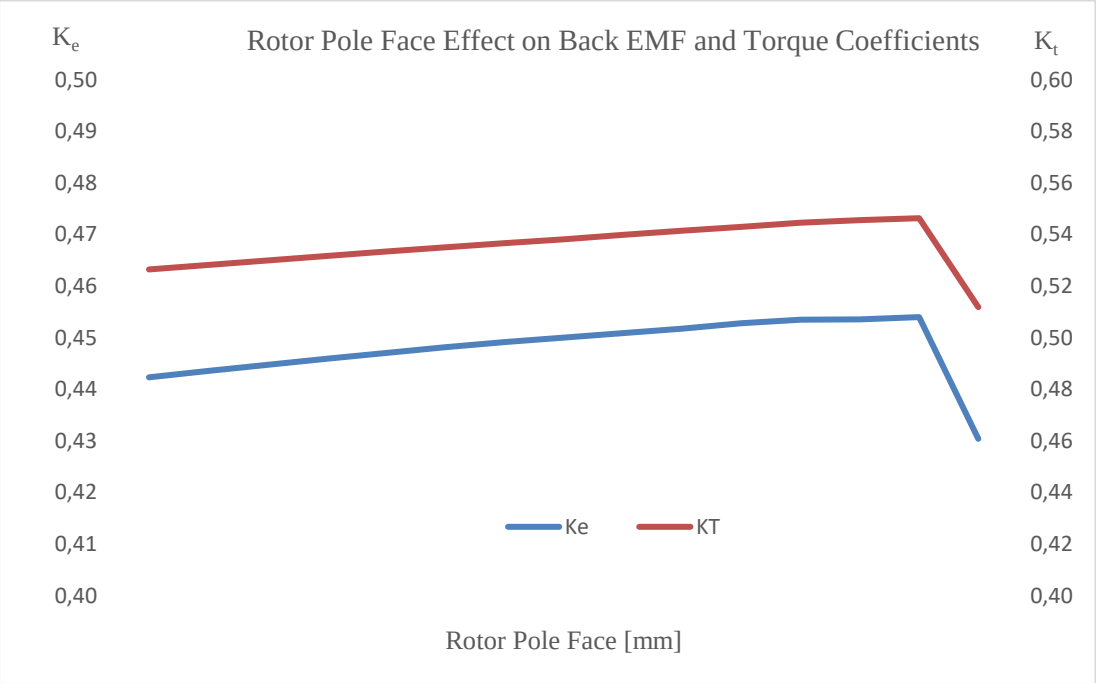

Figure 4.17 : The effect of the rotor pole face on back EMF coefficient (k_e) and torque coefficient (k_t).

The rotor pole face value is given by decreasing from left to right. The leftmost dot represents the highest pole face value, and the rightmost dot represents the lowest pole face value.

As a result of the analysis, when the change of the rotor pole face parameter in specified range on the torque ripple is examined, it is observed that this parameter is quite effective on the torque ripple. An increase in the rotor pole face parameter is caused an increase in torque ripple.

The parametric analysis results are presented for the change of the magnet opening parameter on washing cycle torque results as below in Figure 4.18. In this analysis, all parameters except the magnet opening and rotor pole face were kept the same as the existing motor. The rotor pole face value was analyzed as maximum value.

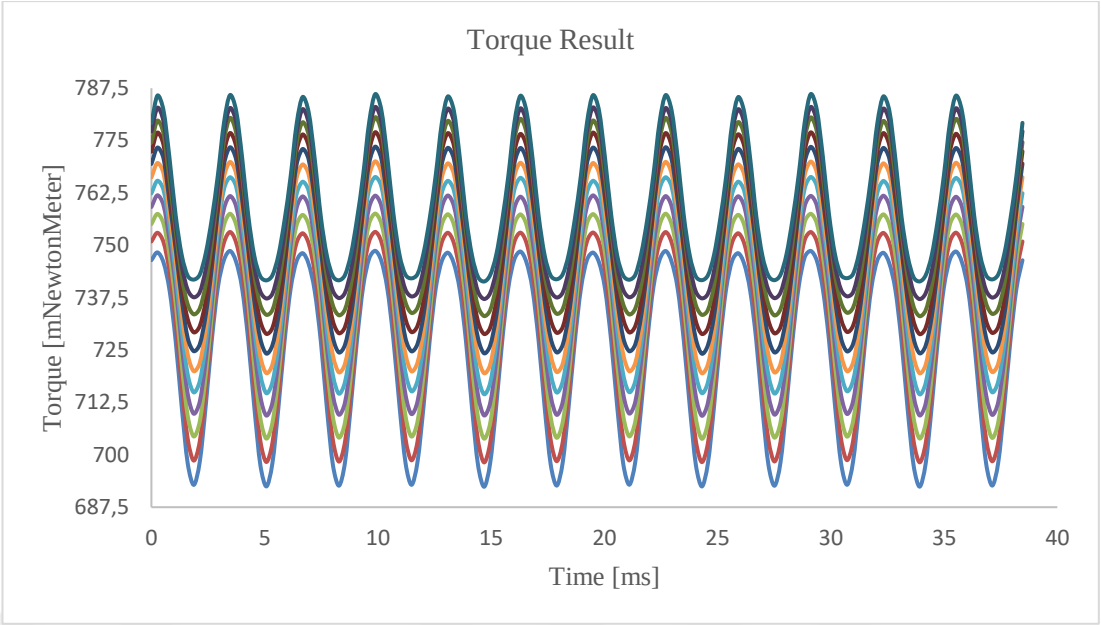

Figure 4.18 : The influence of the magnet opening change on motor torque ripple result.

The top curve is represented the highest magnet opening length. The bottom curve is represented the lowest magnet opening length. The magnet opening length was solved by increasing in the given range.

The parametric analysis results are presented for the change of the magnet opening parameter on back EMF coefficient (k_e) and torque coefficient (k_t) results as below in Figure 4.19.

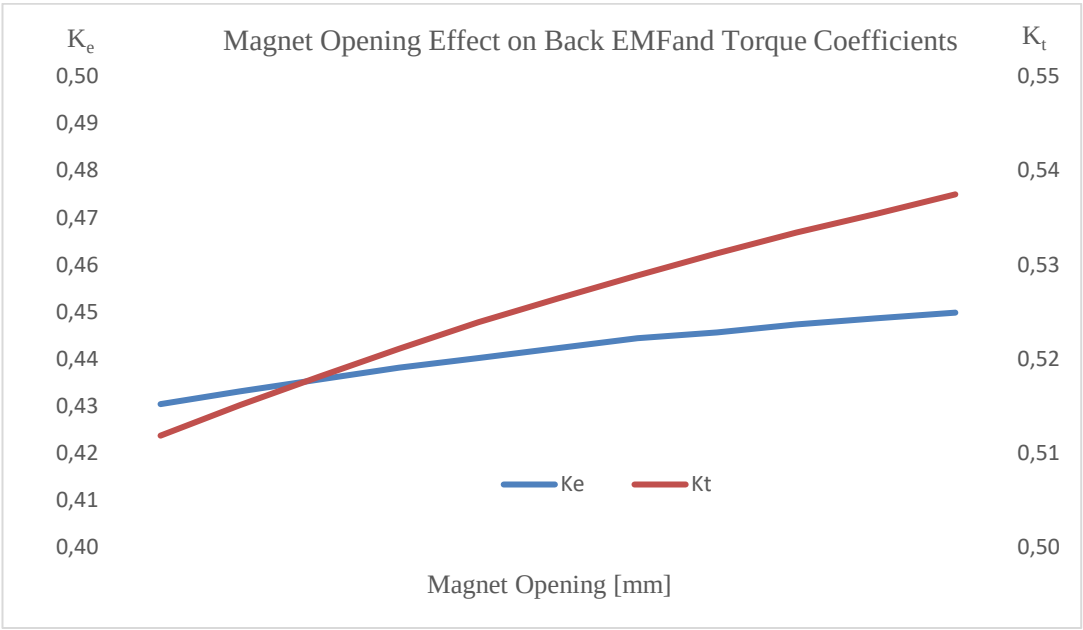

Figure 4.19 : The effect of the magnet opening on back EMF coefficient (k_e) and torque coefficient (k_t).

The magnet opening length is given by increasing from left to right. The leftmost dot represents the lowest magnet opening length, and the rightmost dot represents the highest magnet opening length.

As a result of the analysis, when the change of the magnet opening parameter in specified range on the torque ripple is examined, it is observed that this parameter is effective on the torque ripple. An increase in the magnet opening parameter is caused a decrease in torque ripple.

The parametric analysis results are presented for the change of the magnet thickness parameter on washing cycle torque results as below in Figure 4.20. In this analysis, all parameters except the magnet thickness and rotor pole face were kept the same as the existing motor. The rotor pole face value was analyzed as maximum value.

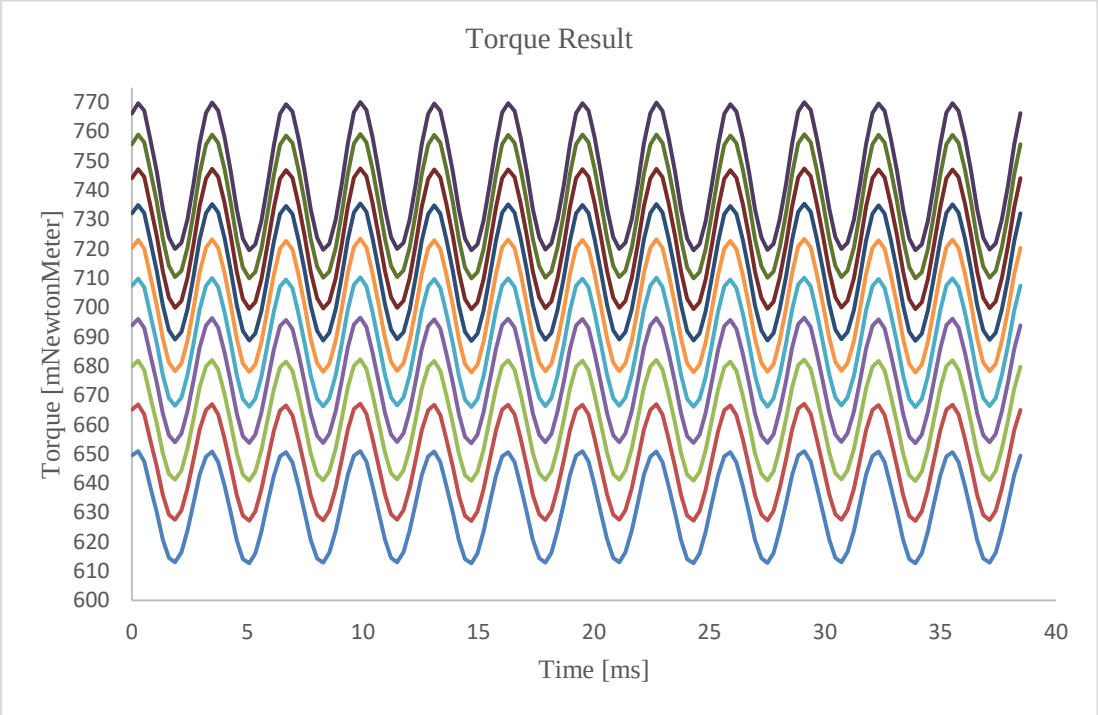

Figure 4.20 : The influence of the magnet thickness change on motor torque ripple result.

The top curve is represented the highest magnet thickness length. The bottom curve is represented the lowest magnet thickness length. The magnet thickness length was solved by increasing in the given range.

The parametric analysis results are presented for the change of the magnet thickness parameter on back EMF coefficient (k_e) and torque coefficient (k_t) results as below in Figure 4.21.

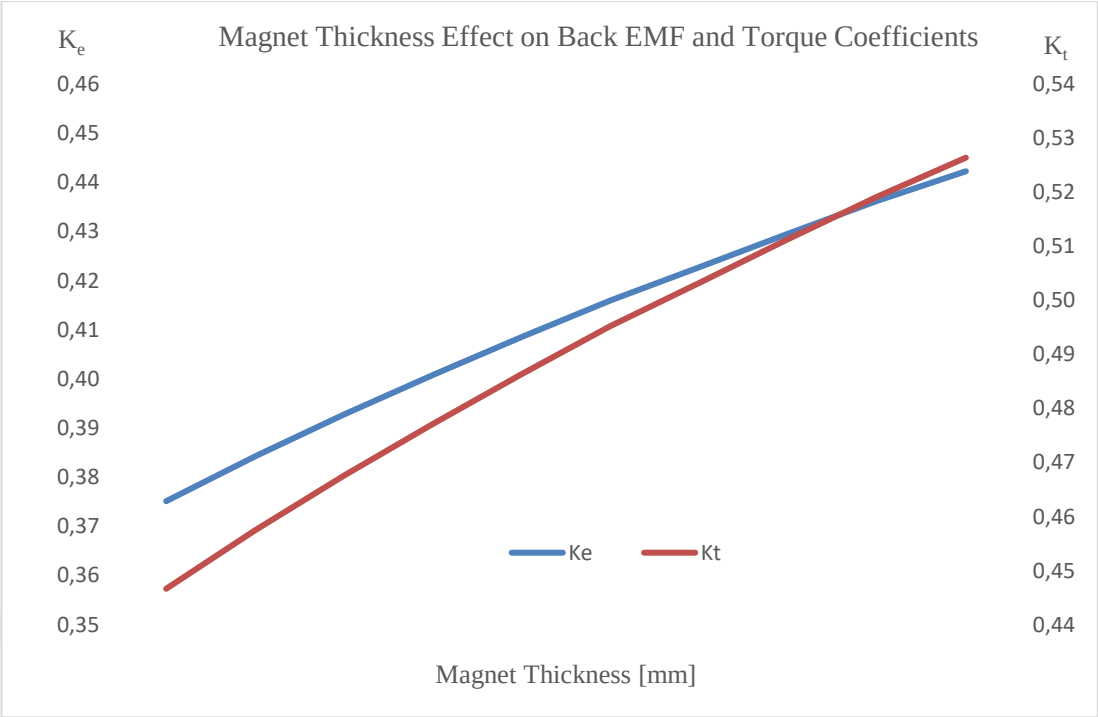

Figure 4.21 : The effect of the magnet thickness on back EMF coefficient (k_e) and torque coefficient (k_t).

The magnet thickness length is given by increasing from left to right. The leftmost dot represents the lowest magnet thickness length, and the rightmost dot represents the highest magnet thickness length.

As a result of the analysis, when the change of the magnet thickness parameter in specified range on the torque ripple is examined, it is observed that this parameter is effective on the torque ripple. An increase in the magnet thickness parameter is caused an increase in torque ripple.

The parametric analysis results are presented for the change of the magnet length and air gap parameters on washing cycle torque results as below in Figure 4.22. Since changes in magnet length directly correspond to air gap change, the evaluation of these parameters is given together considering their interactions with each other. In this analysis, all parameters except the magnet length, air gap and rotor pole face were kept the same as the existing motor. The rotor pole face value was analyzed as maximum value.

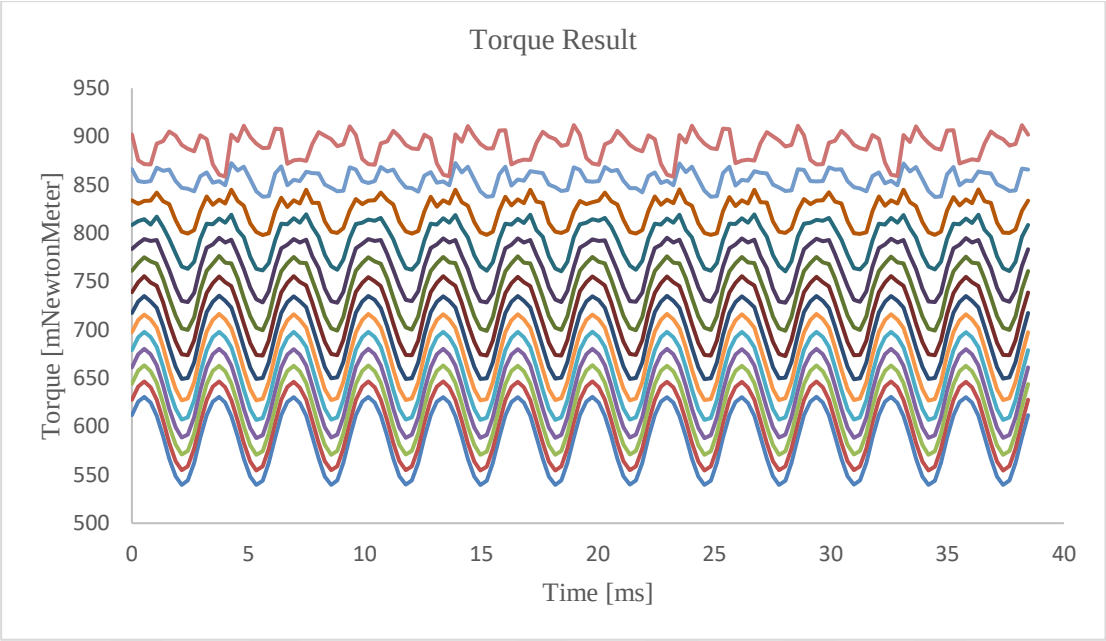

Figure 4.22 : The influence of the air gap change on motor torque ripple result.

The top curve is represented the higher air gap and lower magnet length when compared to the existing motor. The bottom curve is represented the higher magnet length and lower air gap. The magnet length was solved by decreasing and the air gap was solved by increasing in the given range.

The parametric analysis results are presented for the change of the magnet length and air gap parameters on back EMF coefficient (k_e) and torque coefficient (k_t) results as below in Figure 4.23 and Figure 4.24, respectively.

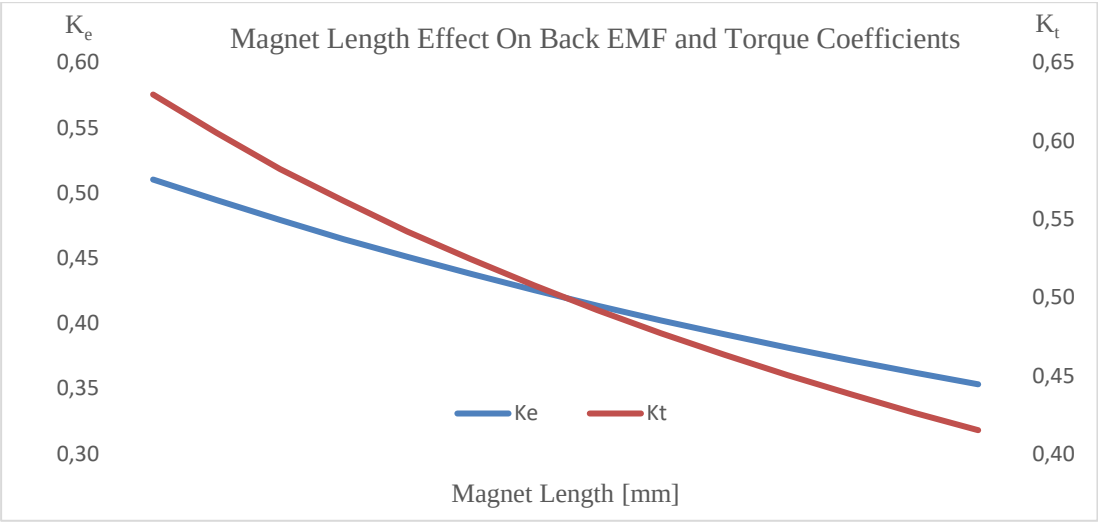

Figure 4.23 : The effect of the magnet length on back EMF coefficient (k_e) and torque coefficient (k_t).

The magnet length is given by decreasing from left to right. The leftmost dot represents the highest magnet length, and the rightmost dot represents the lowest magnet length.

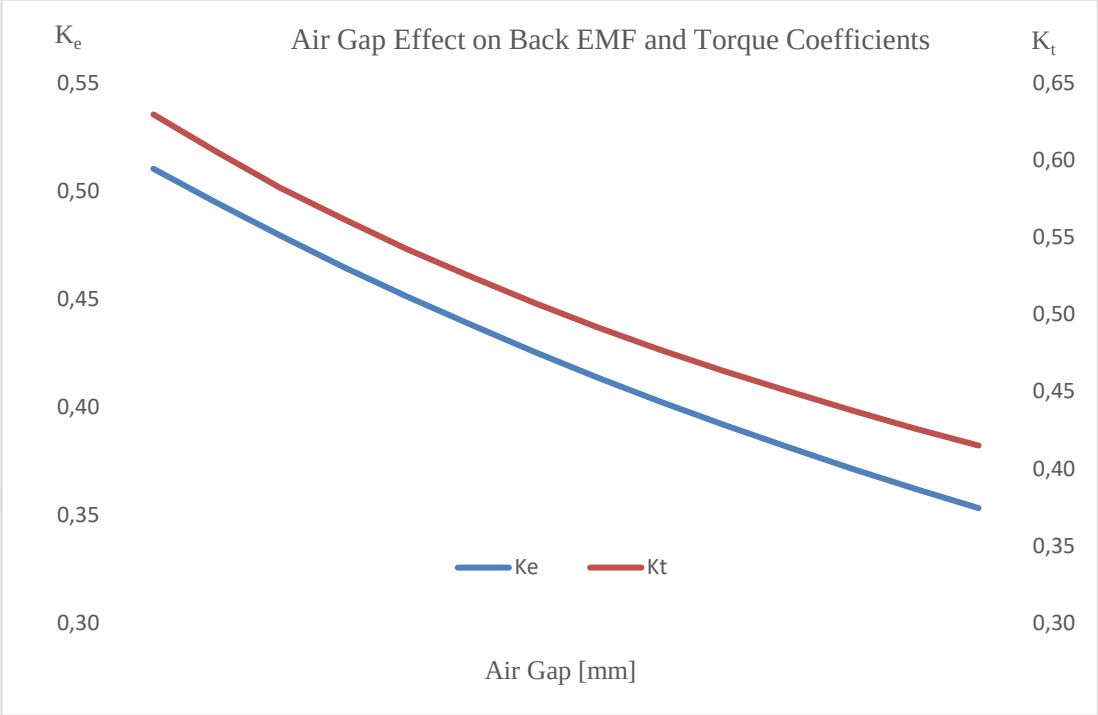

Figure 4.24 : The effect of the air gap on back EMF coefficient (k_e) and torque coefficient (k_t).

The air gap is given by increasing from left to right. The leftmost dot represents the lowest air gap, and the rightmost dot represents the highest air gap.

As a result of the analysis, when the change of the air gap parameter in specified range on the torque ripple is examined, it is observed that this parameter is quite effective on the torque ripple. An increase in the air gap parameter is caused a decrease in torque ripple.

4.3 Multi-Objective Genetic Algorithm (MOGA) Optimization

In this chapter is focused on an optimization process by using multi-objective genetic algorithm (MOGA) according to the parametric model results. The first stage of multi-objective genetic algorithm is to determine the quantities that will most affect the which are the optimization targets, and to evaluate the different multi-objective genetic algorithm optimization methods used for this application in the related literature. In order to be able to evaluate and interpret the effects of geometric parameters on motor

performance more comprehensively, many studies have been presented in the literature related with the multi-objective genetic algorithm optimization.

Recently, a various number of methods have been proposed by researchers to eliminate disturbance effects. It is proven with many researches that the disturbance effects on the machine are reduced by the geometric improvements on motor design [7].

In [18], a genetic algorithm optimization of PMSM in order to ensure the high power density and high speed requirement has been presented. By using high optimization techniques such as genetic algorithm small volume with high power requirement was satisfied. In [19], in order to minimize the cogging torque provided that the same output power, torque or current, rotor structure has been changed in terms of thickness and shape of the magnets and pole span by using a genetic algorithm optimization tool. In addition; genetic algorithm has been used for minimum cogging torque requirement by changing magnet shape [20]. For this purpose, permanent magnet pole slice arrangement was performed with optimization tool in order to be able to define exact values.

Besides, a novel method by using genetic algorithm has been conducted to be able to minimize the magnitude and phase of the harmonic currents for an IPMSM [21]. Providing this goal, genetic algorithm were applied to achieve decreasing the peak to peak torque ripple, reducing the harmonic currents, and increasing the average torque component. As a result of optimization the objectives have been achieved regarding to chosen parameters.

Genetic algorithm is a comprehensive optimization algorithm method which is aimed to obtain the optimal solutions for given problem by maximizing or minimizing a specific function. This algorithm is developed by John Holland in the 1960s and 1970s which is a model matched with biological evolution separation in reference to Charles Darwin's theory of natural selection [33,34].

Genetic algorithm is referred as evolutionary computation because of simulating the breeding biological processes and natural selection. In accordance with this purpose, many terms used in the algorithm are chosen by taking samples from biology literature for example fitness. The fitness function is comed from evolutionary theory and is tried to optimize by genetic algorithm [33,34].

The basic structure of the genetic algorithm is examined, it is seen that it has a structure established from certain components. As the most important components of the algorithm can be expressed as a fitness function definition to be able to optimized, a population of chromosomes, chromosomes extracting to identfiy the reproducement, chromosomes crossovering to obtain next generation and random mutations of chromosomes [33].

In this part, cogging torque optimization of IPMSM is performed by using multi-objective genetic algorithm integrated with ANSYS software. It is obvious that the analysis results to are obtained by parametric modeling are the basic building blocks for the genetic algorithm. In line with the evaluation of the parametric analysis results, the most effective parameters are chosen on disturbance effect and determined ranges for each parameter are reconstructed considering the washing machine application motor requirements and restrictions. The computational complexity and calculation time for the genetic algorithm optimization is reduce with this approach.

Firstly, maximum number of generations, parents, mating pool, children and next generation are defined on the basis of evolutionary theory. The number of evaluations is determined by the optimizer in proportion to the inputs. Then, the cost function to be solved by genetic algorithm is defined. The cost functions reflects the goals that the algorithm is trying to achieve. Inputs are provided for the cost function by adjusting the goal and weights. The preponderance setting has been made for the cost functions defined with the weight content, and the cost function is rearranged according to the input values. The expression of the defined cost funciton in terms of goal and weight is given below in Equation (4.1);

$$Cost1 = (G1 - 1)^2 * W1 \tag{4.1}$$

where,

$$G1 = 1 + (\max(abs(Moving1.Torque)) - X) * (Y / Z) \tag{4.2}$$

According to the Equation (4.1) cost function tried to bring the G1 value closer to 1. The number Y in the Equation (4.2) is used to give the worst case. Other values in the

equation are given as input by converging to the maximum and minimum peak to peak cogging torque values found as a result of parametric optimization.

4.4 Optimization Results

In this part, optimization results are obtained as minimizing the cogging torque by analyzing the genetic algorithm with several geometrical parameters which are the rotor pole face, magnet opening, magnet thickness, magnet length and air gap parameters the investigated spoke type IPMSM at appropriate intervals. As a reminder, since the slit structure is preferred for applications with high speed requirements, only the effect of this parameter on the cogging torque is shown. This parameter is not included in the genetic algorithm optimization process.

In line with the evaluation of the parametric analysis results, the most effective parameters are chosen on disturbance effect and determined ranges for each parameter are reconstructed considering the washing machine application motor requirements and restrictions. The computational complexity and calculation time for the genetic algorithm optimization is reduce with this approach.

The cost-iteration graph obtained as a result of the genetic algorithm is given in the Figure 4.25.

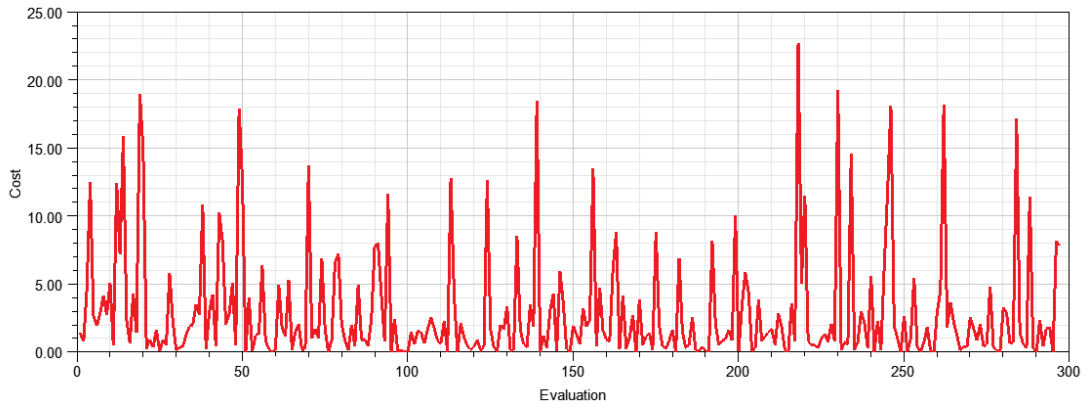

Figure 4.25 : The cost-iteration graph.

The iteration results are evaluated, parameter values that give the optimized cogging torque result are obtained. Considering the requirements for the IPMSM used for the washing machine, the intervals given for the parameters are limited and the optimization is repeated so that the desired result remained within the solution set. In order to achieve the most proper design, the parametric analysis results and genetic

algorithm results are evaluated both the individual and the combined. From the analysis results on the parametric model, the approach of which parameter is effective on the cogging torque and the results that give the lowest cogging torque value in the genetic algorithm are combined and the number of models obtained is reduced to the best two design.

According to the results of the parametric model, it is observed that giving the rotor a pole face quite affected the cogging torque value. It is also realized that changing the magnet length is also affected the cogging torque greatly. Considering to the analyzes performed with the parametric model, the parameters most affecting the cogging torque value are rotor pole face and magnet length.

Since the prototyping of optimized motor is aimed the appropriate results from the genetic algorithm that give these two parameters are taken into consideration as a priority, taking into account the production capabilities. Disturbance effect and simulation results are compared for the two best models obtained as a result of genetic algorithm and parametric optimization. According to these results, the design of the motor to be prototyped is decided.

These two model which are optimized in terms of rotor geometrical parameters cogging torque and torque ripple are investigated comprehensively. Taking into consideration the requirements of the washing machine in order to fully evaluate the infuence of the parameter on motor performance, results which are obtained from genetic algorithm and parametric modeling are evaluated under different scenarios including cogging torque, open circuit back EMF and on load.

4.4.1 Simulation results

For this part; the most crucial parameter to be evaluated while giving the results of the best two designs disturbance effect is the cogging torque. The optimized motors will be given as “Design 1” and “Design 2” after this part.

Cogging torque analysis is performed at no-load condition in Maxwell 2D. The cogging torque period is calculated to be 15 degree. Since the speed is held constant at 1.0 deg/sec, 15 degree is corresponded to be 15 second.

Design 1 cogging torque analysis result is presented as below in Figure 4.26.

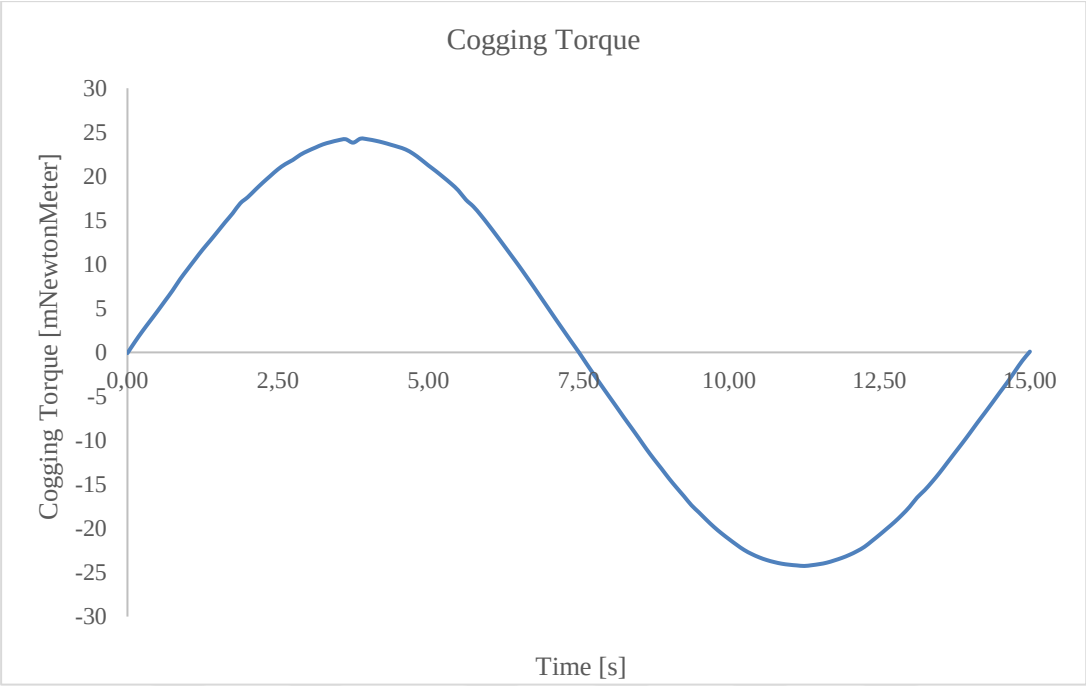

Figure 4.26 : Design 1 cogging torque analysis result.

Design 2 cogging torque analysis result is presented as below in Figure 4.27.

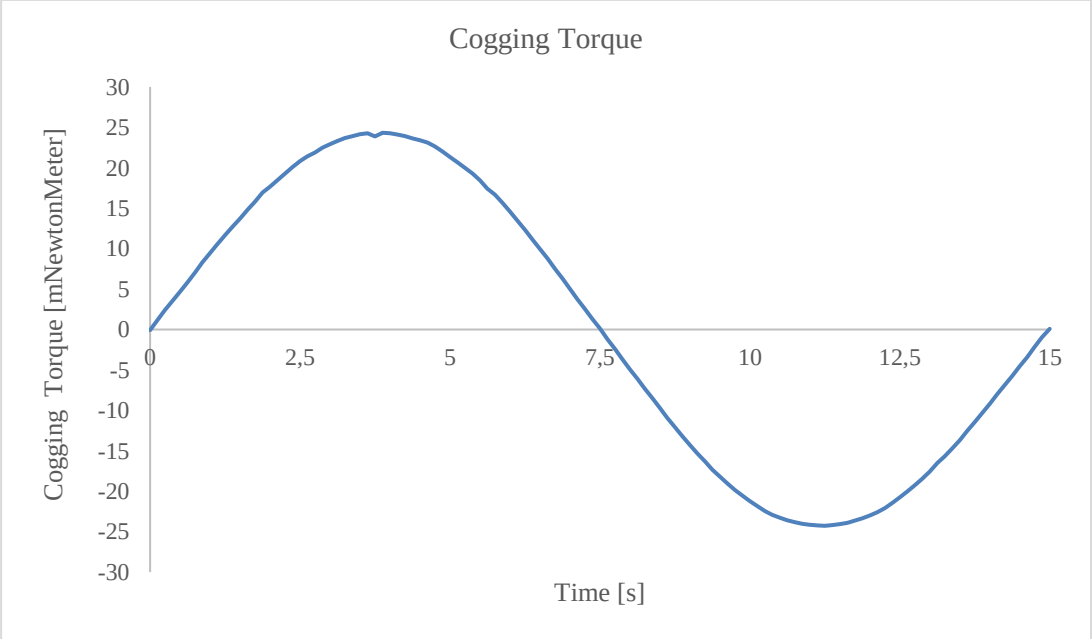

Figure 4.27 : Design 2 cogging torque analysis result.

The design 1 motor torque changing depending on rotor position is presented in Figure 4.28.

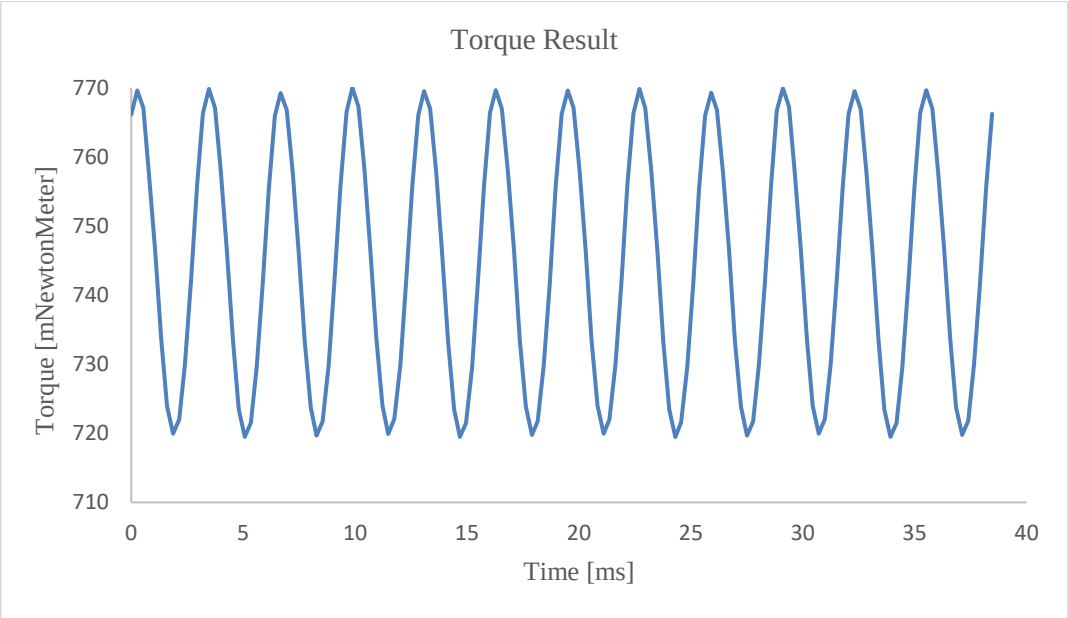

Figure 4.28 : Design 1 motor torque ripple result.

The design 2 motor torque changing depending on rotor position is presented in Figure 4.29.

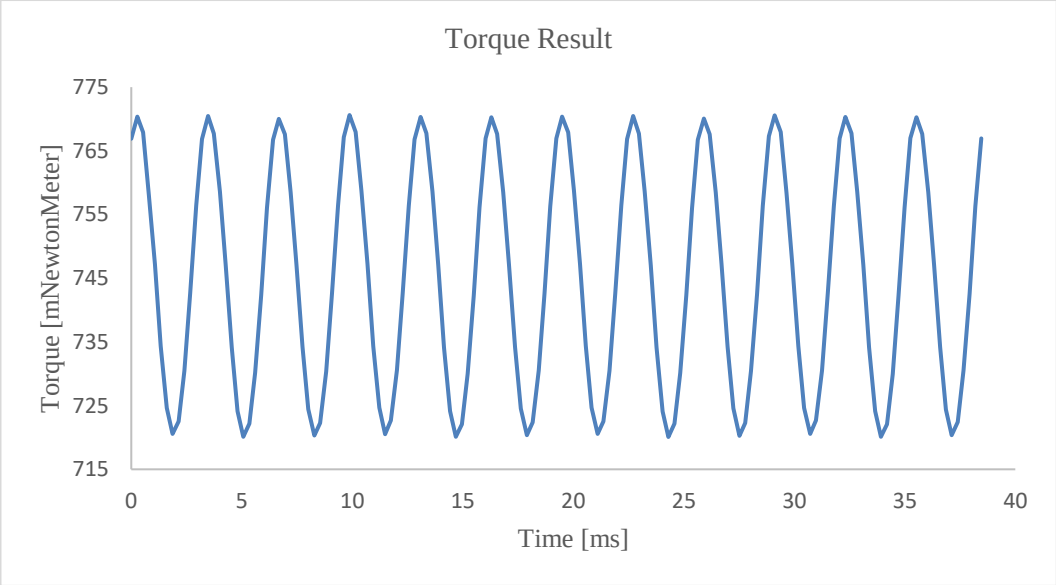

Figure 4.29 : Design 2 motor torque ripple result.

The design 1 motor line and phase voltages are presented in Figure 4.30 and Figure 4.31, respectively.

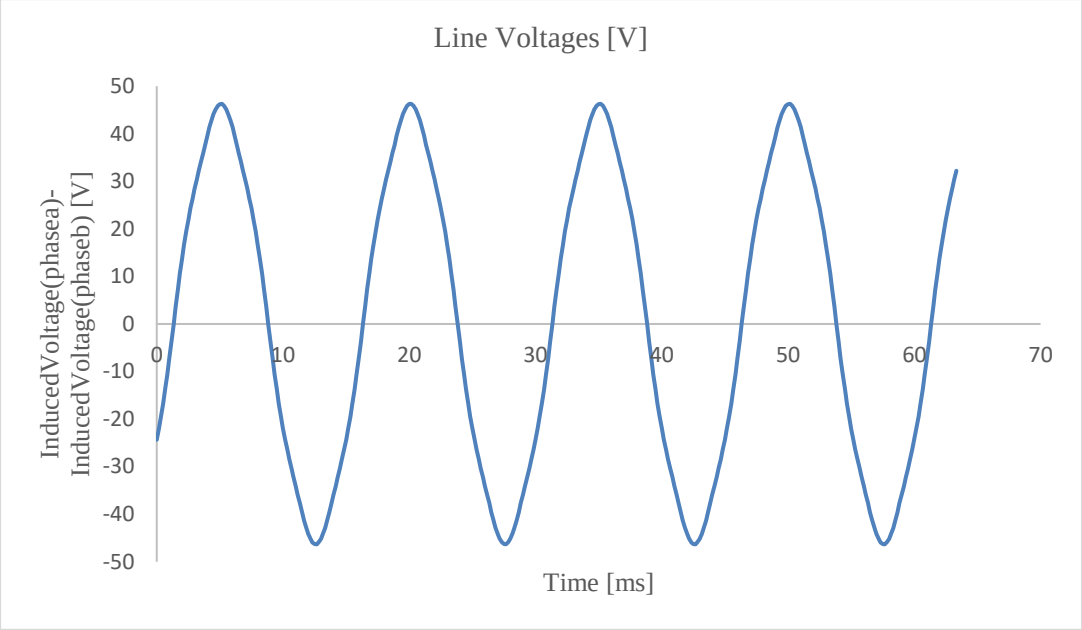

Figure 4.30 : Design 1 motor line voltages.

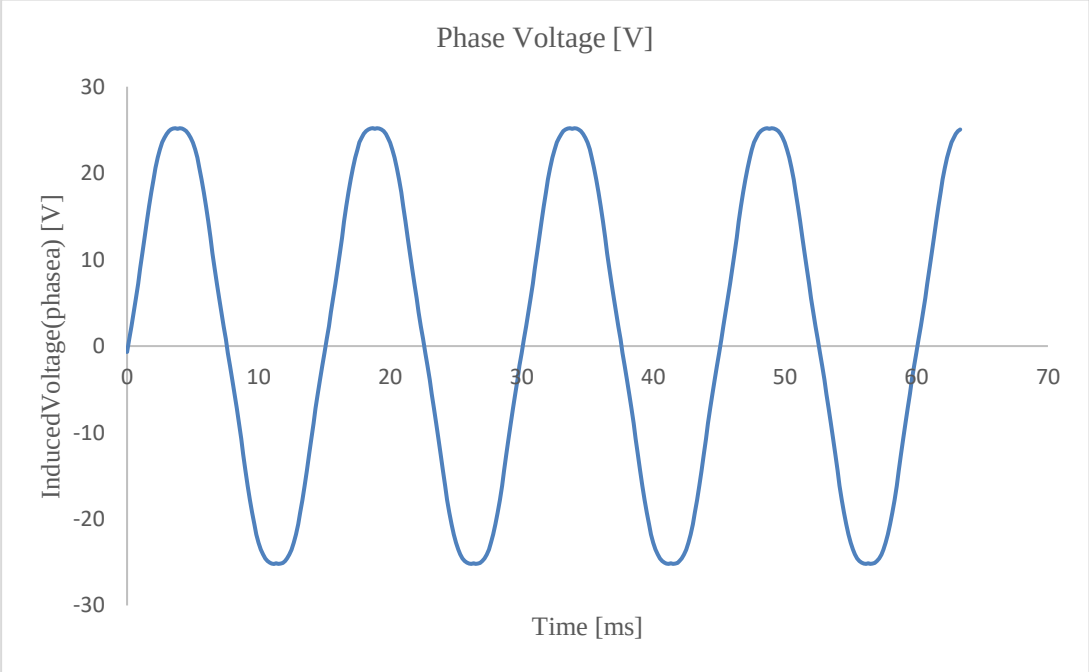

Figure 4.31 : Design 1 motor phase voltages.

The design 2 motor line and phase voltages are presented in Figure 4.32 and Figure 4.33, respectively.

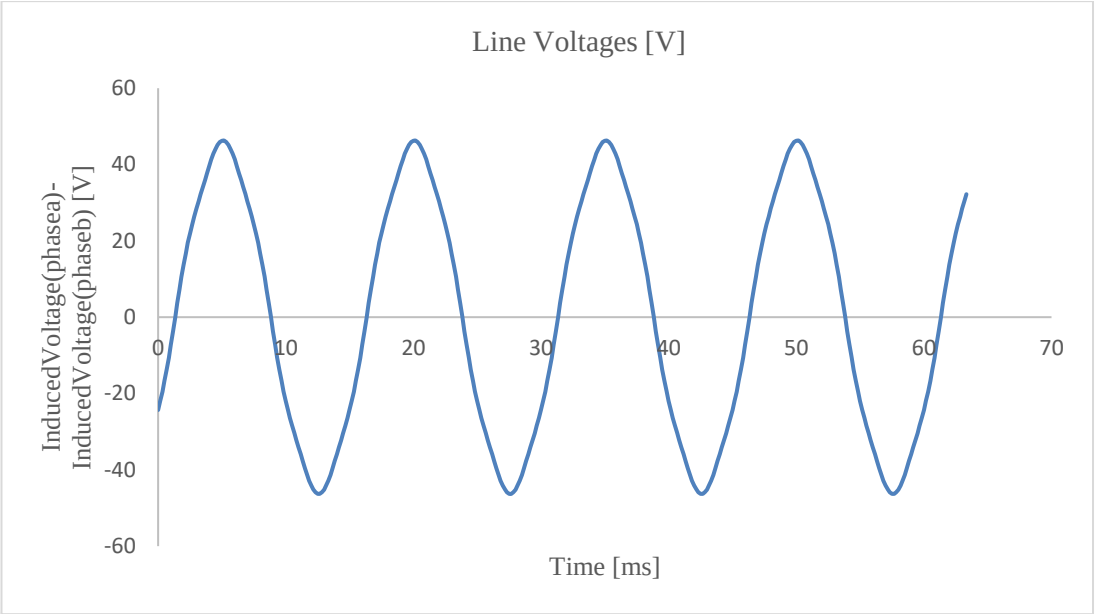

Figure 4.32 : Design 2 motor line voltages.

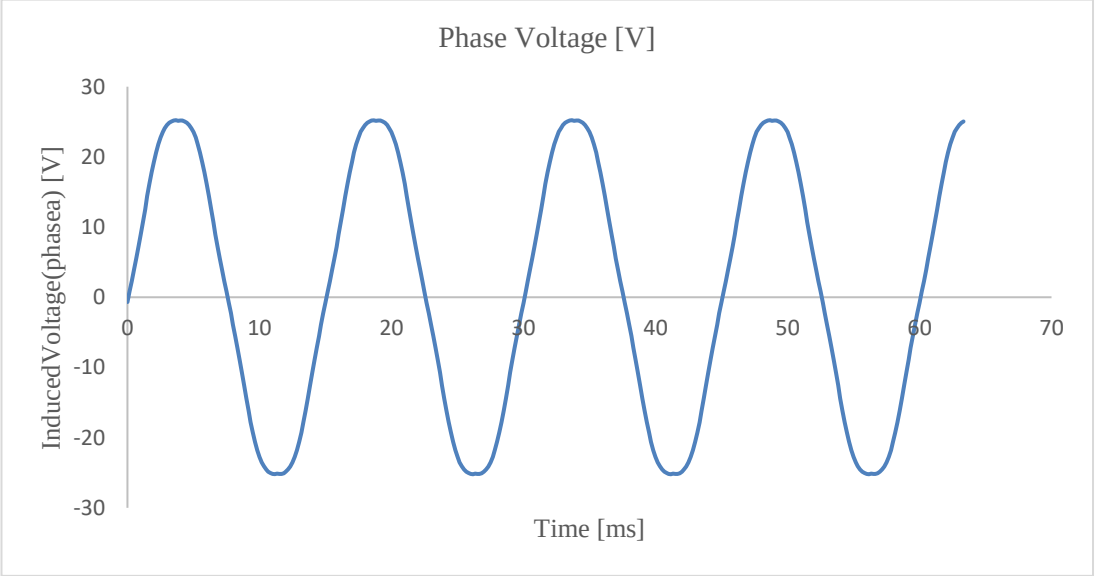

Figure 4.33 : Design 2 motor phase voltages.

The results given in this section are very important in terms of evaluating and comparing the two design in order to prototype.

4.4.2 Comparison and interpretation

In this section, a comparison summary of the simulation results obtained from the previous section with the existing motor is given in Figure 4.34.

Content	Cogging Torque Peak to Peak [mNm]	Torque Ripple (%)	Line Peak to Peak Voltages [V]	Phase Peak to Peak Voltages [V]	Back EMF Coefficient (k_e)	Torque Coefficient (k_t)
Design 1	48,5269	6,79	92,6331	50,4110	0,4422903	0,526
Design 2	48,6119	6,78	92,7099	50,4543	0,4426572	0,527
Existing Motor	86,62	7,43	78,9931	44,7196	0,3771643	0,562

Figure 4.34 : Comparison of Design 1, Design 2 and existing motor simulation results.

If a comprehensive comparison is made between Design 1 and Design 2, it is observed that the Design 1 motor and Design 2 motor effect on reducing existing motor disturbance effect is highly. Since the prototyping of optimized motor is aimed when evaluating the appropriate results from the simulation results was taken into account the production capabilities.

4.4.3 Prototyping

In this part, the resultant design that had been analyzed and simulated in the previous chapters were constructed in a real washing machine application. Considering the producibility capabilities of the prototype, the sample called Design 1 was chosen as resultant design and prototyping was constructed as Figure 4.35 and Figure 4.36.

Figure 4.35 : The resultant design rotor part prototype.

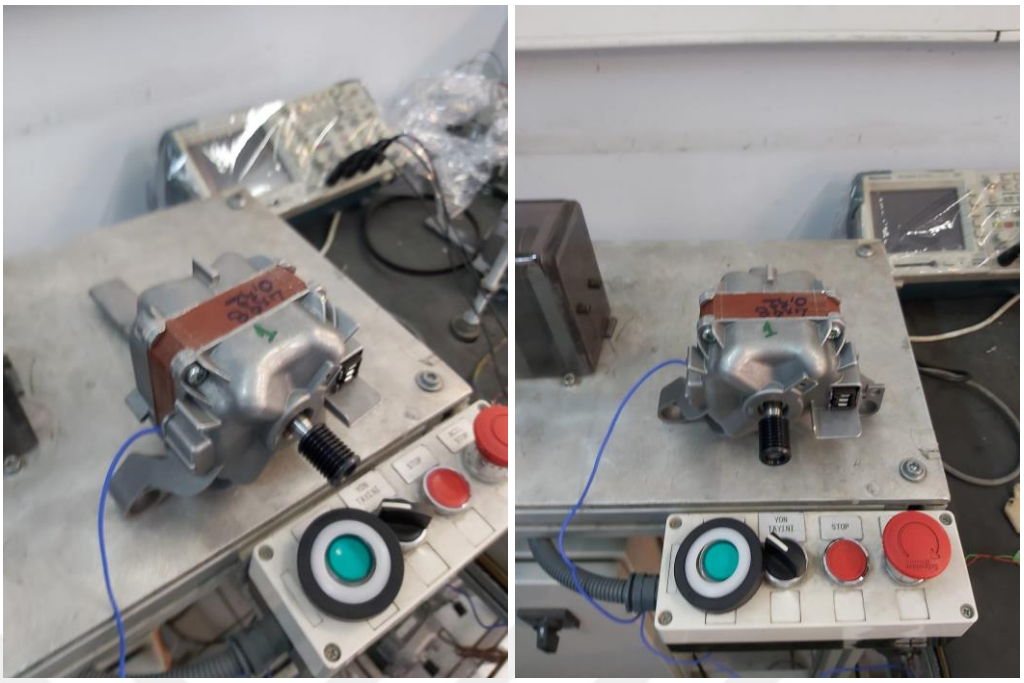

Figure 4.36 : The resultant design prototype.

In this design, the rotor pole face parameter has been created and the magnet length has been reduced when compared to the existing motor design.

5. CONCLUSION

In this thesis, the performance of an existing interior permanent magnet synchronous motor (IPMSM) which is being used in commercial washing machine applications while the disturbante effects reduced has been developed and improved. The space and geometrical dimensions of the motor occupied inside the washing machine was kept unchanged as a design contsraint. Studies on performance optimization with motor control technique were excluded from the scope of this thesis.

The first topics explained in this thesis were related with the disturbance effects. The spoke type IPMSM motors which are widely used the commercial washing machines are needing airgap reduction and stack length reduction in order to meet the demanded power density requirement is caused the noise problem. The source of the undesired noise in the spinning cycle, especially at high speeds, is the motor. The most important components of the effects of harmonic torque distortions on the PMSMs are the back electromotive force (back EMF) harmonics, cogging torque and and torque ripple. It is proven with many researches that the disturbance effects on the machine are reduced by the geometric improvements on motor design and the development of the algorithms used in the motor control. Consequently, unwanted mechanical impacts are reduced such as vibration, noise and rotor stress.

The second section under this thesis are the definition of the specifications of the IPMSM used for a typical horizontal belted-motor driven washing machine. This features were listed as IPMSM structure, equivalent circuit and mathematical modelling. Moreover, it was mentioned about the advantages of the PMSM over other conventional universal motors being used in washing machines. According to the washing machine application requirements; the selection of the PMSM motor was discussed for a belted-motor type washing machine which is composed of two pulleys with the belt transmitting the speed, torque and power from the motor to the drum. Addition to this, the PMSM control method, based on washing machine application was presented. These topics are considered as the basic building blocks formed the

basis of determining the requirements of the selected application and improving the motor design accordingly.

In the third part of this study, the design specifications and design data of a real sample IPMSM used for a typical horizontal belted-motor driven washing machine has been examined. The design criteria for the motor to be used for comparison were evaluated in accordance with the requirements and constraints for the washing machine application. For this purpose, the disturbance effect, simulation and experimental results were investigated for existing IPMSM.

Afterwards, the real sample PMSM used in washing machine application with 12/8 slot-pole ratio was designed in ANSYS 2D software. 2D design steps of the real sample motor used in washing machine applications, which was aimed to improve cogging torque, were presented in ANSYS software program based on finite element method. After this step, disturbance effect, finite element modeling for transient analysis and other simulation results were obtained similar with existing IPMSM. Taking into consideration the requirements of the washing machine in order to fully evaluate the motor performance the designed motor results were evaluated under different scenarios including cogging torque, open circuit back EMF and on load. The results were given in this section are very critical in terms of evaluating and interpreting the performance of the designed motor.

It was aimed to verify 2D design by comparing the results obtained from the finite element analysis with the actual performance of the real sample motor. Considering all compatible results from the disturbance effect, finite element modeling for transient analysis and the other simulation results of the designed motor validation was proved. The simulation results were obtained with the designed model was found to be reliable when compared with the existing motor. Optimization process was continued with this model.

In the next chapter, after confirming the validation and reliability of the established model, the model was converted into a parametric analysis model. Due to the fact that it was proven with many researches that the disturbance effects on the machine were reduced by the geometric improvements on motor design, the rotor of the designed motor was completely parametrically modeled.

The parametric analysis and design optimization were performed on the influence of several geometrical parameters which were the rotor pole face, magnet opening, magnet thickness, magnet length, air gap and rotor slit the investigated spoke type IPMSM. The parametric analysis was configured with definition reasonable ranges for each selected geometrical variable.

In the next step, the effects of determined rotor geometrical parameters on cogging torque and torque ripple were investigated comprehensively. Taking into consideration the requirements of the washing machine in order to fully evaluate the infuence of the parameter on motor performance, results which were obtained from each paramater change were evaluated under different scenarios including cogging torque, open circuit back EMF and on load. Considering to the analyzes performed with the parametric model, the parameters most affecting the cogging torque value were found as rotor pole face and magnet length.

In order to expand the data pool obtained cogging torque optimization of IPMSM was performed by using multi-objective genetic algorithm integrated with ANSYS software. It was obvious that the analysis results obtained by parametric modeling were the basic building blocks for the genetic algorithm. In line with the evaluation of the parametric analysis results, the most effective parameters were chosen on disturbance effect and determined ranges for each parameter were reconstructed considering the washing machine application motor requirements and restrictions. The computational complexity and calculation time for the genetic algorithm optimization was reduce with this approach.

Parametric values with the lowest cogging torque were selected from the data set to provide the cost function determined for the genetic algorithm optimization. From the analysis results on the parametric model, the approach of which parameter was effective on the cogging torque and the results that was given the lowest cogging torque value in the genetic algorithm were combined and the number of models obtained was reduced to the best two design.

Disturbance effect and simulation results were compared for the two best models obtained as a result of genetic algorithm and parametric optimization. According to these results, the design of the motor to be prototyped was decided.

These two model which were optimized in terms of rotor geometrical parameters cogging torque and torque ripple were investigated comprehensively. Taking into consideration the requirements of the washing machine in order to fully evaluate the infuence of the parameter on motor performance, results which were obtained from genetic algorithm and parametric modeling were evaluated under different scenarios including cogging torque, open circuit back EMF and on load. The optimized motors was given as “Design 1” and “Design 2” after this part.

If a comprehensive comparison was made between Design 1 and Design 2, it was observed that the Design 1 motor and Design 2 motor effect on reducing existing motor disturbance effect was highly. Since the prototyping of optimized motor was aimed when evaluating the appropriate results from the simulation results was taken into account the production capabilities. Considering the production capabilities of the prototype, the sample called Design 1 was chosen as resultant design. Concordantly, it was observed that the existing motor peak to peak cogging torque value was calculated 86.62 [mNm] when the cogging torque of the optimized design was calculated 48.53 [mNm] resulting in 56.0% improvement on cogging torque value.

In the final section, the prototyping of the resultant design were established. The resultant design that had been analyzed and simulated in the previous chapters were constructed in a real washing machine application. In this design, the rotor pole face parameter has been created and the magnet length has been reduced when compared to the existing motor design.

All in all, the purpose of the thesis is to develop and to improve the performance of an existing interior permanent magnet synchronous motor (IPMSM) which is being used in commercial washing machine applications while the disturbante effects are reduced. The actual motor used in commercial machine was modeled and analyzed numerically in order to obtain a trustable mathematical model. After obtaining a reliable analysis method and model, the motor was optimized by means of both parametric modeling and multi-objective genetic algorithm. The disturbing effects based on cogging torque and torque ripple were decreased by changing major motor design parameter accoding to the optimization results. In the practical stage of the study the calculated numerical design was prototyped. Verification of the optimized design was proven with simulations. According to the result of the study, the disturbing effect problems in IPMSM used in a commercial washing machine were reduced dramatically and the

new optimized design having less disturbance effects was made ready to be served for the commercial market.

REFERENCES

[1] **Park, K., Jung, D., Chang, H., Bae, J., and Lee, J.** (2008). A study on the reducing of cogging torque of IPMSM. *International Conference on Electrical Machines and Systems*, pp. 3137-3141.

[2] **Jang, H., Cho, S., Lee K.S., and Oh Y.J.** (2018). Design of power density improvement by applying novel shape of slit and notch to outer rib of rotor of spoke-type permanent magnet synchronous motor. *The Open Electrical & Electronic Engineering Journal*, pp. 75-85.

[3] **Candel, M.T.** (2016). *Cogging Torque Reduction for Interior Permanent Magnet Synchronous Motors* (Master Thesis). Technical University of Darmstadt, Institute of Electrical Energy Conversion, DARMSTADT.

[4] **Ravisankar, B., Senthilnathan, N., and Sethupathi, P.** (2021). Analysis and prediction of cogging torque and ripples in output torque of permanent magnet synchronous motor and line start permanent magnet synchronous motor. *Turkish Journal of Computer and Mathematics Education*, Vol.12, No.3, 4586-4595.

[5] **Win, T.** (2014). Speed controller design of permanent magnet synchronous motor used in washing machine. *International Journal of Scientific Engineering and Technology Research*, Vol.03,Issue.15, 3212-3217.

[6] **Murray, A., Palma, M., and Husain, A**. (2008). Performance comparison of permanent magnet synchronous motors and controlled induction motors in washing machine applications using sensorless field oriented control. *Industry Applications Society Annual Meeting*, 11 November.

[7] **Bahrim, F.S., Sulaiman, E., Kumar, R., and Jusoh, L.I** (2017). New cogging torque reduction methods for permanent magnet machine. *IOP Conf. Series: Materials Science and Engineering*, 14 August.

[8] **Aydın, M., Ocak, O., and Çırpanlı Albaş, G.** (2012). Kalıcı mıknatıslı senkron motorların doğrudan sürüşlü beyaz eşya uygulamalarında kullanımı. *EMO Bilimsel Dergi*, Cilt 2, Sayı 3, Syf 7-17.

[9] **Petkovska, L., Cvetkovski, G., and Lefley, P.** (2013). Design consideration of permanent magnet motor for cogging torque reduction. *Proceedings of 16th ISEF'2013 Conference*, Vol. 1, 1 September.

[10] **Abdelmoula, R., Chaieb, M., Neji, R., and Naourez, B.** (2017). Reducing torque ripples in permanent magnet synchronous motor. *Journal of Electrical Systems*, Vol.13, pp. 528-542.

[11] **Yildirim, M., Kurum, H., Miljavec, D., and Corovic, S.** (2018). Influence of material and geometrical properties of permanent magnets on cogging torque of BLDC. *Engineering, Technology & Applied Science Research*, Vol. 8, No. 2, pp. 2656-2662.

[12] **Putek, P.** (2016). *Mitigation of the cogging torque and loss minimization in a permanent magnet machine using shape and topology optimization.* Engineering Computations, Institute for Mathematics and Computer Science, Germany.

[13] **Lim, S., Hong, J.P., and Min, S.** (2012). Low torque ripple rotor design of the interior permanent magnet motor using the multi-phase level-set and phase-field concept. *IEEE Transactions on Magnetics*, Vol. 48, No. 2.

[14] **Yang, Y., Wang, X., Zhang, R., Zhu, C., and Ding, T.** (2005). Research of cogging torque reduction by different slot width pairing in permanent magnet motors. *Elect. Mach. Syst. (ICEMS)*, Vol. 1, pp. 367-370.

[15] **Jin, C. S., Jung, D. S., Kim, K. C., Chun, Y. D., Lee, H. W. and Lee, J.** A study on improvement magnetic torque characteristics of ipmsm for direct drive washing machine. *IEEE Transactions on Magnetics*, Vol. 45, pp. 2811-2814.

[16] **Chen, H., and Lee, C. H. T.** (2019). Parametric sensitivity analysis and design optimization of an interior permanent magnet synchronous motor. *IEEE Transactions on Magnetics*, 28 October.

[17] **Kim, K.** (2021). A study on stator design for electromagnetic noise reduction in washing machine motor. *Turkish Journal of Computer and Mathematics Education*, Vol.12, No.6, pp. 585-589.

[18] **Lai, C., Feng, L., Iyer, V., Mukherjee, K., and Kar, N.C.** (2016). Genetic algorithm based current optimization for torque ripple reduction of interior PMSMs. *XXII International Conference on Electrical Machines (ICEM)*, pp. 1050-1056.

[19] **Sarac, V.** (2019). Performance optimization of permanent magnet synchronous motor by cogging torque reduction. *Journal of electrical engineering*. Vol. 70, No. 3, pp. 218-226.

[20] **Lukaniszyn, M., Wrobel, R., and Jagiela, M.** (2004). Optimization of permanent magnet shape for minimum cogging torque using a genetic algorithm. *IEEE Transactions on Magnetics*. Vol. 40, No. 2, pp. 1228-1231.

[21] **Lai, C., Feng, G., and Iyer L. V.,** (2016). Genetic algorithm based current optimization for torque ripple reduction of interior PMSMs. *XXII International Conference on Electrical Machines (ICEM)*, pp. 1050-1056.

[22] **Agarwal, P., and Srivastava, P.S.** (2014). A comprehensive analysis and implementation of vector control of permanent magnet synchronous motor. *International Journal of Power and Energy Conversion.*

[23] **Ghahfarokhi, P.S., and Faiz, J.** (2013). Design of four-pole permanent magnet motor with different rotor topologies. *Journal of Electromotion 20.*

[24] **Akyol, İ.** (2016). *Position sensorless field oriented control of ipmsm under parameter uncertainties* (Master Thesis). İstanbul Technical University, Department of Control and Automation, İstanbul.

[25] **Bayka, K.** (2014). *Comparison of three ipmsm sensorless position estimation methods through simulations and experiments* (Master Thesis). İstanbul Technical University, Department of Control and Automation, İstanbul.

[26] **Karakaş, S.** (2011). *Vector control of PMSM in washing machine application* (Master Thesis). İstanbul Technical University, Department of Control and Automation, İstanbul.

[27] **Jabbar, M. A., Khambadkone, A. M., and Qinghua, L.** (2001). Design and analysis of exterior and interior type high-speed permanent magnet motors, January.

[28] **Url-1** <*https://community.nxp.com/t5/NXP-Model-Based-Design-Tools/Module-2-PMSM-and-FOC-Theory/m-p/761926*>, date retrieved 05.06.2021.

[29] **Kim, H. .J., Cho, S., Lee, G. S., Jang, H. K., Oh Y. J., and Le J.** (2018). A study on the design of an outer rotor and spoke type pmsm for improving power density. *The Open Electrical & Electronic Engineering Journal*, 20 July.

[30] **Gundogdu, T., and Komurgoz, G.** (2013). The impact of the selection of permanent magnets on the design of permanent magnet machines - a case study: permanent magnet synchronous machine design with high efficiency. *Przeglad Elektrotechniczny*, January.

[31] **Gulbahce, M. O.,** (2013). *Orta güçlü bir girdap akimi freni tasarimi ve sonlu elemanlar yöntemi ile analizi* (Yüksek Lisans Tezi). İstanbul Teknik Üniversitesi, Elektrik Mühendisliği Anabilim Dalı, İstanbul.

[32] **Asl, M. M., and Doroudi, A.** (2014). Finite element analysis of permanent magnet synchronous motors subjected to symmetrical voltage sags. *Iranian Journal of Electrical and Electronic Engineering*. Vol.10, pp. 333-340.

[33] **Carr, J.** (2014). *An Introduction to Genetic Algorithms*, pp 1-40, 16 May.

[34] **Yang, X. S.** (2021). *Genetic Algorithms.* Nature-Inspired Optimization Algorithms, Second Edition.

CURRICULUM VITAE

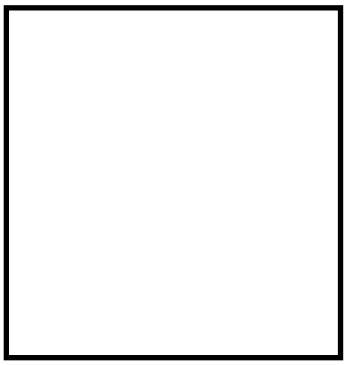

Name Surname **:** Ege ÜNLÜTEPE KESKİN

EDUCATION **:**

- **B.Sc.** **:** 2018, ITU, Faculty of Electrical and Electronics Engineering, Electrical Engineering

PROFESSIONAL EXPERIENCE AND REWARDS:

- October 2018-October 2020 Electronic Control R&D Project Engineer at Arcelik Washing Machine Plant
- R&D Hardware Engineer at Arçelik Washing Machine Plant since October 2020